

Design Guide

Amodel® polyphthalamide (PPA)

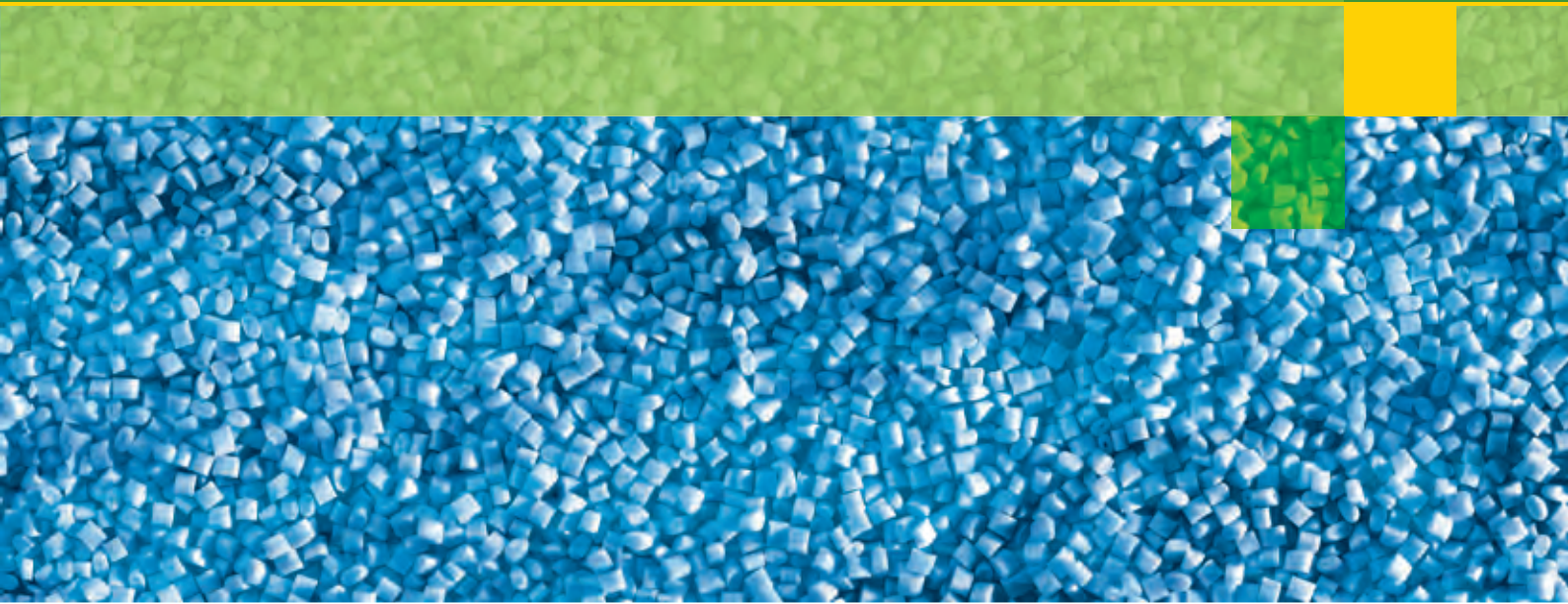


Table of Contents

Introduction	1	Creep	31
Amodel Polyphthalamide (PPA) Resins	1	Tensile Creep	32
Chemistry	1	Isochronous Stress/Strain Curves	34
Crystallinity	2	Tensile Creep Rupture	34
Moisture Effects	3	Flexural Creep	35
Product Data	4	Compressive Creep	36
Amodel Resin Property Tables	4	Fatigue Resistance	36
Nomenclature	4	Fatigue Strength of Amodel Resin	37
Product Selection	5	Moisture Effects	38
Property Data	6	Significance of Moisture Absorption	38
Typical Properties	6	Moisture Absorption and Glass Transition Temperature (T_g)	38
Accelerated Moisture Conditioning	6	Absorption Amount	39
Mechanical Properties	19	Effect of Moisture on Strength and Stiffness	39
Short-Term Mechanical Properties	19	Dimensional Change due to Moisture	40
Tensile Properties	19	Dimensional Change Compared to PA 6,6	41
Test Methods	19	Thermal Properties	42
Tensile Property Comparison	21	Heat Deflection Temperature – HDT	42
Tensile Properties for GR PPA vs. Temperature	21	Deflection Temperature Values for Amodel Resins	43
Tensile Properties of A-1000 GR Grades at Elevated Temperatures	22	Coefficient of Linear Thermal Expansion	43
Flexural Properties	23	Thermal Conductivity	45
Test Methods	23	Specific Heat	46
Flexural Property Comparison	24	Thermal Stability	47
Flexural Properties at Elevated Temperatures	24	Thermogravimetric Analysis (TGA)	47
Shear Properties	26	Thermal Aging	47
Compressive Strength and Modulus	27	Relative Thermal Index (UL)	48
Impact Strength	27	Combustion Properties	50
Izod (Cantilevered Beam) Impact	28	Glow Wire Testing	50
Izod Impact Property Comparison	28	Smoke Density Test (NBS)	51
Charpy (Supported Beam) Impact	29	Vertical Flammability per UL 94	51
Falling Weight Impact Properties	30	Horizontal Burning Test	51
Poisson's Ratio	30	20 MM Vertical Burn Test	51
Long-term Mechanical Properties	31	500 W Vertical Burning Test	52

Electrical Properties	53
Dielectric Breakdown Voltage and Strength -	
ASTM D149	53
Volume Resistivity - ASTM D257	53
Surface Resistivity - ASTM D257	53
Dielectric Constant - ASTM D150	54
Dissipation Factor - ASTM D150	54
UL 746A Short-Term Properties	54
High-Voltage, Low-Current, Dry Arc Resistance -	
ASTM D495	55
Comparative Tracking Index (CTI) – ASTM D3638.	55
High-Voltage Arc-Tracking-Rate (HVTR)	55
Hot Wire Ignition (HWI) - ASTM D3874	56
High-Current Arc Ignition (HAI)	56
High-Voltage Arc Resistance to Ignition	56
UL 746A Properties of Amodel Resins	57
UL Relative Thermal Indices	57
Environmental Resistance	58
Chemical Resistance	58
Chemical Compatibility	62
Gamma Radiation.	62
Design Information	63
Mechanical Design	64
Using Classical Stress/Strain Equations.	67
Limitations of Design Calculations.	67
Deflection Calculations	67
Stress Calculations	67
Reinforcing Fiber Orientation Considerations.	67
Designing for Equivalent Part Stiffness	68
Changing Section Thickness.	68
Adding Ribs to Maintain Stiffness	68
Designing for Sustained Load.	69
Calculating Deflection	69
Calculating Allowable Stress - Creep Rupture.	70
Considering Stress Concentrations	71
Considering Thermal Stresses.	71
Loss of Bolt Tightness Due to Creep	72

Designing for Assembly	73
Interference or Press Fits	73
Calculating the Allowable Interference.	73
Mechanical Fasteners.	74
Self-Tapping Screws	74
Improving Torque Retention	74
Tightening Torque	75
Pull Out Force Calculation.	75
Threaded Inserts.	75
Molded-In Threads	76
Designing with Snap Fits.	76
Tapered Cantilever Beam Equation	77
Designing for Injection Molding.	78
Wall Thickness	78
Wall Thickness Variation	78
Draft Angle	78
Ribs	79
Coring	79
Bosses	79
Undercuts.	80
Secondary Operations	81
Welding.	81
Hot Plate Welding.	81
Vibrational Welding	81
Spin Welding	82
Ultrasonic Welding	82
Adhesive Bonding	83
Coatings and Surface Finishes	84
Vacuum Metallizing	84
Laser Marking.	85
Inkjet Printing	85
Painting	85
Overmolding.	85
Index	87

List of Tables

Table 1: Amodel PPA Base Resin Properties	1	Table 26: UL Criteria for Classifying Materials 5VA or 5VB	52
Table 2: Amodel Resin Nomenclature System	4	Table 27: UL 94 Ratings of Amodel PPA Grades	52
Table 3: Relative Ranking of Selected Properties for Major Amodel PPA Grades	5	Table 28: Dielectric Strength of Selected Amodel Grades	53
Table 4: Glass-Reinforced Grades – Mechanical Properties (US Units)	7	Table 29: Volume and Surface Restivity of Amodel Resins	54
Table 5: Glass-Reinforced Grades – Mechanical Properties (SI Units)	8	Table 30: Dielectric Constant of Amodel Resins	54
Table 6: Glass-Reinforced Grades – Thermal, Electrical, and General Properties	9	Table 31: Dissipation Factor of Amodel Resins	55
Table 7: Toughened Grades – Mechanical Properties (US Units)	10	Table 32: High-Voltage, Low-Current, Dry Arc Resistance Performance Level Categories (PLC)	55
Table 8: Toughened Grades – Mechanical Properties (SI Units)	11	Table 33: Comparative Tracking Index Performance Level Categories	55
Table 9: Toughened Grades – Thermal, Electrical, and General Properties	12	Table 34: High-Voltage Arc-Tracking-Rate Performance Level Categories	56
Table 10: Toughened Glass-Reinforced and Flame Retardant Grades – Mechanical Properties (US Units)	13	Table 35: Hot Wire Ignition Performance Level Categories	56
Table 11: Toughened Glass-Reinforced and Flame Retardant Grades – Mechanical Properties (SI Units)	14	Table 36: High-Current Arc Ignition Performance Level Categories	56
Table 12: Toughened Glass-Reinforced and Flame Retardant Grades – Thermal, Electrical, and General Properties	15	Table 37: High Voltage Arc Resistance to Ignition Performance Level Categories	56
Table 13: Mineral and Mineral/Glass Filled Grades – Mechanical Properties (US Units)	16	Table 38: UL 746A Property PLC for Amodel PPA Grades	57
Table 14: Mineral and Mineral/Glass Filled Grades – Mechanical Properties (SI Units)	17	Table 39: Key to Chemical Resistance Ratings	58
Table 15: Mineral and Mineral/Glass Filled Grades – Thermal, Electrical, and General Properties	18	Table 40: Screening Chemical Resistance Tests – Organic Chemicals	59
Table 16: Izod Test Specimen Dimensions	28	Table 41: Screening Chemical Resistance Tests – Aqueous Chemical Solutions	60
Table 17: Penetration Impact (ASTM D3763) of Impact Modified PPA	30	Table 42: Screening Chemical Resistance Tests – Transportation Fluids	61
Table 18: Poisson's Ratio for Amodel Products	31	Table 43: General Chemical Compatibility Guidelines for Amodel PPA Resins	62
Table 19: Coefficients of Linear Thermal Expansion	44	Table 44: Effect of Gamma Radiation on Amodel AS-1133 HS	62
Table 20: Thermal Conductivity of Amodel PPA Resins	45	Table 45: Design Benefits of Amodel Resin over Metals	63
Table 21: Relative Thermal Indices of Amodel PPA Grades	49	Table 46: Maximum Stress and Deflection Equations	65
Table 22: UL Definitions of GWIT and GWIF	50	Table 47: Area and Moment Equations for Selected Cross Sections	66
Table 23: Glow Wire Results	50	Table 48: Strain Recommendations for Cantilever Snap-Fits	77
Table 24: Smoke Density	51	Table 49: Suitable Automotive Primers	84
Table 25: UL Criteria for Classifying Materials V-0, V-1, or V-2	52	Table 50: Suppliers of Laser Marking Equipment	84
		Table 51: Suppliers of InkJet Printing Equipment	85

List of Figures

Figure 1: Modulus Changes with Temperature	2	Figure 27: Shear Strength of 30%-33% GR Resins.	26
Figure 2: Modulus versus Temperature for Amodel Base Resins	2	Figure 28: Compressive Strength of 30%-33% GR Resins	27
Figure 3: Effect of Moisture on T_g	3	Figure 29: Compressive Strength of A-1000 Resins vs. Temperature	27
Figure 4: Dimension Change vs. Water Immersion Time	3	Figure 30: Compressive Modulus A-1000 Resins vs. Temperature	27
Figure 5: Typical Stress/Strain Curve for Amodel ET-1000.	19	Figure 31: Izod Impact Test Specimen	28
Figure 6: Typical Stress/Strain Curve for Amodel A-1933	20	Figure 32: Izod Impact Strength of 30%-33% GR Resins, ASTM D256.	28
Figure 7: Secant and Tangent Methods for Estimating Modulus	20	Figure 33: Izod Impact of Amodel ET-1000 Compared to PA and PC	29
Figure 8: Tensile Strength of 30%-33% GR Resins	20	Figure 34: Notch Radius Sensitivity of ET-1000 HS and PC.	29
Figure 9: Tensile Modulus of 30%-33% GR Resins	20	Figure 35: Low Temperature Izod of Amodel PPA Grades	29
Figure 10: Tensile Elongation of 30%-33% GR Resins	21	Figure 36: Charpy Impact Test Specimen	29
Figure 11: Tensile Strength of 33% GR PPA vs. Temperature	21	Figure 37: Notched Charpy Impact Strength of 30%-33% GR Resins.	30
Figure 12: Tensile Modulus of 33% GR PPA vs. Temperature	21	Figure 38: Apparent Modulus at 23°C (73°F) and 13.8 MPa (2 kpsi)	33
Figure 13: Tensile Elongation of 33% GR PPA vs. Temperature	21	Figure 39: Apparent Modulus at 23°C (73°F) and 34.5 MPa (5 kpsi)	33
Figure 14: Tensile Strength of GR A-1000 PPA Grades vs. Temperature.	22	Figure 40: Apparent Modulus at 125°C (257°F) and 13.8 MPa (2 kpsi)	33
Figure 15: Tensile Modulus of GR A-1000 PPA Grades vs. Temperature.	22	Figure 41: Apparent Modulus at 125°C (257°F) and 34.5 MPa (5 kpsi)	33
Figure 16: Tensile Elongation of GR A-1000 PPA Grades vs. Temperature.	22	Figure 42: Apparent Modulus at 175°C (347°F) and 13.8 MPa (2 kpsi)	33
Figure 17: Tensile Strength of Mineral/Glass PPA Grades vs. Temperature.	22	Figure 43: Apparent Modulus at 175°C (347°F) and 34.5 MPa (5 kpsi)	33
Figure 18: Tensile Modulus of Mineral/Glass PPA Grades vs. Temperature.	23	Figure 44: Isochronous Stress-Strain of A-1133 HS PPA.	34
Figure 19: Flexural Strength of 30-33% GR Resins	24	Figure 45: Isochronous Stress-Strain of A-1145 HS PPA.	34
Figure 20: Flexural Modulus of 30-33% GR Resins	24	Figure 46: Tensile Creep Rupture of AS-1133 HS	35
Figure 21: Flex Strength of GR PPA Resins vs. Temperature	24	Figure 47: Apparent Flex Modulus at 69 Mpa (10 kpsi) at 23°C (73°F)	35
Figure 22: Flex Modulus of GR PPA Resins vs. Temperature	24	Figure 48: Apparent Flex Modulus at 14 Mpa (2 kpsi) at 83°C (181°F)	35
Figure 23: Flex Strength of GR A-1000 PPA Grades vs. Temperature.	25	Figure 49: Apparent Compressive Modulus of AS-1133 HS	36
Figure 24: Flex Modulus of GR A-1000 PPA Grades vs. Temperature.	25	Figure 50: Flex Fatigue of GR Resins at 23°C (73°F) and 32 Hz	37
Figure 25: Flex Strength of Mineral/Glass PPA Resins vs. Temperature	25	Figure 51: Flex Fatigue of AS-1145 Resin at Elevated Temperature.	37
Figure 26: Flex Modulus of Mineral/Glass PPA Resins vs. Temperature	25	Figure 52: Moisture Absorption of GR Resins	39

Figure 53: Effect of Moisture on Tensile Strength of GR Resins	40	Figure 82: Wall Thickness Transition	78
Figure 54: Effect of Moisture on Flex Modulus of GR Resins	40	Figure 83: Draft - Designing for Mold Release	78
Figure 55: Dimensional Change of 33% GR PPA	40	Figure 84: Draft - Recommended Rib Design	79
Figure 56: Dimensional Change of 40% Mineral Filled PPA.	41	Figure 85: Boss Design - General Guidelines	80
Figure 57: Dimensional Comparison of GR PA 6,6 to GR PPA at 100% RH	41	Figure 86: Thermostat Housing Showing Beads	80
Figure 58: Mold Temperature and Annealing Effects on HDT of Amodel AS-1133 HS.	42	Figure 87: Undercut Diagram	80
Figure 59: HDT of 30% - 33% GR Resins	43	Figure 88: Joint Design for Hot Plate Welding	81
Figure 60: Thermal Conductivity of Glass Reinforced Amodel PPA.	45	Figure 89: Lap Shear Joint Configuration	82
Figure 61: Amodel A-1000 PPA, Specific Heat vs. Temperature	46	Figure 90: Shear Joint Configuration	82
Figure 62: Amodel A-4000, Specific Heat vs. Temperature	46	Figure 91: Typical Energy-Directing Joint Configuration	83
Figure 63: Amodel A-5000, Specific Heat vs. Temperature	46	Figure 92: Lap Shear Bond Strength.	84
Figure 64: Amodel A-6000, Specific Heat vs. Temperature	46	Figure 93: Side Impact Bond Strength	84
Figure 65: Thermogravimetric Analysis of A-1000 in Air	47		
Figure 66: Thermal Aging Comparison - Tensile Strength	47		
Figure 67: Thermal Aging Comparison - Izod Impact	48		
Figure 68: Adding Ribs to Increase Stiffness	69		
Figure 69: Cantilever Beam, Bending Load Example	69		
Figure 70: Tensile Creep Rupture, Amodel A-1133 HS Resin	70		
Figure 71: Stress Concentration Factor at Inside Corners	71		
Figure 72: Thermal Stress Example.	71		
Figure 73: Bolt Torque Retention.	72		
Figure 74: Designing for Mechanical Fasteners	74		
Figure 75: Boss Design for Self-Tapping Screws	74		
Figure 76: Torque Developed During Screw Installation	75		
Figure 77: Boss Design for Ultrasonic Inserts	75		
Figure 78: Cantilever Type Snap Fit.	76		
Figure 79: Boss Design for Self-Tapping Screws	76		
Figure 80: Snap Fit Design Using Tapered Beam	77		
Figure 81: Proportionality Constant (K) for Tapered Beam	77		

Amodel Polyphthalamide (PPA) Resins

Amodel polyphthalamide (PPA) resins were commercialized in 1991. Polyphthalamide resin technology can produce a wide range of polymers that includes both semi-crystalline and amorphous resins. Since 1991, several base polymer formulations have been commercialized to meet specific industry needs. All of the commercial Amodel products are semi-crystalline.

The semi-crystalline grades of Amodel PPA resins have excellent mechanical properties, outstanding dimensional stability, exceptional elevated thermal performance, and good processing characteristics. Amodel resins bridge the cost/performance gap between the high-volume, moderate-performance engineering resins, such as thermoplastic polyesters and aliphatic nylons, and the low-volume, high-cost specialty thermoplastics, such as polyetheretherketone (PEEK).

The Amodel product portfolio contains well over 100 different grades. Each grade has been designed to have a unique balance of properties that are important for specific application and processing requirements. Applications for Amodel PPA have been developed in a wide range of industries including automotive/transportation, industrial equipment, water handling, telecommunications, electrical/electronic, coatings and composites, food service, and consumer goods.

This manual is intended to be an easy to use reference tool for designers and fabricators interested in Amodel PPA as a solution to their material needs. It includes property data for select grades of the portfolio as well as part design and processing recommendations.

Chemistry

Amodel resins are classified in the general chemical family known as polyamides. Polyamides may be produced by the reaction of a difunctional organic acid with a difunctional amine, or the self-condensation of either an ω -amino acid or a lactam. Polyamides can be produced from a wide variety of acids and amines, and a number of polyamides are commercially important.

A naming convention for polyamides has evolved. The convention is to name the polyamide using the number of carbon atoms in the monomers with the diamine

Table 1: Amodel PPA Base Resin Properties

Base Resin	T _g		T _m	
	°C	°F	°C	°F
A-1000	123	253	313	595
A-4000	100	212	325	617
A-5000	89	192	294	561
A-6000	88	190	310	590

component first. Thus, a polyamide made from hexamethylene diamine and adipic acid is called polyamide 66 or nylon 66, and one made from hexamethylene diamine and dodecanedioic acid would be nylon 6,12.

When an aromatic diacid is used instead of an aliphatic diacid, the nomenclature is modified to reflect the isomeric form of the aromatic diacid, and the term polyphthalamide may be used to distinguish these polymers from those of solely aliphatic raw materials.

Polyamide 6,T produced by the condensation of hexamethylene diamine with terephthalic acid, has long been recognized for its excellent dimensional stability, low moisture absorption, high strength, and heat resistance. The fundamental problem preventing its commercialization has been that its high crystalline melting point of 370°C (698°F) is above its thermal decomposition temperature. Therefore, it cannot be processed by most conventional melt processing techniques, such as injection molding or extrusion. In addition, its melting point, among other factors, complicates the polymerization process.

The basic polyamide 6,T technology has been modified by adding comonomers to produce the Amodel family of polyphthalamide (PPA) resins which are composed of proprietary compositions of matter. Varying the amount and nature of the comonomers leads to a family of resins. All of these resins have melting points lower than polyamide 6,T and exhibit rapid crystallization. The thermal properties of the Amodel PPA base resins are shown in Table 1.

These base resins when combined with mineral, glass-fiber, and/or other compounding ingredients provide a wide range of injection molding compounds that offer an excellent balance of processing and thermal/mechanical performance. Compounds based on A-1000 base resin require molds using oil for temperature control, but compounds based on the other base resins can be processed using water controlled molds.

Crystallinity

Thermoplastics are often divided into two classes, amorphous and semi-crystalline. One of the major differences between amorphous and semi-crystalline polymers is the way their properties change in response to changes in temperature. Figure 1 shows a typical response of modulus to temperature change for amorphous and semi-crystalline polymers.

When the temperature is raised, the modulus of amorphous polymers generally decreases slowly until the glass transition temperature (T_g) is reached. At temperatures above the T_g , the modulus decreases rapidly. Therefore, amorphous thermoplastics are rarely used at temperatures higher than their glass transition temperature.

In the case of semi-crystalline polymers, the modulus also gradually decreases with increasing temperature. At or near the glass transition temperature, the modulus decreases rapidly to a lower but still useful level. Continuing to increase the temperature causes the modulus to remain at or near this new level (the crystalline plateau) until the melting point temperature (T_m) is reached. At T_m , the modulus decreases rapidly again. Semi-crystalline polymers are often used at temperatures above their glass transition temperatures, but below their melting points, particularly when they are modified with glass fibers and/or mineral fillers.

When semi-crystalline polymers are processed, the amount of crystallinity can be affected by processing conditions. For example, Amodel A-1000 PPA based products require mold surface temperatures of at least 135°C (275°F) for development of the maximum amount of crystallinity during injection molding. Products based on Amodel A-4000 or A-6000 base resin will give high crystallinity at mold temperatures of about 80°C (176°F).

Above the T_m , a semi-crystalline polymer melts, changing from the solid state to the liquid state.

The thermal capability of a semi-crystalline polymer is defined to a large extent by its T_g and T_m , as these values indicate the temperature ranges where the polymer has high stiffness (below T_g), moderate stiffness (between T_g and T_m), or no useful stiffness (above T_m). Figure 2 shows the modulus versus temperature behavior of the Amodel base resins as measured by dynamic mechanical analysis (DMA).

Figure 1: Modulus Changes with Temperature

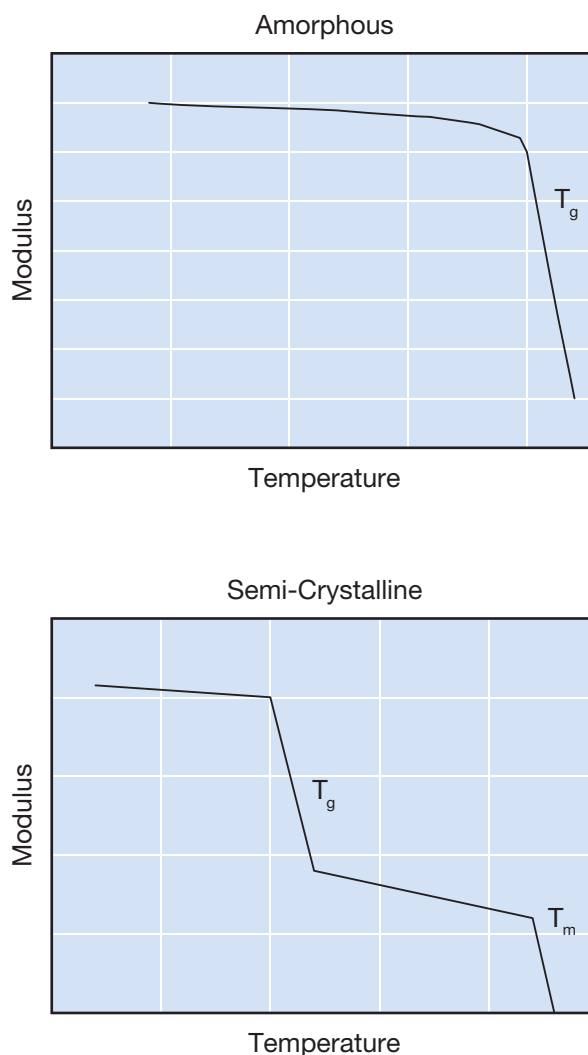
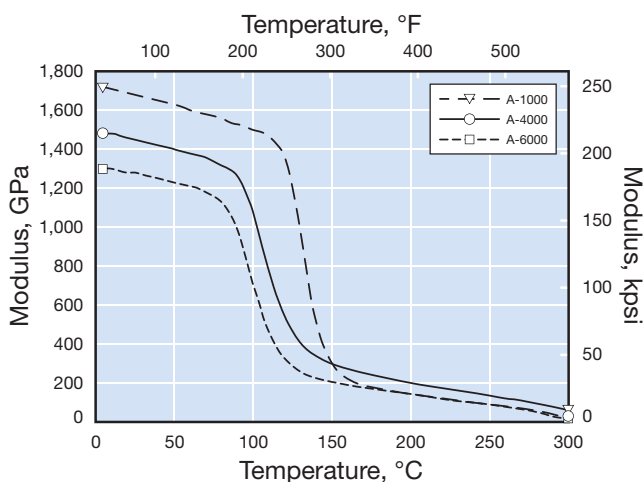


Figure 2: Modulus versus Temperature for Amodel Base Resins



Moisture Effects

Like other polymers, polyphthalamide resins absorb moisture from the environment. In general, polyphthalamides will absorb less water than aliphatic polyamides, like PA 6,6, and they will absorb the moisture at a slower rate.

When an article made from Amodel grade based on A-1000 base resin reaches equilibrium with a 100% relative humidity (RH) atmosphere, the increase in weight due to moisture absorption will be roughly 5% to 6% of the polyphthalamide resin weight.

Figure 3 compares the glass transition temperatures of Amodel A-1000 resin and PA 6,6 at a range of moisture contents. These materials absorb moisture at different rates and they have different maximum moisture adsorption amounts. The most useful and practical comparison is achieved by plotting the T_g versus the equilibrium moisture content at various relative humidities.

Comparing dry PA 6,6 to dry Amodel A-1000 resin, Amodel resin has a T_g advantage of about 60°C (108°F). If the comparison is made at the 50% RH equivalent moisture content, the T_g advantage of Amodel resin is about 89°C (160°F). The exceptional dimensional stability and property retention of Amodel polyphthalamide is due largely to the higher T_g and the fact that the T_g remains well above room temperature, even at the moisture content appropriate for 100% RH. The T_g of PA 6,6, on the other hand, falls to -15°C (5°F) at moisture contents consistent with equilibria at 50% to 60% RH.

Figure 4 compares the dimensional change of Amodel A-1000 resin to that of PA 6,6 after being immersed in water at 23°C (73°F). Results shown are for 3.2 mm (0.125 inch) thick plaques. After one year (about 8,800 hours), the dimensional change of the PA resin is approximately three times that of the PPA resin.

Not only do polyphthalamides absorb less moisture than typical polyamides, they do so much more slowly. The diffusion coefficient for water in Amodel A-1000 resin is approximately 20% of that for PA 6,6 at 23°C (73°F).

Figure 3: Effect of Moisture on T_g

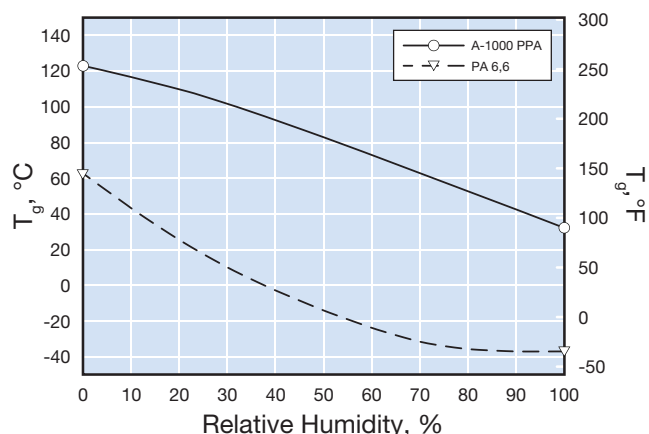
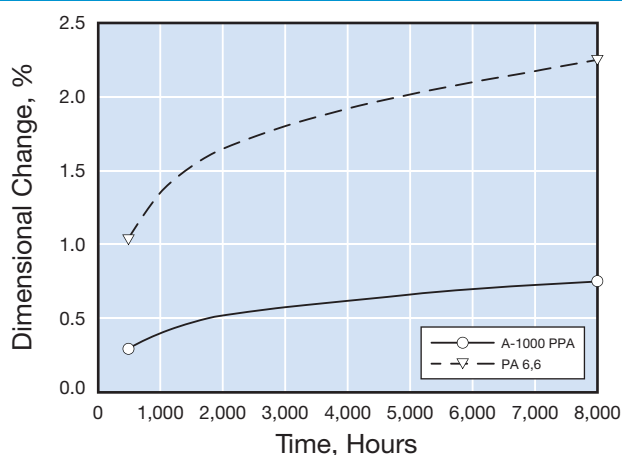


Figure 4: Dimension Change vs. Water Immersion Time



Amodel Resin Property Tables

Amodel PPA resins are typically combined with reinforcements, fillers, impact modifiers, flame retardants, colorants, and other additives to achieve a wide range of performance profiles. Currently the family contains over 100 commercial grades. This document provides detailed property information on 12 grades that were selected to be representative of the product family. Your Solvay representative can help you select the most cost-effective material for your application.

The base polymers are translucent white due to crystallinity, and the natural color of a specific product will vary depending on the additives used. Most grades are available in natural and black. Other colors can often be provided. Discuss your color requirements with your Solvay representative.

Nomenclature

The grade designations used for Amodel PPA resins are designed to communicate important compositional information. The nomenclature system is illustrated in Table 2.

Table 2: Amodel Resin Nomenclature System

Position	Characteristic	Meaning/Example
1st letter	Product family	A = Amodel E = extra
Next letter(s)	Optional descriptor	E = electrical/electronic F = flame retardant P = paintable/plateable S = thick-wall parts (>3 mm) T = toughened
-	Hyphen	
1st digit	Base resin	1 = A-100x base resin 4 = A-400x base resin 5 = A-500x base resin 6 = A-600x base resin 9 = A-900x base resin
2nd digit	Filler or reinforcement type	0 = unfilled 1 = glass 2 = mineral A 3 = mineral A + glass 4 = mineral B 5 = mineral B + glass 6 = carbon or graphite fiber 9 = glycol resistant
3rd and 4th digits	Filler or reinforcement amount	33 = 33% by weight 45 = 45% by weight, etc.
Space		
Next 1 or 2 letters	Suffix	HN = heat stabilized, not lubricated HS = heat stabilized HSL = heat stabilized and lubricated L = lubricated, not heat stabilized NL = neither lubricated nor heat stabilized VO Z = UL 94 VO at 0.8mm (0.032 inch)
Space		
Next 2 letters	Color Code	NT = natural, unpigmented BK = black WH = white, etc.

Product Selection

Solvay Specialty Polymers has the broadest and deepest portfolio of PPA resins in the industry. Table 3 shows the relative performance of several Amodel products to assist you in selecting the right product for your specific application. The products listed here are a good representation of the portfolio. However, there are many other grades not listed and one of these may

be the perfect fit for you. It is recommended that you contact a Solvay Specialty Polymers representative before making a final product selection decision. Additional product selection resources and technical data can be found on the website.

Table 3: Relative Ranking of Selected Properties for Major Amodel PPA Grades⁽¹⁾

	Strength at RT	Stiffness at RT	Stiffness at 100°C	Impact - Notched	Deflection Temperature	Specific Gravity
Glass-Reinforced Grades						
A-1133 HS	9	6	8	4	7	6
A-1145 HS	9	8	8	7	7	7
A-6135 HN	8	7	6	5	8	4
A-4133 HS	7	6	5	4	9	4
Toughened Grades						
AT-1002 HS	2	2	2	8	2	1
ET-1000 HS	1	1	1	9	1	1
Toughened Glass-Reinforced Grades						
AT-1116 HS	5	4	4	7	4	3
AT-6115 HS	4	3	3	6	4	3
Flame Retardant Grades						
AFA-6133 V0 Z	6	8	7	5	6	8
Mineral and Mineral/Glass Filled Grades						
A-1240 L	3	4	4	2	3	6
A-1565 HS	4	9	9	1	5	10
AS-1566 HS	8	9	9	3	6	9

⁽¹⁾ Properties ranked from 1 to 10, 10 being highest

Property Data

Typical Properties

The typical property data contained in the following short term property tables fall within the normal range of product properties. Actual properties of individual batches will vary within specification limits.

These values should not be used to establish specification limits, nor should they be used alone as the basis for part design.

Accelerated Moisture Conditioning

In general, polyamides absorb moisture from the atmosphere, and the absorbed moisture can affect some properties. To provide the design engineer with more relevant property information, polyamide suppliers customarily list properties as molded (dry) and also after moisture absorption. The convention is to list a 50% RH value, that is intended to provide the property value after the material has achieved equilibrium with a 50% relative humidity environment. This convention is appropriate for polyamide 6,6, because that polymer absorbs moisture quickly and many properties change significantly due to moisture.

This approach is really not appropriate for polyphthalamides, because these materials absorb moisture slowly and most properties don't change significantly due to moisture content. However to be consistent with the industry, values after moisture absorption were generated. The correct way of preparing the samples with absorbed moisture is to place them in a 50% RH environment and wait until constant weight, i.e. moisture equilibrium, is reached. The moisture absorption rate of Amodel PPA is so slow, that over two years would be required. So a method of accelerating the moisture absorption was developed.

The accelerated moisture conditioning method used was to boil the test specimens in an aqueous solution containing 80 grams of potassium acetate per 100 grams of water for 96 hours. This procedure was developed empirically to approximate the moisture uptake of samples that were placed in a constant humidity chamber until equilibrium was achieved. Because the temperatures involved in this conditioning are between 100°C and 130°C (212°F and 266°F), some annealing takes place, and the 50% RH modulus values are sometimes a few percent higher than the "dry, as molded" values.

In addition, exposure to the aqueous conditioning media at these relatively high temperatures combined with an exposure time of 96 hours results in some hydrolysis of the glass/resin matrix interface. In many cases, the properties that depend on glass/resin adhesion, such as tensile strength, notched Izod, etc., are about 10% lower than would have been obtained had the samples been allowed to condition to 50% RH in air at room temperature.

Table 4: Glass-Reinforced Grades – Mechanical Properties (US Units)

Property	Temperature	Method		Units	A-1133	A-1145	A-6135	AS-4133
		ASTM	ISO		HS	HS	HN	HS
Tensile Strength	23°C (73°F)	D638		kpsi	32.0	37.5	29.4	29.0
Tensile Strength 50% RH	23°C (73°F)	D638		kpsi	28.0	33.0	25.5	25.0
Tensile Strength	23°C (73°F)		527	kpsi	33.8	38.1	30.6	30.6
	100°C (212°F)		527	kpsi	21.5	25.1	17.6	18.1
	150°C (302°F)		527	kpsi	11.5	12.3	13.4	12.7
	175°C (347°F)		527	kpsi	10.4	11.0	11.9	11.5
Tensile Elongation	23°C (73°F)	D638		%	2.5	2.6	1.9	2.5
Tensile Elongation 50% RH	23°C (73°F)	D638		%	2.1	2.1	2.1	2.2
Tensile Elongation	23°C (73°F)		527	%	2.5	2.7	2.0	2.6
	100°C (212°F)		527	%	2.9	2.5	4.3	4.3
	150°C (302°F)		527	%	8.7	7.2	4.9	6.6
	175°C (347°F)		527	%	8.5	6.5	4.7	6.6
Tensile Modulus	23°C (73°F)	D638		Mpsi	1.90	2.50	2.00	1.70
Tensile Modulus 50% RH	23°C (73°F)	D638		Mpsi	1.90	2.50	1.77	1.70
Tensile Modulus	23°C (73°F)		527	Mpsi	1.94	2.44	1.67	1.83
	100°C (212°F)		527	Mpsi	1.57	1.62	1.06	0.99
	150°C (302°F)		527	Mpsi	0.97	1.16	0.91	0.77
	175°C (347°F)		527	Mpsi	0.62	0.78	0.77	0.70
Flexural Strength	23°C (73°F)	D790		kpsi	46.0	52.6	45.0	42.0
Flexural Strength 50% RH	23°C (73°F)	D790		kpsi	36.9	42.7	36.1	35.0
Flexural Strength	23°C (73°F)		178	kpsi	46.3	54.7	43.5	42.9
	100°C (212°F)		178	kpsi	33.0	38.7	24.7	25.6
	150°C (302°F)		178	kpsi	13.5	16.1	17.8	16.1
	175°C (347°F)		178	kpsi	11.5	13.7	16.2	14.4
Flexural Modulus	23°C (73°F)	D790		Mpsi	1.65	2.00	1.65	1.60
Flexural Modulus 50% RH	23°C (73°F)	D790		Mpsi	1.65	2.00	1.59	1.60
Flexural Modulus	23°C (73°F)		178	Mpsi	1.68	2.31	1.65	1.51
	100°C (212°F)		178	Mpsi	1.42	1.89	0.96	1.04
	150°C (302°F)		178	Mpsi	0.58	0.78	0.71	0.67
	175°C (347°F)		178	Mpsi	0.52	0.71	0.67	0.61
Shear Strength	23°C (73°F)	D732		kpsi	14.7	15.6	12.7	13.0
Shear Strength 50% RH	23°C (73°F)	D732		kpsi	12.9	13.3	10.7	11.0
Compressive Strength	23°C (73°F)	D695		kpsi	26.9	28.1	21.4	26.0
Poisson's Ratio	23°C (73°F)				0.41	0.41	0.39	0.41
Izod Impact, Notched	23°C (73°F)	D256		ft-lb/in	1.5	2.1	1.6	1.5
Izod Impact, Notched 50% RH	23°C (73°F)	D256		ft-lb/in	1.1	1.9	1.3	1.5
Izod Impact, Unnotched	23°C (73°F)	D4812		ft-lb/in	14	21	15	19
Izod Impact, Notched	23°C (73°F)		180/1A	ft-lb/in ²	4.2	4.9	4.3	4.6
Izod Impact, Unnotched	23°C (73°F)		180/1U	ft-lb/in ²	23	29	30	28
Charpy Impact	23°C (73°F)		179/1eA	ft-lb/in ²	4.5	4.9	4.4	5.1
Charpy Impact, Unnotched	23°C (73°F)		179/1eU	ft-lb/in ²	35	44	28	32
Rockwell Hardness	23°C (73°F)	D785		R	125	125	125	124

Table 5: Glass-Reinforced Grades – Mechanical Properties (SI Units)

Property	Temperature	Method		Units	A-1133	A-1145	A-6135	AS-4133
		ASTM	ISO		HS	HS	HN	HS
Tensile Strength	23°C (73°F)	D638		MPa	221	259	202	200
Tensile Strength 50% RH	23°C (73°F)	D638		MPa	193	228	178	172
Tensile Strength	23°C (73°F)		527	MPa	233	263	211	211
	100°C (212°F)		527	MPa	148	173	121	125
	150°C (302°F)		527	MPa	80	85	93	87
	175°C (347°F)		527	MPa	72	76	82	79
Tensile Elongation	23°C (73°F)	D638		%	2.5	2.6	1.9	2.5
Tensile Elongation 50% RH	23°C (73°F)	D638		%	2.1	2.1	2.1	2.2
Tensile Elongation	23°C (73°F)		527	%	2.5	2.7	2.0	2.6
	100°C (212°F)		527	%	2.9	2.5	4.3	4.3
	150°C (302°F)		527	%	8.7	7.2	4.9	6.6
	175°C (347°F)		527	%	8.5	6.5	4.7	6.6
Tensile Modulus	23°C (73°F)	D638		GPa	13.1	17.2	13.8	11.7
Tensile Modulus 50% RH	23°C (73°F)	D638		GPa	13.1	17.2	12.2	11.7
Tensile Modulus	23°C (73°F)		527	GPa	13.4	16.8	11.5	12.6
	100°C (212°F)		527	GPa	10.8	11.2	7.3	6.8
	150°C (302°F)		527	GPa	6.7	8.0	6.3	5.3
	175°C (347°F)		527	GPa	4.3	5.4	5.3	4.8
Flexural Strength	23°C (73°F)	D790		MPa	317	363	310	290
Flexural Strength 50% RH	23°C (73°F)	D790		MPa	254	294	249	241
Flexural Strength	23°C (73°F)		178	MPa	319	377	300	296
	100°C (212°F)		178	MPa	227	267	171	176
	150°C (302°F)		178	MPa	93	111	123	111
	175°C (347°F)		178	MPa	80	95	112	100
Flexural Modulus	23°C (73°F)	D790		GPa	11.4	13.8	11.4	11.0
Flexural Modulus 50% RH	23°C (73°F)	D790		GPa	11.4	13.8	10.9	11.0
Flexural Modulus	23°C (73°F)		178	GPa	11.6	15.9	11.4	10.4
	100°C (212°F)		178	GPa	9.8	13.0	6.6	7.2
	150°C (302°F)		178	GPa	4.0	5.4	4.9	4.6
	175°C (347°F)		178	GPa	3.6	4.9	4.6	4.2
Shear Strength	23°C (73°F)	D732		MPa	101	108	88	90
Shear Strength 50% RH	23°C (73°F)	D732		MPa	89	92	74	76
Compressive Strength	23°C (73°F)	D695		MPa	185	194	148	179
Poisson's Ratio	23°C (73°F)				0.41	0.41	0.39	0.41
Izod Impact, Notched	23°C (73°F)	D256		J/m	80	110	85	80
Izod Impact, Notched 50% RH	23°C (73°F)	D256		J/m	60	100	70	70
Izod Impact, Unnotched	23°C (73°F)	D4812		J/m	770	1105	780	1030
Izod Impact, Notched	23°C (73°F)		180/1A	kJ/m ²	8.8	10.3	9.1	9.7
Izod Impact, Unnotched	23°C (73°F)		180/1U	kJ/m ²	49	61	62	59
Charpy Impact	23°C (73°F)		179/1eA	kJ/m ²	9.5	10.3	9.2	10.7
Charpy Impact, Unnotched	23°C (73°F)		179/1eU	kJ/m ²	73	93	60	68
Rockwell Hardness	23°C (73°F)	D785		R scale	125	125	125	124

Table 6: Glass-Reinforced Grades – Thermal, Electrical, and General Properties

Property	Method		Units	A-1133	A-1145	A-6135	AS-4133
	ASTM	ISO		HS	HS	HN	HS
Thermal							
Deflection Temperature Under Load, 264 psi	D648		°C	285	287	291	300
			°F	545	549	556	572
Deflection Temperature Under Load, 1.8 MPa		75AF	°C	280	281	288	294
			°F	536	538	550	561
Vicat Softening Temperature	D1525	306	°C	303	304	301	314
			°F	577	580	573	597
Melting Point	D3418	11357-3	°C	313	310	310	327
			°F	595	590	590	620
Flammability, 3.2 mm (1⁄8 inch) bar	UL-94			HB	HB	HB	HB
Electrical							
Dielectric Strength at 3.2 mm (1⁄8 inch)	D149		V/mil	533	584	—	510
			kV/mm	21	23	—	21
Dielectric Strength at 1.6 mm (1⁄16 inch)	D149		V/mil	813	—	—	813
			kV/mm	32	—	—	32
Volume Resistivity	D257		ohm-cm	1x10 ¹⁶	1x10 ¹⁶	—	1x10 ¹⁶
Surface Resistivity	D257		ohms	1x10 ¹⁵	—	—	1x10 ¹⁵
Comparative Tracking Index	D3638		volts	550	550	—	>600
Dielectric Constant at 60 Hz	D150			4.4	4.6	—	3.8
Dielectric Constant at 100 Hz	D150			5.1	—	—	4.6
Dielectric Constant at 10 ⁶ Hz	D150			4.2	4.4	—	3.6
Dielectric Constant at 10 ⁹ Hz	D150			3.7	—	—	3.6
Dissipation Factor at 60 Hz	D150			0.005	0.005	—	0.004
Dissipation Factor at 10 ⁶ Hz	D150			0.017	0.016	—	0.012
Dissipation Factor at 10 ⁹ Hz	D150			0.016	—	—	0.013
General							
Specific Gravity	D792	1183A		1.48	1.59	1.45	1.45
Moisture Absorption, 24 hours	D570	62	%	0.2	0.1	0.3	0.3
Mold Shrinkage, Flow Direction	D955	294-4	%	0.4	0.2	0.6	0.5
Mold Shrinkage, Transverse Direction	D955	294-4	%	0.8	0.6	0.9	1.0

Table 7: Toughened Grades – Mechanical Properties (US Units)

Property	Temperature	Method		Units	AT-1002	ET-1000
		ASTM	ISO		HS	HS
Tensile Strength	23°C (73°F)	D638		kpsi	12.1	10.0
Tensile Strength 50% RH	23°C (73°F)	D638		kpsi	11.1	9.1
Tensile Stress at Yield	23°C (73°F)		527	kpsi	10.9	10.2
Tensile Stress at Break	23°C (73°F)		527	kpsi	9.9	8.7
Tensile Stress at Yield	100°C (212°F)		527	kpsi	5.6	4.9
Tensile Stress at Break	100°C (212°F)		527	kpsi		
Tensile Elongation at Yield	23°C (73°F)	D638		%	5.0	6.0
Tensile Elongation at Break	23°C (73°F)	D638		%	10-12	20.0
Tensile Elongation at Break 50% RH	23°C (73°F)	D638		%	30.0	18
Tensile Strain at Yield	23°C (73°F)		527	%	5.0	5.0
Tensile Strain at Break	23°C (73°F)		527	%	10.0	7.0
Tensile Strain at Yield	100°C (212°F)		527	%	3.7	4.3
Tensile Strain at Break	100°C (212°F)		527	%	>95	>95
Tensile Modulus	23°C (73°F)	D638		kpsi	400	350
Tensile Modulus 50% RH	23°C (73°F)	D638		kpsi	400	350
Tensile Modulus	23°C (73°F)		527	kpsi	400	350
Tensile Modulus	100°C (212°F)		527	kpsi	305	290
Flexural Strength	23°C (73°F)	D790		kpsi	14.9	15.8
Flexural Strength 50% RH	23°C (73°F)	D790		kpsi	10.6	12.4
Flexural Strength	23°C (73°F)		178	kpsi	11.5	10.2
Flexural Strength	100°C (212°F)		178	kpsi	7.2	6.4
Flexural Modulus	23°C (73°F)	D790		kpsi	320	330
Flexural Modulus 50% RH	23°C (73°F)	D790		kpsi	330	310
Flexural Modulus	23°C (73°F)		178	kpsi	330	260
Flexural Modulus	100°C (212°F)		178	kpsi	250	190
Shear Strength	23°C (73°F)	D732		kpsi	9.3	8.5
Shear Strength 50% RH	23°C (73°F)	D732		kpsi	8.3	
Poisson's Ratio	23°C (73°F)				0.38	0.39
Izod Impact, Notched	23°C (73°F)	D256		ft-lb/in	2.4	17.0
Izod Impact, Notched 50% RH	23°C (73°F)	D256		ft-lb/in	2.6	20.0
Izod Impact, Unnotched	23°C (73°F)	D4812		ft-lb/in	No break	No break
Izod Impact, Notched	23°C (73°F)		180/1A	ft-lb/in ²	6.0	34.9
Izod Impact, Unnotched	23°C (73°F)		180/1U	ft-lb/in ²	84	No break
Charpy Impact	23°C (73°F)		179/1eA	ft-lb/in ²	6.4	36.9
Charpy Impact, Unnotched	23°C (73°F)		179/1eU	ft-lb/in ²	No break	No break
Rockwell Hardness	23°C (73°F)	D785		R	119	120

Table 8: Toughened Grades – Mechanical Properties (SI Units)

Property	Temperature	Method		Units	AT-1002	ET-1000
		ASTM	ISO		HS	HS
Tensile Strength	23°C (73°F)	D638		MPa	83	69
Tensile Strength 50% RH	23°C (73°F)	D638		MPa	76	63
Tensile Stress at Yield	23°C (73°F)		527	MPa	75	70
Tensile Stress at Break	23°C (73°F)		527	MPa	68	60
Tensile Stress at Yield	100°C (212°F)		527	MPa	39	34
Tensile Stress at Break	100°C (212°F)		527	MPa		
Tensile Elongation at Yield	23°C (73°F)	D638		%	5.0	6.0
Tensile Elongation at Break	23°C (73°F)	D638		%	10-12	20.0
Tensile Elongation at Break 50% RH	23°C (73°F)	D638		%	30.0	18.0
Tensile Strain at Yield	23°C (73°F)		527	%	5.0	5.0
Tensile Strain at Break	23°C (73°F)		527	%	10.0	7.0
Tensile Strain at Yield	100°C (212°F)		527	%	3.7	4.3
Tensile Strain at Break	100°C (212°F)		527	%	>95	>95
Tensile Modulus	23°C (73°F)	D638		GPa	2.8	2.4
Tensile Modulus 50% RH	23°C (73°F)	D638		GPa	2.8	2.4
Tensile Modulus	23°C (73°F)		527	GPa	2.8	2.4
Tensile Modulus	100°C (212°F)		527	GPa	2.1	2.0
Flexural Strength	23°C (73°F)	D790		MPa	103	109
Flexural Strength 50% RH	23°C (73°F)	D790		MPa	73	85
Flexural Strength	23°C (73°F)		178	MPa	80	70
Flexural Strength	100°C (212°F)		178	MPa	50	44
Flexural Modulus	23°C (73°F)	D790		GPa	2.2	2.3
Flexural Modulus 50% RH	23°C (73°F)	D790		GPa	2.3	2.2
Flexural Modulus	23°C (73°F)		178	GPa	2.3	1.8
Flexural Modulus	100°C (212°F)		178	GPa	1.8	1.3
Shear Strength	23°C (73°F)	D732		MPa	64	59
Shear Strength 50% RH	23°C (73°F)	D732		MPa	57	
Poisson's Ratio	23°C (73°F)				0.38	0.39
Izod Impact, Notched	23°C (73°F)	D256		J/m	130	905
Izod Impact, Notched 50% RH	23°C (73°F)	D256		J/m	140	1065
Izod Impact, Unnotched	23°C (73°F)	D4812		J/m	No break	No break
Izod Impact, Notched	23°C (73°F)		180/1A	kJ/m ²	13	74
Izod Impact, Unnotched	23°C (73°F)		180/1U	kJ/m ²	177	No break
Charpy Impact	23°C (73°F)		179/1eA	kJ/m ²	14	78
Charpy Impact, Unnotched	23°C (73°F)		179/1eU	kJ/m ²	No break	No break
Rockwell Hardness	23°C (73°F)	D785			119	120

Table 9: Toughened Grades – Thermal, Electrical, and General Properties

Property	Method		Units	A-1002 HS	ET-1000 HS
	ASTM	ISO			
Thermal					
Deflection Temperature Under Load, 264 psi	D648		°C	121	120
			°F	250	248
Deflection Temperature Under Load, 1.8 MPa		75AF	°C	118	109
			°F	244	228
Vicat Softening Temperature	D1525	306	°C	286	283
			°F	547	542
Melting Point	D3418	11357-3	°C	315	310
			°F	599	590
Flammability, 3.2 mm (1/8 inch) Bar	UL-94			HB	HB
Electrical					
Dielectric Strength at 3.2 mm (1/8 inch)	D149		V/mil	431	—
			kV/mm	17	—
Volume Resistivity	D257		ohm-cm	1x10 ¹⁶	—
Surface Resistivity	D257		ohm	8x10 ¹³	—
Comparative Tracking Index	D3638		volts	>600	—
Dielectric Constant at 60 Hz	D150			3.3	—
Dielectric Constant at 10 ⁶ Hz	D150			3.3	—
Dissipation Factor at 60 Hz	D150			0.004	—
Dissipation Factor at 10 ⁶ Hz	D150			0.016	—
General					
Specific Gravity	D792	1183A		1.13	1.13
Moisture Absorption, 24 hours	D570	62	%	0.5	0.7
Mold Shrinkage, Flow Direction	D955	294-4	%	2.0	1.5
Mold Shrinkage, Transverse Direction	D955	294-4	%	2.1	1.5

Table 10: Toughened Glass-Reinforced and Flame Retardant Grades – Mechanical Properties (US Units)

Property	Temperature	Method		Units	AFA-6133		
		ASTM	ISO		AT-1116 HS	AT-6115 HS	VO Z
Tensile Strength	23°C (73°F)	D638		kpsi	23.3	17.7	28.8
Tensile Strength 50% RH	23°C (73°F)	D638		kpsi	19.0	13.9	24.1
Tensile Strength	23°C (73°F)		527	kpsi	23.2	16.5	27.0
	100°C (212°F)		527	kpsi	9.5	9.9	16.5
	150°C (302°F)		527	kpsi			10.9
	175°C (347°F)		527	kpsi			9.2
Tensile Elongation	23°C (73°F)	D638		%	3.8	3.4	1.7
Tensile Elongation 50% RH	23°C (73°F)	D638		%	2.8	5.3	1.7
Tensile Elongation	23°C (73°F)		527	%	3.7	3.9	1.6
	100°C (212°F)		527	%	4.2	7.7	2.4
	150°C (302°F)		527	%			5.1
	175°C (347°F)		527	%			4.9
Tensile Modulus	23°C (73°F)	D638		Mpsi	0.94	0.78	2.33
Tensile Modulus 50% RH	23°C (73°F)	D638		Mpsi	1.03	0.97	1.99
Tensile Modulus	23°C (73°F)		527	Mpsi	1.00	0.78	2.10
	100°C (212°F)		527	Mpsi	0.97	0.45	1.33
	150°C (302°F)		527	Mpsi			0.86
	175°C (347°F)		527	Mpsi			0.74
Flexural Strength	23°C (73°F)	D790		kpsi	32.8	24.0	32.5
Flexural Strength 50% RH	23°C (73°F)	D790		kpsi	29.1	16.7	33.2
Flexural Strength	23°C (73°F)		178	kpsi	28.6	24.7	37.6
	100°C (212°F)		178	kpsi	20.5	9.7	23.3
	150°C (302°F)		178	kpsi			14.6
	175°C (347°F)		178	kpsi			12.7
Flexural Modulus	23°C (73°F)	D790		Mpsi	0.87	0.64	1.90
Flexural Modulus 50% RH	23°C (73°F)	D790		Mpsi	0.90	0.50	1.93
Flexural Modulus	23°C (73°F)		178	Mpsi	0.97	0.62	1.83
	100°C (212°F)		178	Mpsi	0.72	0.34	1.17
	150°C (302°F)		178	Mpsi			0.72
	175°C (347°F)		178	Mpsi			0.67
Shear Strength	23°C (73°F)	D732		kpsi	10.1	8.2	11.6
Shear Strength 50% RH	23°C (73°F)	D732		kpsi	9.5	6.4	9.0
Compressive Strength	23°C (73°F)	D695		kpsi	18.0	14.5	21.1
Poisson's Ratio	23°C (73°F)				0.40	0.39	0.37
Izod Impact, Notched	23°C (73°F)	D256		ft-lb/in	1.8	1.7	1.6
Izod Impact, Notched 50% RH	23°C (73°F)	D256		ft-lb/in	0.9	1.5	1.5
Izod Impact, Unnotched	23°C (73°F)	D4812		ft-lb/in	18	16	13
Izod Impact, Notched	23°C (73°F)		180/1A	ft-lb/in ²	3.8	5.5	3.9
Izod Impact, Unnotched	23°C (73°F)		180/1U	ft-lb/in ²	25	26	21
Charpy Impact	23°C (73°F)		179/1eA	ft-lb/in ²	4.3	5.2	6.6
Charpy Impact, Unnotched	23°C (73°F)		179/1eU	ft-lb/in ²	41	36	22
Rockwell Hardness	23°C (73°F)	D785		R scale	124	116	125

Table 11: Toughened Glass-Reinforced and Flame Retardant Grades – Mechanical Properties (SI Units)

Property	Temperature	Method		Units	AFA-6133		
		ASTM	ISO		AT-1116 HS	AT-6115 HS	VO Z
Tensile Strength	23°C (73°F)	D638		MPa	161	122	199
Tensile Strength 50% RH	23°C (73°F)	D638		MPa	131	96	166
Tensile Strength	23°C (73°F)		527	MPa	160	114	186
	100°C (212°F)		527	MPa	66	68	114
	150°C (302°F)		527	MPa			75
	175°C (347°F)		527	MPa			63
Tensile Elongation	23°C (73°F)	D638		%	3.8	3.4	1.7
Tensile Elongation 50% RH	23°C (73°F)	D638		%	2.8	5.3	1.7
Tensile Elongation	23°C (73°F)		527	%	3.7	3.9	1.6
	100°C (212°F)		527	%	4.2	7.7	2.4
	150°C (302°F)		527	%			5.1
	175°C (347°F)		527	%			4.9
Tensile Modulus	23°C (73°F)	D638		GPa	6.5	5.4	16.1
Tensile Modulus 50% RH	23°C (73°F)	D638		GPa	7.1	6.7	13.7
Tensile Modulus	23°C (73°F)		527	GPa	6.9	5.4	14.5
	100°C (212°F)		527	GPa	6.7	3.1	9.2
	150°C (302°F)		527	GPa			5.9
	175°C (347°F)		527	GPa			5.1
Flexural Strength	23°C (73°F)	D790		MPa	226	165	224
Flexural Strength 50% RH	23°C (73°F)	D790		MPa	201	115	229
Flexural Strength	23°C (73°F)		178	MPa	197	170	259
	100°C (212°F)		178	MPa	141	67	161
	150°C (302°F)		178	MPa			101
	175°C (347°F)		178	MPa			88
Flexural Modulus	23°C (73°F)	D790		GPa	6.0	4.4	13.1
Flexural Modulus 50% RH	23°C (73°F)	D790		GPa	6.2	3.4	13.3
Flexural Modulus	23°C (73°F)		178	GPa	6.7	4.3	12.6
	100°C (212°F)		178	GPa	5.0	2.4	8.1
	150°C (302°F)		178	GPa			5.0
	175°C (347°F)		178	GPa			4.6
Shear Strength	23°C (73°F)	D732		MPa	70	56	80
Shear Strength 50% RH	23°C (73°F)	D732		MPa	66	44	62
Compressive Strength	23°C (73°F)	D695		MPa	124	100	145
Poisson's Ratio	23°C (73°F)				0.40	0.39	0.37
Izod Impact, Notched	23°C (73°F)	D256		J/m	95	90	85
Izod Impact, Notched 50% RH	23°C (73°F)	D256		J/m	45	80	80
Izod Impact, Unnotched	23°C (73°F)	D4812		J/m	945	825	710
Izod Impact, Notched	23°C (73°F)		180/1A	kJ/m ²	8.1	11.6	8
Izod Impact, Unnotched	23°C (73°F)		180/1U	kJ/m ²	53	54	44
Charpy Impact	23°C (73°F)		179/1eA	kJ/m ²	9.1	11.0	14.0
Charpy Impact, Unnotched	23°C (73°F)		179/1eU	kJ/m ²	85	75	47
Rockwell Hardness	23°C (73°F)	D785		R scale	124	116	125

Table 12: Toughened Glass-Reinforced and Flame Retardant Grades – Thermal, Electrical, and General Properties

Property	Method		Units	AT-1116	AT-6115	AFA-6133
	ASTM	ISO		HS	HS	VO Z
Thermal						
Deflection Temperature Under Load, 264 psi	D648		°C	254	271	277
			°F	489	519	531
Deflection Temperature Under Load, 1.8 MPa		75AF	°C	258	265	282
			°F	497	509	540
Vicat Softening Temperature	D1525	306	°C	295	296	291
			°F	563	565	556
Melting Point	D3418	11357-3	°C	310	307	310
			°F	590	585	590
Flammability, 3.2 mm (1⁄8 inch) Bar	UL 94			HB	HB	V-0
Electrical						
Dielectric Strength at 3.2 mm (1⁄8 inch)	D149		V/mil	—	533	609
			kV/mm	—	21	24
Dielectric Strength at 1.6 mm (1⁄16 inch)	D149		V/mil		711	686
			kV/mm		28	27
Volume Resistivity	D257		ohm-cm	—	1x10 ¹⁶	1x10 ¹⁶
Surface Resistivity	D257		ohm		1x10 ¹⁵	1x10 ¹⁵
Comparative Tracking Index	D3638		volts	—	—	—
Dielectric Constant at 60 Hz	D150			—	—	—
Dielectric Constant at 100 Hz	D150			—	4.0	4.8
Dielectric Constant at 10 ⁶ Hz	D150			—	3.3	4.1
Dielectric Constant at 10 ⁹ Hz	D150			—	3.1	3.7
Dissipation Factor at 60 Hz	D150			—	—	—
Dissipation Factor at 100 Hz	D150			—	—	—
Dissipation Factor at 10 ⁶ Hz	D150			—	0.013	0.011
Dissipation Factor at 10 ⁹ Hz	D150			—	0.011	—
General						
Specific Gravity	D792	1183A		1.28	1.22	1.68
Moisture Absorption, 24 hours	D570	62	%	0.2	0.2	0.2
Mold Shrinkage, Flow Direction	D955	294-4	%	0.6	1.0	0.3
Mold Shrinkage, Transverse Direction	D955	294-4	%	0.6	1.1	0.6

Table 13: Mineral and Mineral/Glass Filled Grades – Mechanical Properties (US Units)

Property	Temperature	Method		Units	A-1240	A-1565	AS-1566
		ASTM	ISO		L	HS	HS
Tensile Strength	23°C (73°F)	D638		kpsi	15.0	19.0	30.0
Tensile Strength 50% RH	23°C (73°F)	D638		kpsi	13.5	17.9	25.4
Tensile Strength	23°C (73°F)		527	kpsi	15.1	20.0	29.0
	100°C (212°F)		527	kpsi	10.1	13.3	18.4
	150°C (302°F)		527	kpsi	4.2	6.7	7.6
	175°C (347°F)		527	kpsi	3.5	4.7	6.3
Tensile Elongation	23°C (73°F)	D638		%	1.6	1.2	1.7
Tensile Elongation 50% RH	23°C (73°F)	D638		%	1.2	1.2	1.8
Tensile Elongation	23°C (73°F)		527	%	1.6	1.0	1.4
	100°C (212°F)		527	%	1.9	1.3	1.5
	150°C (302°F)		527	%	9.1	2.4	3.4
	175°C (347°F)		527	%	7.3	1.8	3.1
Tensile Modulus	23°C (73°F)	D638		Mpsi	1.30	3.00	2.90
Tensile Modulus 50% RH	23°C (73°F)	D638		Mpsi	1.20	3.02	3.03
Tensile Modulus	23°C (73°F)		527	Mpsi	1.45	2.86	3.26
	100°C (212°F)		527	Mpsi	0.81	2.23	2.49
	150°C (302°F)		527	Mpsi	0.16	0.83	1.06
	175°C (347°F)		527	Mpsi	0.13	0.74	0.90
Flexural Strength	23°C (73°F)	D790		kpsi	30.0	30.5	42.0
Flexural Strength 50% RH	23°C (73°F)	D790		kpsi	25.6	28.4	38.1
Flexural Strength	23°C (73°F)		178	kpsi	24.9	30.6	41.2
	100°C (212°F)		178	kpsi	17.6	23.6	29.7
	150°C (302°F)		178	kpsi	4.0	10.1	13.9
	175°C (347°F)		178	kpsi	3.2	8.1	11.0
Flexural Modulus	23°C (73°F)	D790		Mpsi	1.10	2.60	2.70
Flexural Modulus 50% RH	23°C (73°F)	D790		Mpsi	1.00	2.61	2.88
Flexural Modulus	23°C (73°F)		178	Mpsi	1.00	1.32	2.98
	100°C (212°F)		178	Mpsi	0.87	0.99	2.44
	150°C (302°F)		178	Mpsi	0.16	0.36	1.06
	175°C (347°F)		178	Mpsi	0.13	0.33	0.93
Shear Strength	23°C (73°F)	D732		kpsi	13.9	10.3	11.6
Shear Strength 50% RH	23°C (73°F)	D732		kpsi	13.5	7.2	9.1
Compressive Strength	23°C (73°F)	D695		kpsi	26.8	27.4	25.3
Poisson's Ratio	23°C (73°F)				0.29	0.31	0.35
Izod Impact, Notched	23°C (73°F)	D256		ft-lb/in	0.9	0.7	1.2
Izod Impact, Notched 50% RH	23°C (73°F)	D256		ft-lb/in	0.6	0.6	1.0
Izod Impact, Unnotched	23°C (73°F)	D4812		ft-lb/in	7	7	13
Izod Impact, Notched	23°C (73°F)		180/1A	ft-lb/in ²	2.2	1.9	3.1
Izod Impact, Unnotched	23°C (73°F)		180/1U	ft-lb/in ²	11	15	21
Charpy Impact	23°C (73°F)		179/1eA	ft-lb/in ²	1.9	1.6	2.9
Charpy Impact, Unnotched	23°C (73°F)		179/1eU	ft-lb/in ²	14	21	16
Rockwell Hardness	23°C (73°F)	D785		R scale	125	124	122

Table 14: Mineral and Mineral/Glass Filled Grades – Mechanical Properties (SI Units)

Property	Temperature	Method		Units	A-1240	A-1565	AS-1566
		ASTM	ISO		L	HS	HS
Tensile Strength	23°C (73°F)	D638		MPa	103	131	207
Tensile Strength 50% RH	23°C (73°F)	D638		MPa	93	123	175
Tensile Strength	23°C (73°F)		527	MPa	104	138	200
	100°C (212°F)		527	MPa	70	92	127
	150°C (302°F)		527	MPa	29	46	53
	175°C (347°F)		527	MPa	24	32	44
Tensile Elongation	23°C (73°F)	D638		%	1.6	1.2	1.7
Tensile Elongation 50% RH	23°C (73°F)	D638		%	1.2	1.2	1.8
Tensile Elongation	23°C (73°F)		527	%	1.6	1.0	1.4
	100°C (212°F)		527	%	1.9	1.3	1.5
	150°C (302°F)		527	%	9.1	2.4	3.4
	175°C (347°F)		527	%	7.3	1.8	3.1
Tensile Modulus	23°C (73°F)	D638		GPa	9.0	20.7	20.0
Tensile Modulus 50% RH	23°C (73°F)	D638		GPa	8.3	20.8	20.9
Tensile Modulus	23°C (73°F)		527	GPa	10.1	20.0	22.8
	100°C (212°F)		527	GPa	5.6	15.4	17.2
	150°C (302°F)		527	GPa	1.1	5.7	7.3
	175°C (347°F)		527	GPa	0.9	5.1	6.2
Flexural Strength	23°C (73°F)	D790		MPa	207	210	290
Flexural Strength 50% RH	23°C (73°F)	D790		MPa	177	196	263
Flexural Strength	23°C (73°F)		178	MPa	172	211	284
	100°C (212°F)		178	MPa	121	162	205
	150°C (302°F)		178	MPa	27	70	96
	175°C (347°F)		178	MPa	22	56	76
Flexural Modulus	23°C (73°F)	D790		GPa	7.6	17.9	18.6
Flexural Modulus 50% RH	23°C (73°F)	D790		GPa	6.9	18.0	19.8
Flexural Modulus	23°C (73°F)		178	GPa	7.0	9.1	20.8
	100°C (212°F)		178	GPa	6.0	6.8	16.8
	150°C (302°F)		178	GPa	1.1	2.5	7.3
	175°C (347°F)		178	GPa	0.9	2.3	6.4
Shear Strength	23°C (73°F)	D732		MPa	96	71	80
Shear Strength 50% RH	23°C (73°F)	D732		MPa	93	50	63
Compressive Strength	23°C (73°F)	D695		MPa	185	189	174
Poisson's Ratio	23°C (73°F)				0.29	0.31	0.35
Izod Impact, Notched	23°C (73°F)	D256		J/m	50	35	65
Izod Impact, Notched 50% RH	23°C (73°F)	D256		J/m	30	30	55
Izod Impact, Unnotched	23°C (73°F)	D4812		J/m	345	395	700
Izod Impact, Notched	23°C (73°F)		180/1A	kJ/m ²	4.7	4.0	6.6
Izod Impact, Unnotched	23°C (73°F)		180/1U	kJ/m ²	24	31	44
Charpy Impact	23°C (73°F)		179/1eA	kJ/m ²	4.1	3.4	6.2
Charpy Impact, Unnotched	23°C (73°F)		179/1eU	kJ/m ²	29	44	34
Rockwell Hardness	23°C (73°F)	D785		R	125	124	122

Table 15: Mineral and Mineral/Glass Filled Grades – Thermal, Electrical, and General Properties

Property	Method		Units	A-1240	A-1565	AS-1566
	ASTM	ISO		L	HS	HS
Thermal						
Deflection Temperature Under Load, 264 psi	D648		°C	179	271	278
			°F	355	520	532
Deflection Temperature Under Load, 1.8 MPa		75AF	°C	174	271	280
			°F	346	520	536
Vicat Softening Temperature	D1525	306	°C	302	296	298
			°F	575	565	569
Melting Point	D3418	11357-3	°C	310	311	311
			°F	590	592	592
Flammability, 3.2 mm (1⁄8 inch) Bar	UL-94			HB	HB	HB
Electrical						
Dielectric Strength at 1.6 mm (1⁄16 inch)	D149		V/mil	—	—	737
			kV/mm	—	—	29
Volume Resistivity	D257		ohm-cm	9x10 ¹⁵	4x10 ¹⁴	1x10 ¹⁶
Surface Resistivity	D257		ohm	—	—	1x10 ¹⁵
Comparative Tracking Index	D3638		volts	550	>600	—
Dielectric Constant at 60 Hz	D150			—	—	—
Dielectric Constant at 100 Hz	D150			4.2	—	5.7
Dielectric Constant at 10 ⁶ Hz	D150			4.0	—	4.7
Dissipation Factor at 60 Hz	D150			—	—	—
Dissipation Factor at 100 Hz	D150			0.006	—	—
Dissipation Factor at 10 ⁶ Hz	D150			0.017	—	0.011
General						
Specific Gravity	D792	1183A		1.54	1.90	1.84
Moisture Absorption, 24 hours	D570	62	%	0.1	0.1	0.1
Mold Shrinkage, Flow Direction	D955	294-4	%	1.0	0.3	0.3
Mold Shrinkage, Transverse Direction	D955	294-4	%	1.0	0.5	0.5

Mechanical Properties

The mechanical properties of a material are of fundamental importance to engineers when designing a part. The designer must match the mechanical properties of various candidate materials to the performance requirements of each application in order to determine which material is suitable for a given part design. Conversely, the designer can use the material property values to achieve an optimum part design.

To assist the designer, the material properties listed in this manual have been grouped into short-term or instantaneous and long-term or time-dependent properties. The short-term properties generally measure strength at failure while the long-term properties show how the material properties are affected by temperature, continuous loading, or chemical exposure as a function of time.

Short-Term Mechanical Properties

Short-term mechanical properties typically include tensile strength and modulus, flexural strength and modulus, several impact tests, compressive strength, shear strength, and surface hardness. These properties are usually reported at room temperature, and other temperatures as appropriate. Since some polymers absorb atmospheric moisture which may affect the properties, the moisture content may also be specified, often using the Relative Humidity (RH) convention.

The data sheets provided by the material suppliers typically list short-term properties, and their primary utility is for comparing similar materials. When using data sheets to compare materials, it is very important to insure that the same test methods have been used and that the data is reported in similar units.

The utility of short-term mechanical properties in design is limited. Typically, the properties are measured using molded test specimens that have been specifically designed to yield reproducible results, under carefully controlled environmental conditions, using specified loading rates. These measurements often provide the highest value obtainable for any property and material.

When parts are fabricated by a molding process they will likely contain a number of features such as stress concentrations, weld lines, corners or other aspects that may reduce strength. The strength of a material in an actual component may also be reduced, or in some cases enhanced, by reinforcing fiber orientation, relative degree of crystallinity, or thermal history (annealing). In addition, short-term properties do not provide any insight regarding time-related effects or the influence of chemical environments.

Tensile Properties

Test Methods

There are two widely accepted methods of testing tensile properties, ASTM method D638 and ISO method 527. These test methods measure the same property, but slightly different test specimens and test procedures are used. If the same material is tested using both procedures, the results will be similar but not the same. Therefore, only values obtained using the same method should be compared. In this document, whenever a tensile property value is given, the test method is also given, and in many cases values by both methods are provided.

Regardless of which test method is used, tensile properties are determined by clamping each end of a test specimen in the jaws of a testing machine that applies a unidirectional axial force to the specimens at a specified rate. The force required to separate the jaws divided by the minimum cross-sectional area of the test specimen is defined as the tensile stress. The test specimen will elongate as a result of the stress being applied. The amount of elongation divided by the original length of the test specimen is the strain.

When the applied stress is plotted against the resulting strain, a curve similar to that shown in Figure 5 for Amodel ET-1000 HS resin is obtained. This is known as a "Stress-Strain" curve and is very useful in determining the short term behavior of a material when a load is applied. The curve of a ductile metal would have a similar shape.

Figure 6 shows a typical stress/strain curve for a non-ductile material, Amodel A-1933 PPA. Strain at failure is much lower than that of the unreinforced grade. The addition of glass-fiber reinforcement improves the strength and stiffness but reduces the elongation or strain at failure.

Figure 5: Typical Stress/Strain Curve for Amodel ET-1000

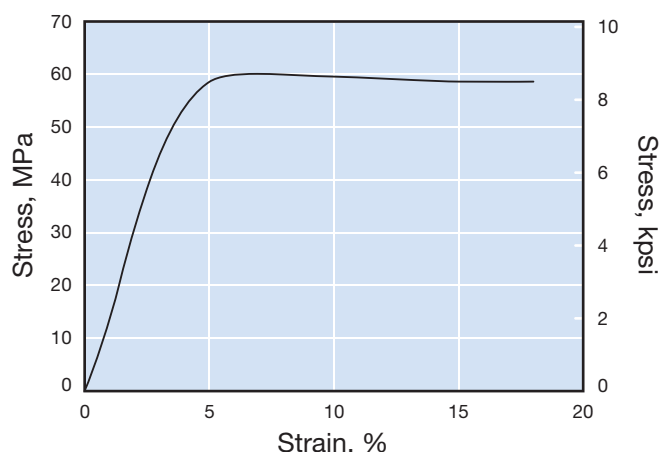


Figure 6: Typical Stress/Strain Curve for Amodel A-1933

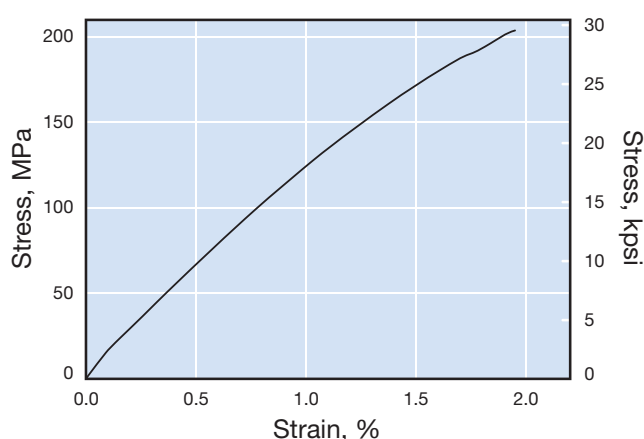
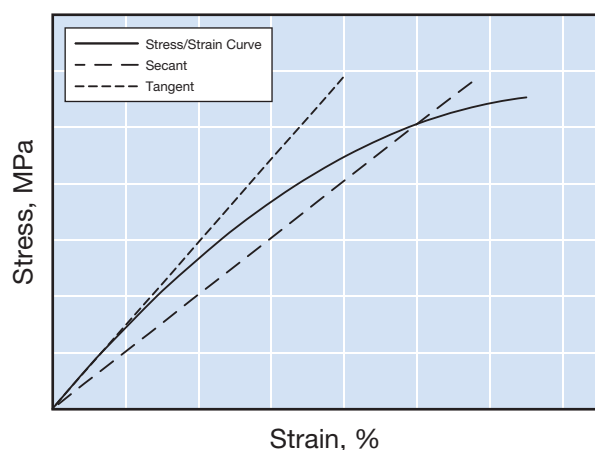


Figure 7: Secant and Tangent Methods for Estimating Modulus



The initial portion of the stress/strain curve is also of special interest because its slope relates to the stiffness or modulus of the material as shown in Figure 7.

This figure shows that the strain is directly proportional to stress up to a certain amount of stress. This region is known as the "Hookean" or elastic region. The maximum stress level that results in a proportional amount of strain is known as the proportional limit.

The tensile or elastic modulus is the slope of the stress/strain curve when a specimen is subjected to a tensile loading. Since the stress/strain plot is non-linear above the proportional limit, some conventions have been developed to standardize the measurements and reduce the variability in test results. One method uses the slope of a line drawn tangent to the curve. Another method utilizes the slope of a secant drawn through the origin and some arbitrarily designated strain level, usually 1%. The tangent method has been removed from the ISO test method and replaced with a slope calculation based

Figure 8: Tensile Strength of 30%-33% GR Resins

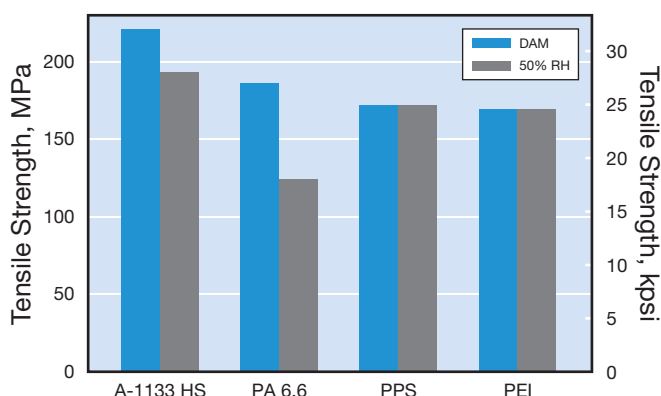
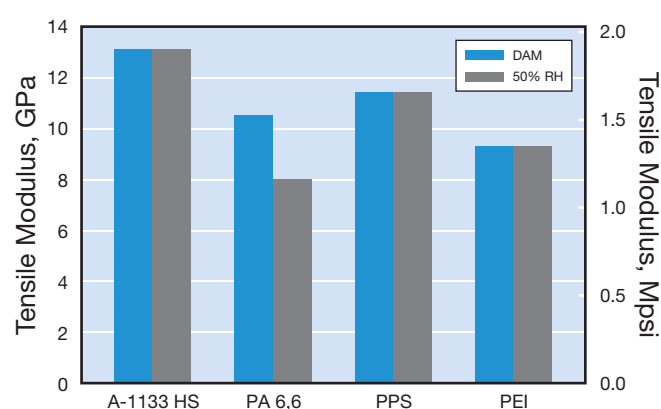


Figure 9: Tensile Modulus of 30%-33% GR Resins



on specified strain values of 0.0005 and 0.0025. Alternatively, computerized machines can use the least squares method to calculate the slope over the same strain region.

The tangent method was used for the tensile data run by ASTM D638 presented in this brochure.

Ductile polymers undergo yield prior to rupture. At this point, the material undergoes additional elongation without an increase in stress. The stress level at which yield occurs is often referred to as tensile strength at yield or tensile stress at yield. The elongation achieved at this point is called the elongation at yield, yield strain or tensile strain at yield. As the test proceeds, the specimen continues to elongate until rupture occurs. The stress level at this point is called tensile strength at break or ultimate tensile strength or tensile stress at break. Tensile strength is defined as the greater of measured stresses which could be either the stress at yield or the stress at rupture.

Figure 10: Tensile Elongation of 30%-33% GR Resins

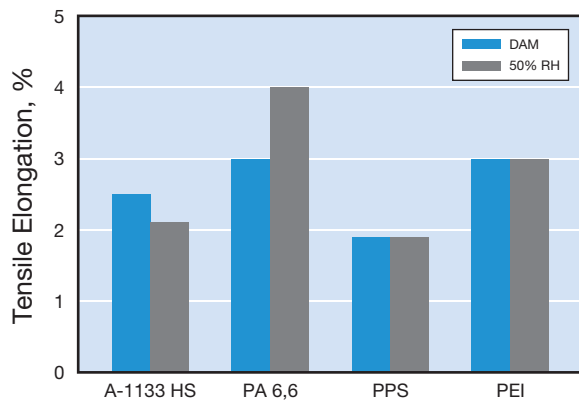
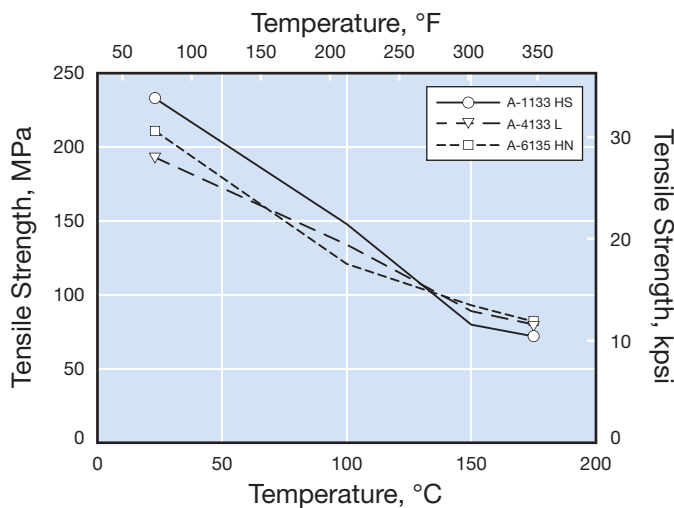


Figure 11: Tensile Strength of 33% GR PPA vs. Temperature



Tensile Property Comparison

Amodel A-1133 HS resin has higher tensile strength at room temperature than 33% GR polyamide (PA) 6,6, 30% GR polyphenylene sulfide (PPS), and 30% GR polyetherimide (PEI), as shown in Figure 8. Even after moisture conditioning, the Amodel PPA is stronger than the other resins.

The tensile modulus of 33% GR Amodel PPA is compared to the same resins in Figure 9. The Amodel resin has a higher modulus as molded and shows no decline when moisture conditioned, while the PA 6,6 exhibits a reduction of over 20%.

This same comparison for tensile elongation is shown in Figure 10. The tensile elongation of the resins is low due to the glass-fiber reinforcement. Moisture conditioning the PA 6,6 results in an increase in elongation due to the reduction in T_g .

Figure 12: Tensile Modulus of 33% GR PPA vs. Temperature

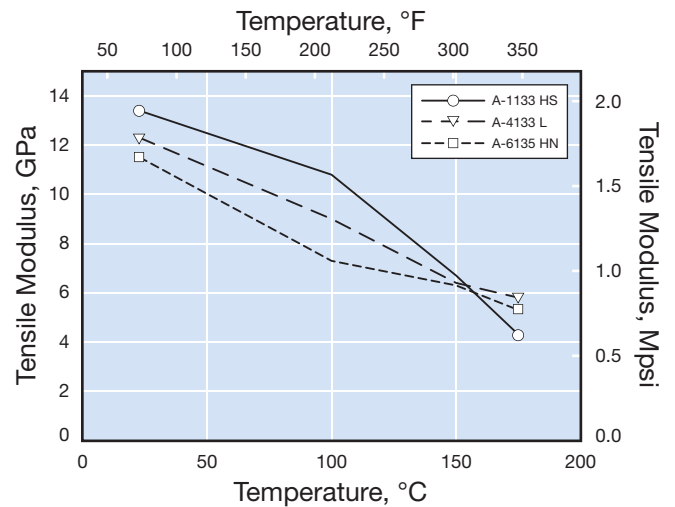
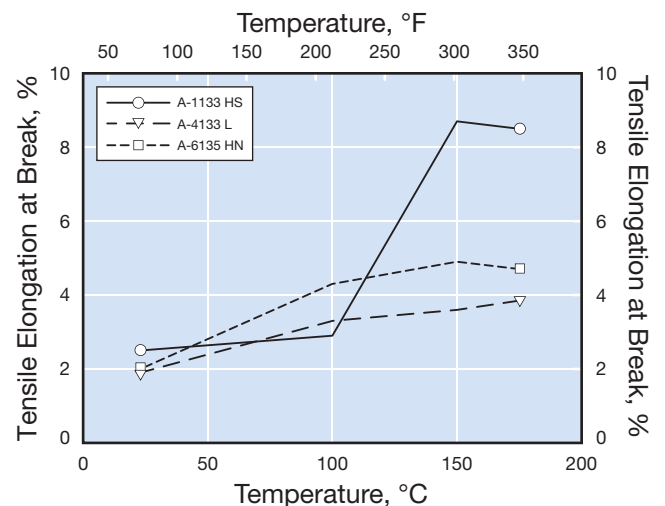


Figure 13: Tensile Elongation of 33% GR PPA vs. Temperature



Tensile Properties for GR PPA vs. Temperature

Figures 11 through 13 show the tensile properties of GR grades of Amodel PPA based upon A-1000, A-4000, and A-6000 base resins from RT to 175°C (347°F). Amodel A-1133 HS has the highest strength and stiffness at room temperature, but A-4133 L and A-6135 HN have better strength and stiffness above 150°C (302°F).

Figure 14: Tensile Strength of GR A-1000 PPA Grades vs. Temperature

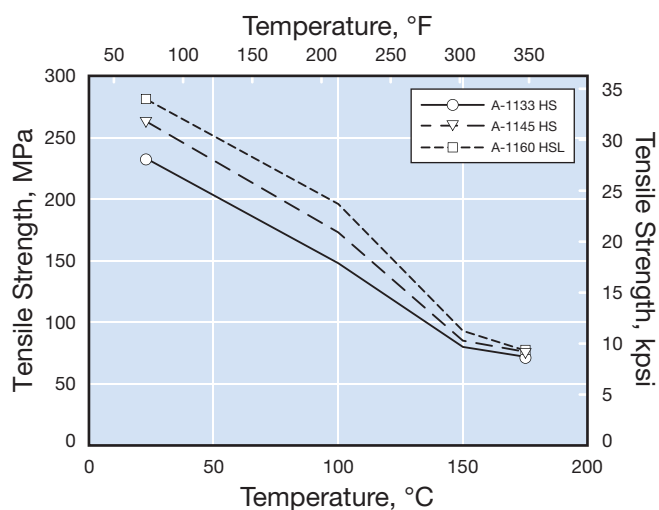


Figure 16: Tensile Elongation of GR A-1000 PPA Grades vs. Temperature

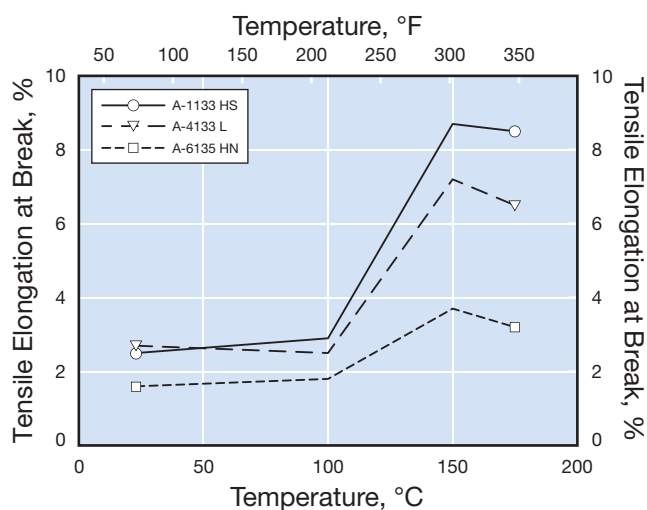


Figure 15: Tensile Modulus of GR A-1000 PPA Grades vs. Temperature

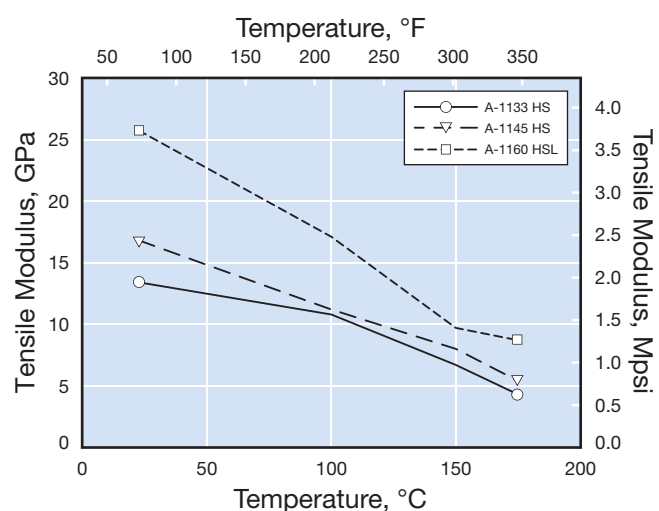
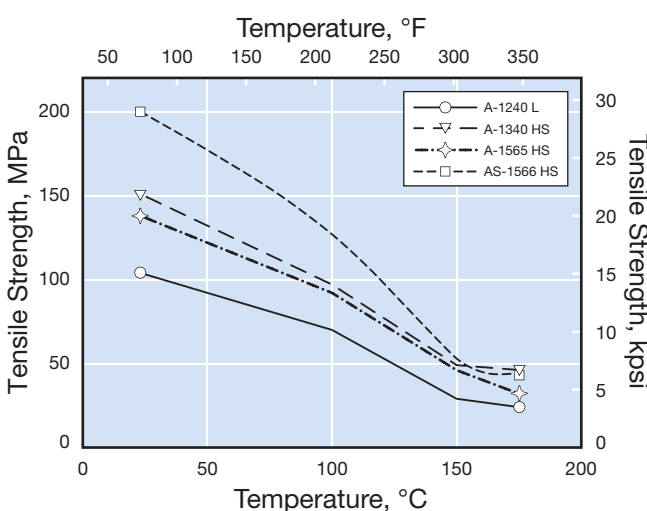


Figure 17: Tensile Strength of Mineral/Glass PPA Grades vs. Temperature

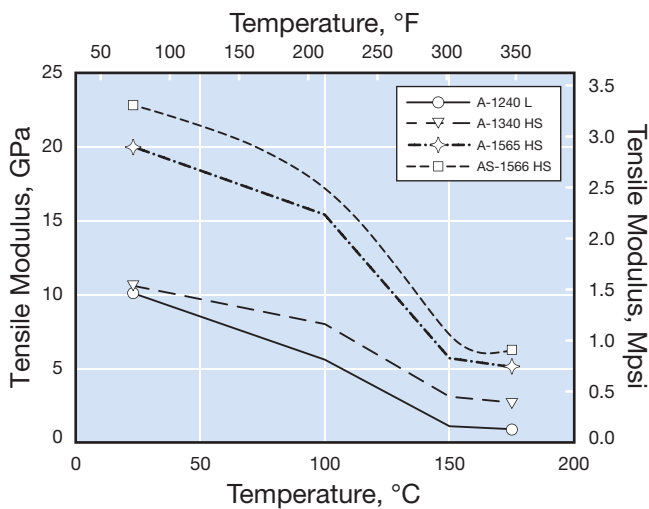


Tensile Properties of A-1000 GR Grades at Elevated Temperatures

Figures 14 through 16 shows the tensile properties of three glass-reinforced grades of Amodel PPA, based on the A-1000 base resin containing 33%, 45% and 60% glass-fiber over the temperature range of RT to 175°C (347°F). The tensile strength and modulus increase with glass fiber content, which is typical of semi-crystalline thermoplastics.

Both strength and modulus decrease as temperatures rise. Elongation increases with increasing temperature. As a semi-crystalline material, Amodel resins show a slow but steady loss in mechanical properties from ambient temperature up to the glass transition temperature (T_g). At the T_g , there is a more significant loss over a narrow temperature range, followed by another gradual decline. This behavior is typical of all semi-crystalline thermoplastics.

Figure 18: Tensile Modulus of Mineral/Glass PPA Grades vs. Temperature



Flexural Properties

Like tensile strength and modulus, the flexural strength and modulus of a plastic material can be increased by adding glass fibers into the plastic resin. Treatment of the glass fibers can produce a strong chemical bond between the plastic and the glass that enhances both tensile and flexural properties over a wide range of environmental conditions. As the amount of glass fiber reinforcement is increased in the plastic, both the flexural strength and modulus increase.

Test Methods

Flexural properties of thermoplastic materials are determined in accordance with either ASTM D790 or ISO 178. ASTM D790 includes a three point loading test, Method I and a four point loading test, Method II. In this document, whenever D790 is referenced, Method 1 was used. ISO 178, Plastics - Determination of Flexural Properties, specifies three point loading.

The two test methods differ in test specimen dimensions, apparatus specifications, maximum deflection, and calculation details. The three point loading refers to the specimen being supported at two points separated by a specified span and a vertical load applied to the top of the test specimen at a point midway between the supports. The test specimen deforms or bends as a result of the load. The specimen is deflected until rupture occurs or the maximum fiber strain is reached. The flexural strength is defined as the maximum fiber stress at the moment of rupture or maximum strain. The maximum strain specified by the ISO 178 method is 3.5 %, while ASTM D790 specifies 5%.

When the flexural properties of one material are determined by both methods, the results obtained by the ASTM are different from those obtained using the ISO method. Data by both methods are shown in the property tables. When comparing materials, ensure that the data being compared was obtained using the same test method and test condition.

The flexural modulus of elasticity is the ratio, within the elastic limit, of the stress in the outermost fiber of the object being stressed to corresponding strain. As in tensile testing, the modulus is calculated from the slope of the load deflection curve in the linear "Hookean" region.

Flexural testing provides information about the relative strength and stiffness of materials when subjected to bending loads. The material with the higher flexural strength can endure higher bending loads without fracture. Parts produced from a material with a higher flexural modulus will deflect less when subjected to a bending load than parts made of a lower modulus material.

Glass fibers and mineral additives increase the flexural strength and modulus of Amodel PPA compared to the unfilled resin. The resultant higher modulus may be desirable in many applications.

Figure 19: Flexural Strength of 30-33% GR Resins

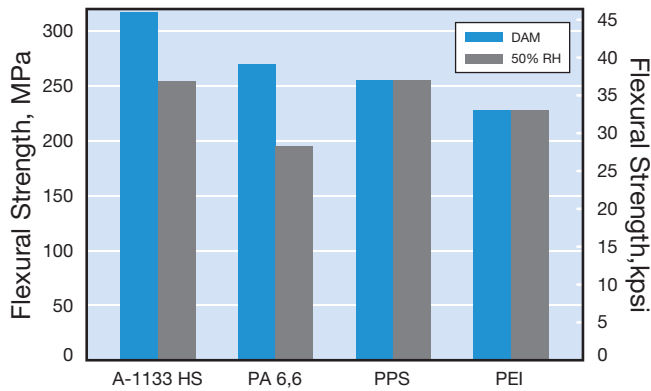
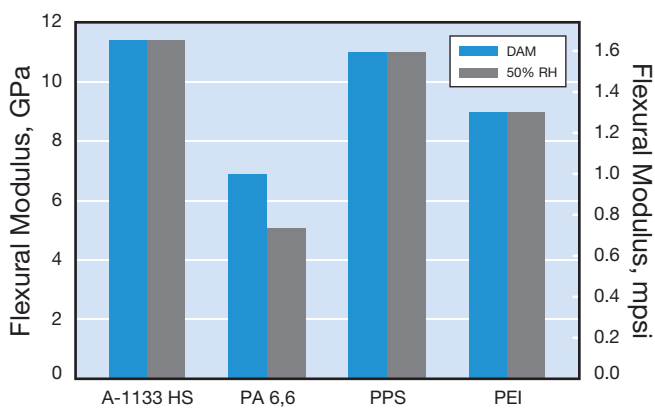


Figure 20: Flexural Modulus of 30-33% GR Resins



Flexural Property Comparison

The flexural strength of 33% GR Amodel PPA is compared to that of comparable PPS, PEI, and PA 6,6 materials in Figure 19. Amodel PPA's strength is superior to the other resins, and although it declines somewhat with moisture conditioning it is still higher than most of the other materials as molded.

This comparison for flexural modulus is shown in Figure 20. The flexural modulus of the Amodel resin shown is quite high and it is not affected by moisture conditioning. The modulus of the PA 6,6 material declines significantly with moisture conditioning.

Figure 21: Flex Strength of GR PPA Resins vs. Temperature

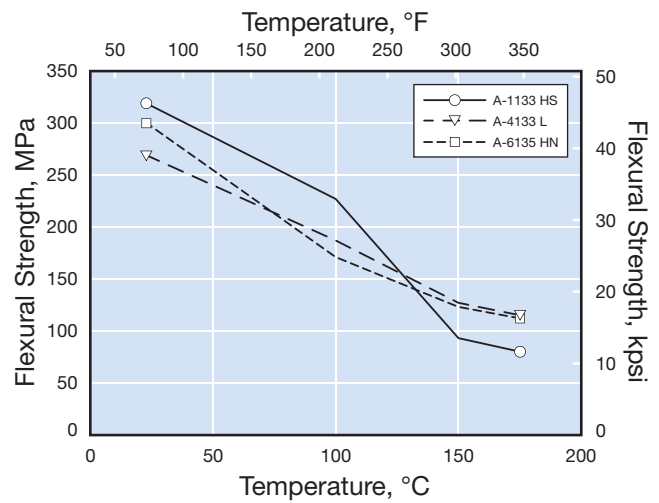
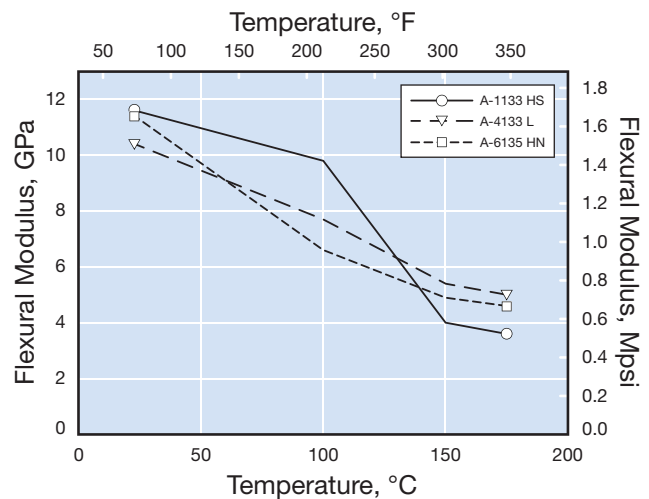


Figure 22: Flex Modulus of GR PPA Resins vs. Temperature



Flexural Properties at Elevated Temperatures

Figures 21 and 22 show the flexural properties of three glass-reinforced Amodel grades based on A-1000, A-4000, A-6000 base resins from room temperature up to 175°C. The grade based on A-1000 has higher strength and stiffness and room temperature, but the grades based on A-4000 and A-6000 are better at temperatures above 125°C.

Figure 23: Flex Strength of GR A-1000 PPA Grades vs. Temperature

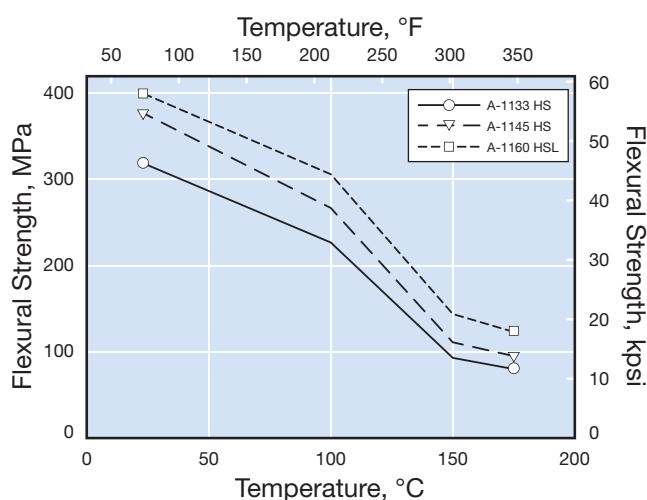
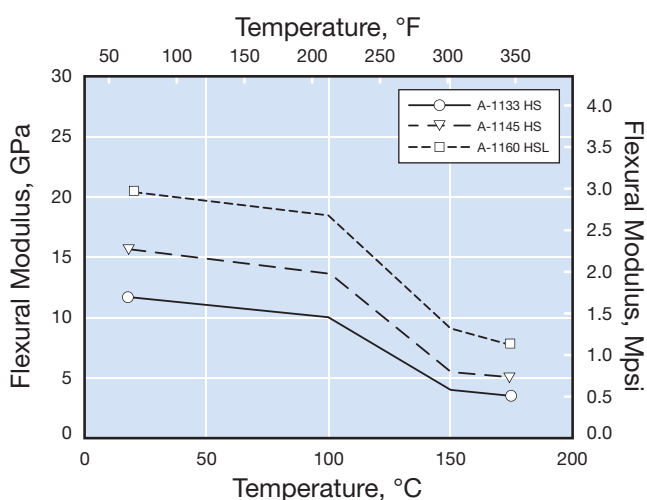


Figure 24: Flex Modulus of GR A-1000 PPA Grades vs. Temperature



Figures 23 and 24 present the flexural properties of Amodel PPA resins based on A-1000 containing different glass reinforcement levels. As expected, the higher glass content grades have the higher strength and stiffness across the temperature range.

Figure 25: Flex Strength of Mineral/Glass PPA Resins vs. Temperature

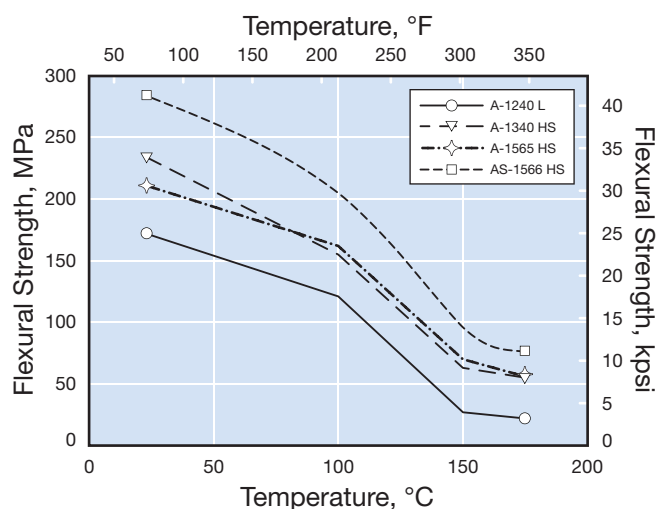
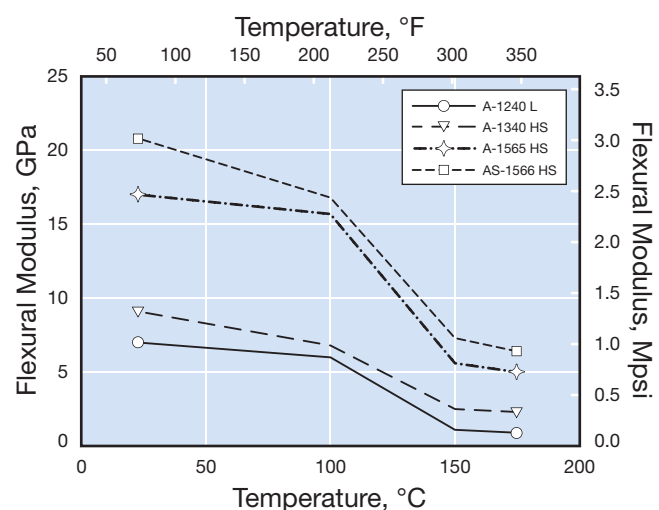


Figure 26: Flex Modulus of Mineral/Glass PPA Resins vs. Temperature



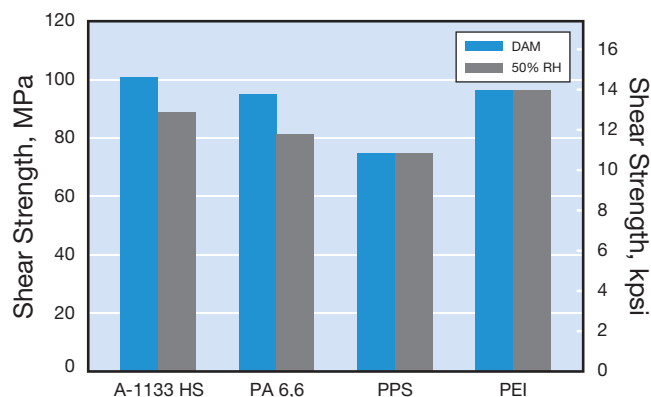
Shear Properties

Shear strength is the resistance to yield or fracture of two planes moving relative to one another in the direction of load. Shear strength can also be defined as the maximum load required to shear the specimen being tested in such a manner that the moving plane has completely cleared the stationary plane. Shear strength values are important in designing structural components because in actual applications the maximum stress on a component is often a shear stress.

Shear strength was determined in accordance with ASTM D732. In this test, a plaque molded from the material to be tested is placed on a plate with a circular hole in it. A circular punch whose diameter is slightly smaller than the hole in the plate is pushed through the molded plaque, punching out a circular disc. The maximum stress is reported as the shear strength, and is calculated by dividing the load required to shear the specimen by the sheared area, which is calculated by multiplying the circumference of the hole by the thickness of the plaque.

Figure 27 compares the shear strength of Amodel PPA to PA 6,6, PPS, and PEI. The shear strength of Amodel PPA is comparable to that of PA 6,6 and PEI and superior to that of PPS.

Figure 27: Shear Strength of 30%-33% GR Resins



Compressive Strength and Modulus

Compressive strength and modulus are measured in accordance with ASTM D695. The test specimen is molded from the material to be tested and then placed between parallel plates. These plates then exert a compressive force on the specimen, while the force and the distance between the parallel plates is monitored. The compressive strain is given by the change in the distance between the plates. The stress at failure, calculated by dividing the force by the cross-sectional area, is the compressive strength, and the slope of the stress/strain curve is the compressive modulus.

Impact Strength

Because polymers are viscoelastic, their properties depend upon the rate at which a load is applied. When the loading rate is rapid, the part is said to be subjected to impact loading. If a plastic part is to survive an impact without damage, it must be able to absorb the kinetic energy transferred by the collision.

The ability of a plastic part to absorb energy is a function of its shape, size, thickness, and the type of plastic used to make the part. The impact resistance testing methods most frequently used may not adequately provide the designer with information that can be used analytically. These tests are most useful for determining relative impact resistance and comparing the notch sensitivities of materials. While the results may not adequately predict practical toughness in actual applications, they will serve to offer comparisons between materials.

Figure 28: Compressive Strength of 30%-33% GR Resins

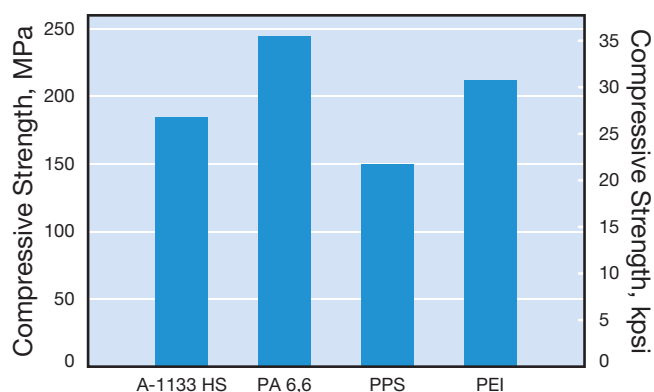


Figure 29: Compressive Strength of A-1000 Resins vs. Temperature

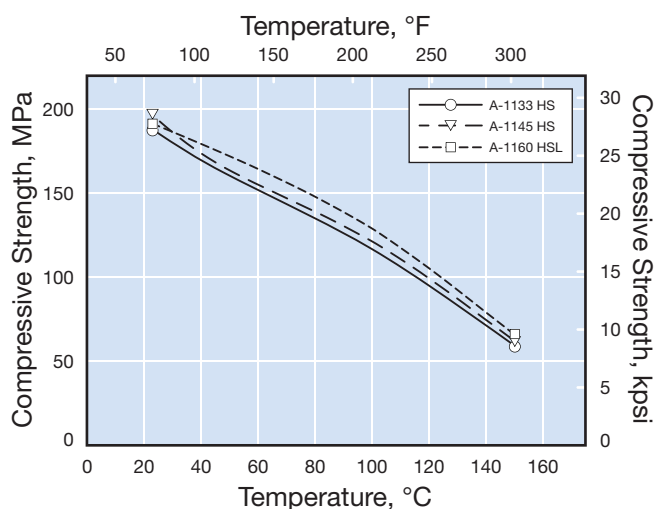


Figure 30: Compressive Modulus A-1000 Resins vs. Temperature

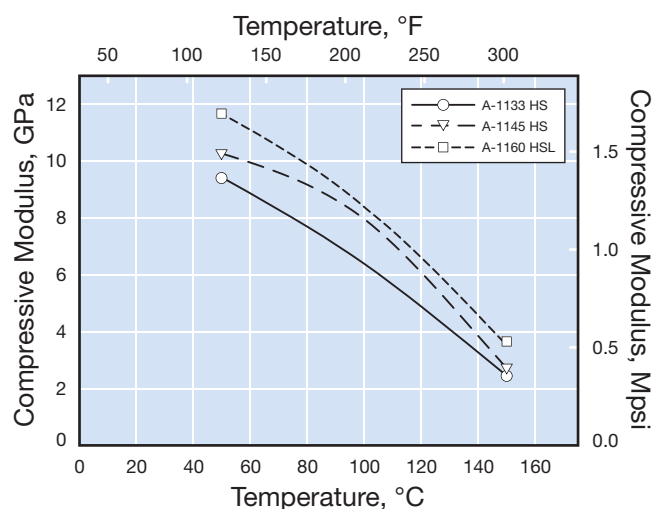


Figure 31: Izod Impact Test Specimen

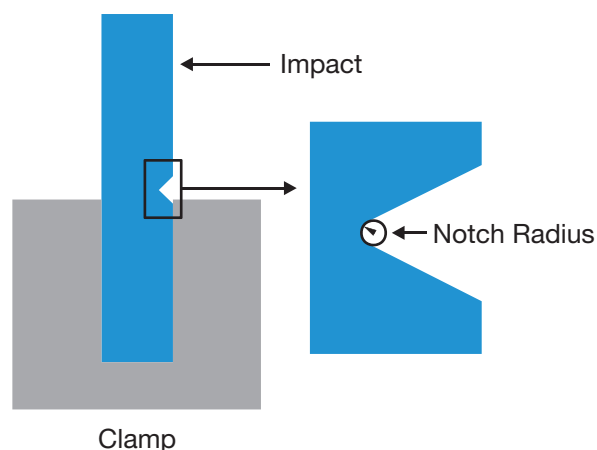


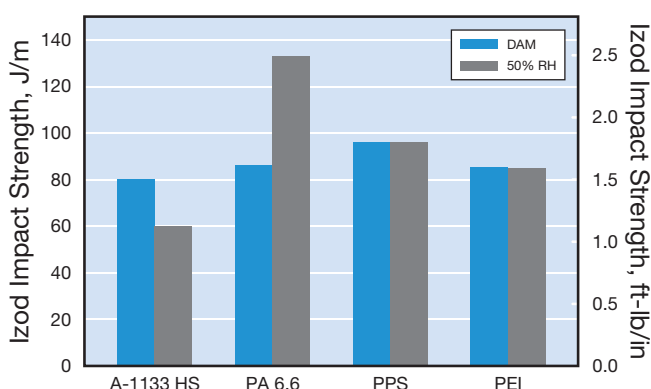
Table 16: Izod Test Specimen Dimensions

Dimension	ISO 180		ASTM D256	
	mm	inch	mm	inch
Length	80.00	3.150	63.50	2.500
Width	10.00	0.394	12.70	0.500
Thickness	4.00	0.157	3.20	0.125
Notch Radius	0.25	0.010	0.25	0.010

Izod (Cantilevered Beam) Impact

Izod impact can be determined using ASTM D256, Impact Resistance of Plastics and Electrical Insulating Materials, or ISO 180, Plastics – Determination of Izod Impact Strength. In both of these tests, a test specimen, as illustrated in Figure 31, with a notch of specified radius cut in its edge is struck by a swinging pendulum. After the impact, the pendulum continues to swing, but with less energy due to the collision. The methods differ in the dimensions of the test specimen and in the way the results are calculated. When using ASTM D256, the energy lost is divided by the width of the specimen remaining after notching, and the units are either Joules per meter (J/m) or foot-pounds per inch (ft-lb/in). When using ISO 180, the amount of energy lost is multiplied by 1,000 and divided by the product of the remaining width and the specimen thickness, and the units are either kilojoules per square meter (kJ/m²) or foot-pounds per square inch (ft-lb/in²).

Figure 32: Izod Impact Strength of 30%-33% GR Resins, ASTM D256



Izod impact can also be run on un-notched specimens. The applicable test methods are ASTM D4812 or ISO 180U. The major difference between these methods and the notched methods is that the full width of the specimen is used in the calculation.

Data using both methods are included in this document. The dimensions for the test specimens used are given in Table 16.

Izod Impact Property Comparison

Figure 32 shows a comparison of the notched Izod impact strength of 33% glass-fiber reinforced Amodel PPA to glass-fiber reinforced grades of PA 6,6, PPS, and PEI. The glass-fiber reinforcement adds strength to these materials but reduces elongation and all of these materials have low Izod values. PA 6,6 shows an increase in impact strength when moisture conditioned.

Figure 33 shows the Izod impact strength of a toughened grade of Amodel PPA, ET-1000 HS, and that of high impact grades of PA 6,6 and PA 6, as well as polycarbonate (PC) and a polycarbonate-polyester (PC/PBT) blend. The Amodel grade has impact strength comparable or better than the other materials. Figure 34 shows that this grade is not as sensitive to notch radius as most amorphous polymers are.

Figure 35 shows that ET-1000 HS has good Izod impact at temperatures lower than room temperature, but Amodel AT-1001 L has superior impact resistance at temperatures as low as -40°C.

Figure 33: Izod Impact of Amodel ET-1000 Compared to PA and PC

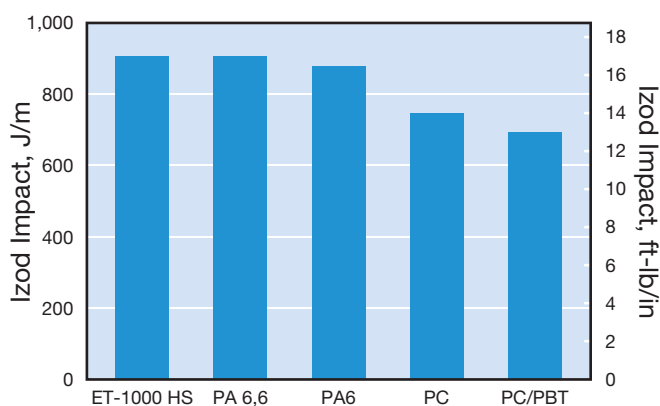
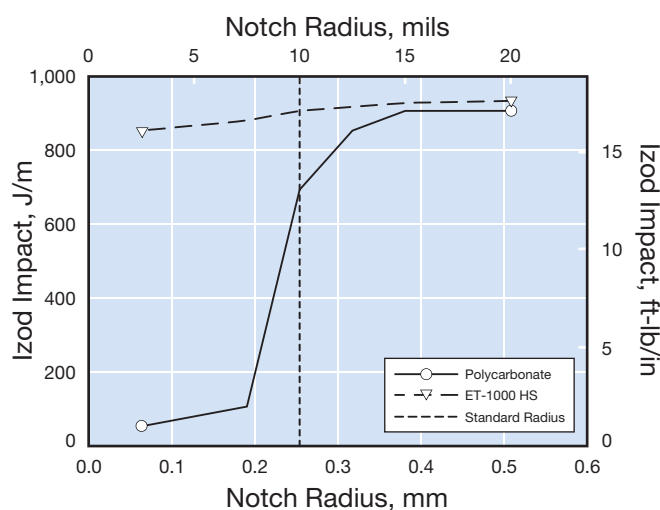


Figure 34: Notch Radius Sensitivity of ET-1000 HS and PC



Charpy (Supported Beam) Impact

Charpy is similar to Izod because a test specimen is struck by a falling pendulum and the energy the break the specimen measured. The primary difference is that in the Charpy test the specimen is supported at both ends and struck in the middle, as shown in Figure 36. The test methods used were ISO 179/1eA and 179/1eU.

Figure 35: Low Temperature Izod of Amodel PPA Grades

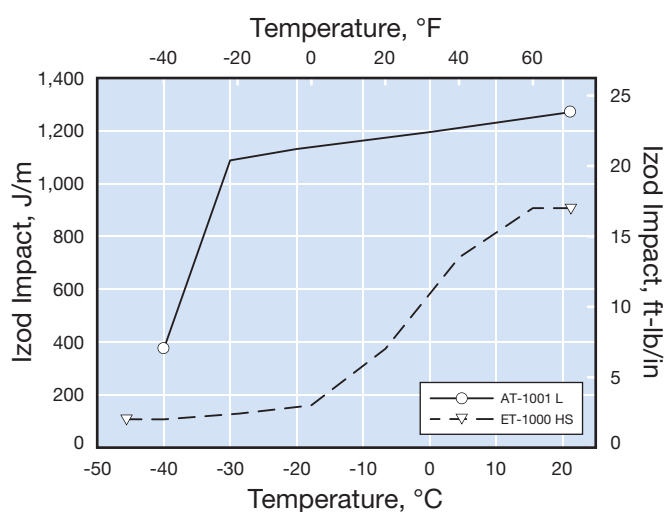


Figure 36: Charpy Impact Test Specimen

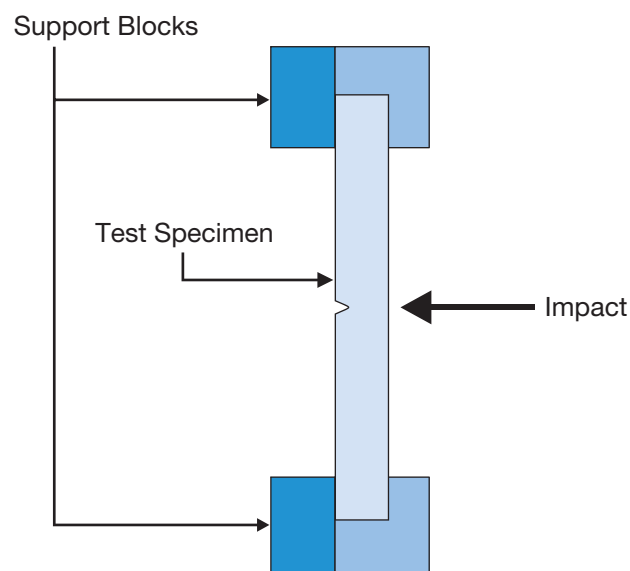
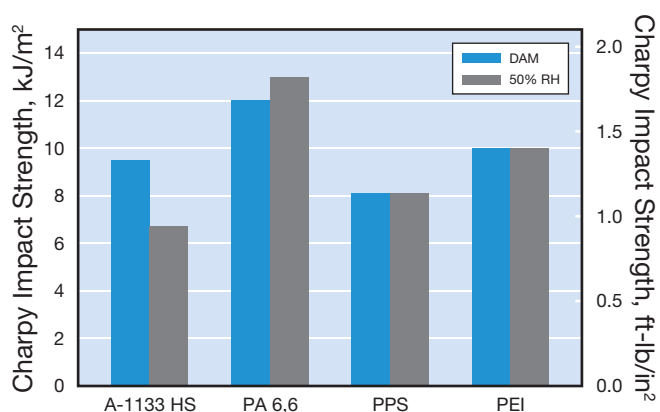


Figure 37: Notched Charpy Impact Strength of 30%-33% GR Resins



Falling Weight Impact Properties

ASTM D3763, High-Speed Puncture Properties of Plastics Using Load and Displacement Sensors, was used to measure the practical toughness of Amodel polyphthalamide resins.

In this test, an injection molded specimen is clamped down over a 76 mm (3 inch) diameter hole and a weighted plunger is dropped from a predetermined height to give it a predetermined impact velocity. The plunger assembly consists of a 12.7 mm (0.500 inch) diameter steel rod with a hemispherical end. The plunger assembly is attached to a load cell which measures the energy needed to cause a sample to fail.

Specimens can fail in either a brittle or a ductile mode. In a ductile failure mode, the specimen is permanently deformed to the shape of the plunger, but remains in one piece after the penetration by the plunger. In a brittle failure mode, the specimen does not have sufficient ductility to be deformed without failure, and therefore breaks into two or more pieces when impacted by the plunger.

This method is preferred to ASTM D3029, because although the impact values obtained are similar in nature to the "stair step" falling weight impact test, the instrumented test results are obtained via a computerized data reduction technique and fewer samples are required.

Table 17: Penetration Impact (ASTM D3763) of Impact Modified PPA

Grade	Condition	Max Load		Total Energy	
		N	lb	J	ft-lb
AT-1001 L	DAM	4,900	1,100	54	40
AT-1002 HS	DAM	4,400	1,000	54	40
AT-1002 HS	50% RH	4,000	900	47	35
AT-5001	DAM	4,400	1,000	54	40
AT-5001	50% RH	4,000	900	50	37
ET-1000 HS	DAM	4,670	1,050	54	40
ET-1001 L	DAM	5,600	1,260	64	47

Poisson's Ratio

Poisson's ratio is a measure of the strain characteristics imposed on a material transverse to the applied load. Poisson's ratio is the ratio of lateral strain to longitudinal strain within the proportional limit. To illustrate, consider a cylindrical bar subjected to tensile stress, the length (L) increases and simultaneously its diameter (D) decreases.

In this case, Poisson's ratio (ν) would be calculated by:

$$\nu = \frac{-\frac{\Delta D}{D}}{\frac{\Delta L}{L}}$$

Most plastic materials have a Poisson's ratio between 0.3 and 0.5.

Table 18 gives the Poisson's ratios for various Amodel formulations at 23°C (73°F), "dry, as molded".

Table 18: Poisson's Ratio for Amodel Products

Grade	Poisson's Ratio, ν
ET-1000 HS	0.40
A-1115 HS	0.41
AS-1133 HS	0.41
AS-1145 HS	0.41
A-1230 L	0.31
A-1240 L	0.29
A-1340 HS	0.38

Long-term Mechanical Properties

In order for any engineered component fabricated from a polymeric resin to perform within specified parameters throughout its intended design life, the design engineer must consider the long term effects of a number of factors. A variety of stress loads as well as property changes due to environmental factors must be taken into consideration. To assess the time related effects of stress on the behavior of polymeric materials, creep and fatigue properties are measured. A wide variety of environmental factors can also affect the performance of an engineered component and this subject is discussed in detail in the section entitled "Environmental Resistance" starting on page 58. However, certain environmental factors are so pervasive that it was deemed appropriate to consider them in this section. These are the effects of moisture absorption and long-term exposure to high ambient temperatures.

This section will present data generated to assist the design engineer with the analysis of design life requirements. The data in this section includes:

- Creep modulus in tension, flexure, and compression modes
- Tensile creep rupture
- Fatigue endurance
- Property changes due to moisture absorption
- Dimensional changes due to moisture absorption
- Property changes due to long-term exposure to elevated temperatures

The long term property data presented in this manual has been generated to show trends and property loss for a number of Amodel PPA grades under a variety of representative conditions. Due to the time required to generate the data, not all grades or sets of conditions can be included. The data are intended to show trends as a function of filler/reinforcement systems so that the designer may make educated decisions.

In some instances, attempts to generate data on long term properties utilize "accelerated" test conditions to speed data acquisition. Caution should be taken when evaluating data generated in this manner as it is often non-linear. This is especially true when measuring property loss as a function of elevated temperature and/or chemical exposure. Thermal "thresholds" such as the glass transition temperature (T_g) and ultimately, the melting point are the main contributors to this non-linear behavior.

Creep

When a material is subjected to stress, an immediate strain occurs. For small strains, this strain is proportional to the stress and calculable from the appropriate modulus. If the application of stress continues for an extended period of time, additional strain may be observed. This behavior is referred to as creep and the additional strain as creep strain.

While creep is observed in metals, the phenomenon is more significant with plastics. Their lower modulus means that at the same stress level, the magnitude of the strain is larger and a higher proportion of ultimate strain. In general, the closer the initial strain is to the ultimate strain, the more likely it is that creep is significant.

The reality of creep must be factored into a design to insure long term satisfactory performance. The initial task is to determine if the creep will have a significant effect on the dimensions or function of the part. If the stress levels are low enough so that any dimensional change will be insignificant, creep may be ignored. However, if the stress levels are such that creep will result in unacceptable deformation, an alternative design must be considered. This may include investigating a material with a higher creep modulus, or incorporation of an alternate design such as a metallic insert to serve as the load bearing member. Additional discussion can be found in the Design section.

In general, glass and mineral/glass reinforced grades creep less than the unreinforced grades. The time required to observe measurable creep will also be shorter for the unreinforced grades. Apparent or creep modulus will decrease at elevated temperatures with a corresponding increase in creep. At temperatures above the glass transition temperature (T_g), the apparent modulus of the unreinforced grades is so low that even relatively low loads can result in significant creep, and therefore these unreinforced grades are usually not recommended for use in structural applications above these temperatures. Structural applications that will be exposed to elevated temperatures should be specified in the glass or mineral/glass reinforced grades.

Creep can occur in tension, compression, or flexural modes. Therefore, to evaluate creep properties, strain is measured as a function of time while a specimen is subjected to a constant tensile, compressive or flexural load at specified environmental conditions. The procedure followed is described in ASTM D2990, Standard Test Methods for Tensile, Compressive, and Flexural Creep and Creep-Rupture of Plastics. ISO Method 899, Plastics - Determination of Creep Behaviour is similar, but because of differences in the test specimen may not yield exactly the same results. The general trends shown by either method should be comparable, but material comparisons should only be done using data generated by the same method.

The normal progression of creep occurs in these three stages:

- A rapid initial deformation
- Continued deformation at a slow and constant rate
- Yield followed by rupture for ductile materials, or rupture for non-ductile materials

The significance of data from creep tests is that they can be used to calculate the time dependent creep strain and creep modulus for use in stress calculations and to determine the safe stress levels for specific time and temperature conditions. If the creep tests are conducted until failure occurs at various stress levels, a creep rupture curve can be produced.

Another aspect of creep may further complicate the analysis: under a given stress, creep will occur at the expected rate based on the apparent modulus. However, depending on how the stress is applied, the initial creep can result in stress relaxation. For example, if a plastic part is clamped with a bolt torqued to achieve a compressive stress on the plastic. As creep strain occurs, the compressive stress will drop, resulting in less creep. The compressive stress will drop until an equilibrium is established at a lower stress level. A "single point" analysis would indicate that torque retention would drop to a failure level, while, in reality, an acceptable equilibrium is reached before failure levels occur.

Further discussion of the influence of creep on part design, including examples, can be found on page 70.

Tensile Creep

Tensile creep was measured at three temperatures: 23°C (73°F); 125°C (257°F); and 175°C (347°F) and two stress levels: 13.8 MPa (2000 psi) and 34.5 MPa (5000 psi). Test specimens were 3.2 mm (0.125 inch) thick injection molded ASTM D638 Type I tensile bars. Samples were placed under test in the "dry, as molded" condition. The samples tested at the two elevated temperatures were placed in air circulating ovens. Although the strain is measured, the results are typically presented as the apparent modulus, which is calculated by dividing the strain by the applied stress. The apparent modulus is the value design engineers use in their mechanical design calculations when designing components that must perform when subjected to sustained load.

The materials tested were A-1133 HS (33% glass-fiber) and A-1145 HS (45% glass-fiber). The results of the room temperature testing are shown in Figures 38 and 39.

The results of the tensile creep testing at 125°C (257°F) are shown in Figures 40 and 41, and at 175°C (347°F) in Figures 42 and 43.

Figure 38: Apparent Modulus at 23°C (73°F) and 13.8 MPa (2 kpsi)

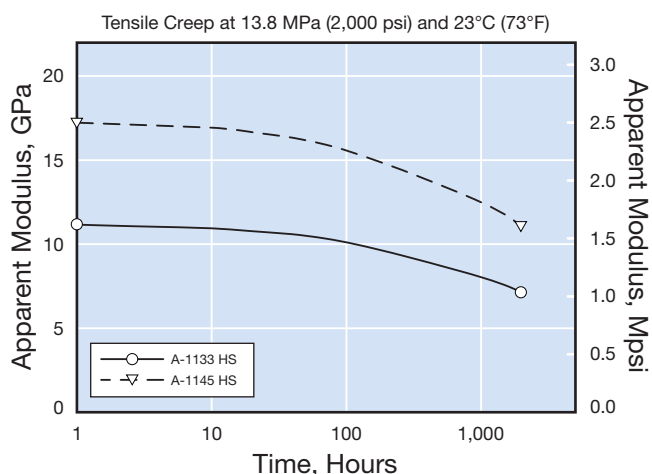


Figure 41: Apparent Modulus at 125°C (257°F) and 34.5 MPa (5 kpsi)

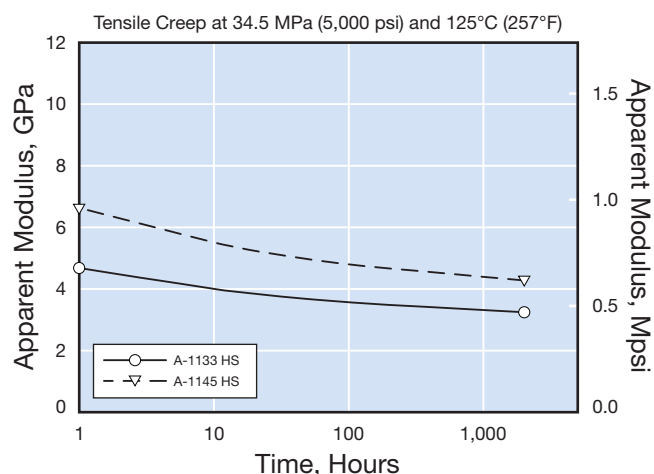


Figure 39: Apparent Modulus at 23°C (73°F) and 34.5 MPa (5 kpsi)

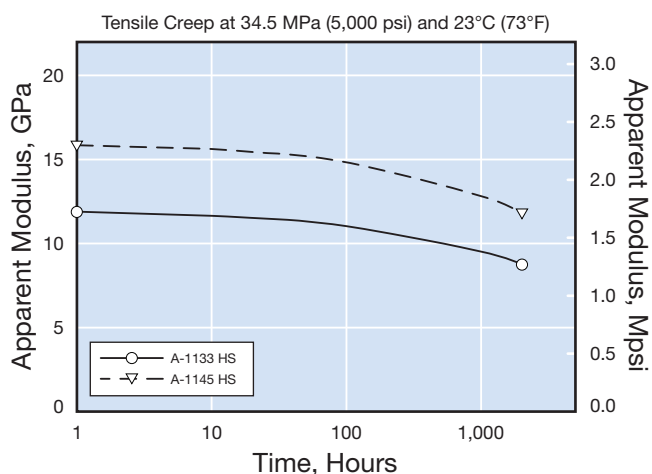


Figure 42: Apparent Modulus at 175°C (347°F) and 13.8 MPa (2 kpsi)

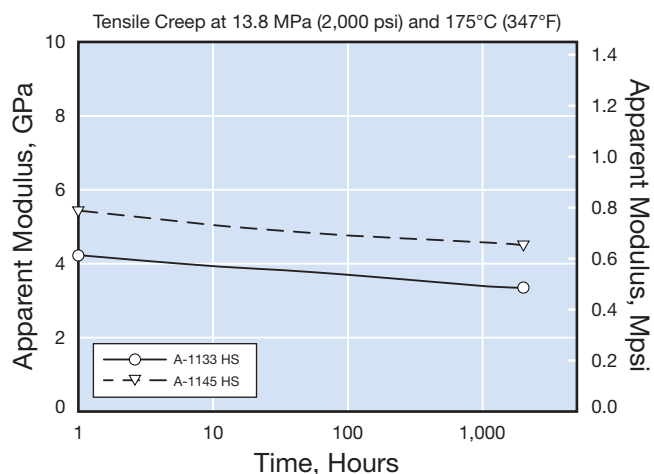


Figure 40: Apparent Modulus at 125°C (257°F) and 13.8 MPa (2 kpsi)

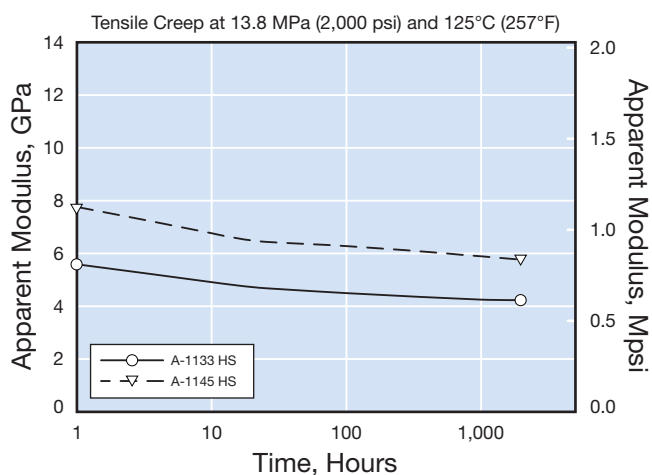
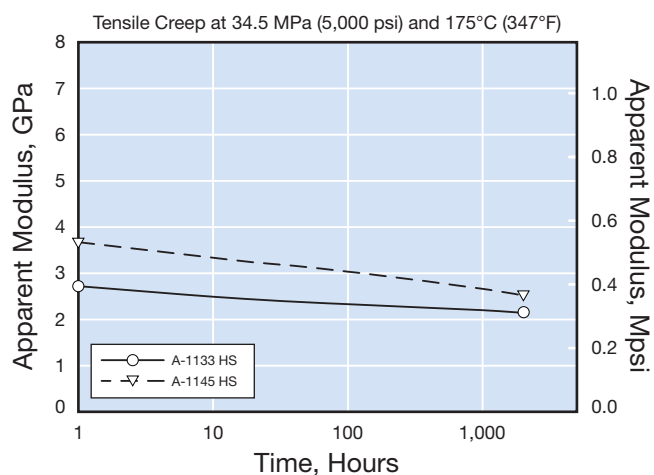


Figure 43: Apparent Modulus at 175°C (347°F) and 34.5 MPa (5 kpsi)



Isochronous Stress/Strain Curves

Another format for presenting creep data is through the use of isochronous (equal time) stress versus strain curves. To prepare an isochronous curve, plot the stresses and the resultant strains for a single time interval and draw a smooth curve through the points. Repeat this process for each time interval.

This method has the advantage of providing a concise summary of a large amount of data. The apparent modulus at any point can be calculated by dividing the stress by the indicated strain. (Please note that the figures show strain expressed in %; actual strain is the plotted value divided by 100.)

The isochronous stress/strain curves for Amodel A-1133 HS resin at 23°C, 125°C, and 175°C are shown in Figure 44.

Figure 45 shows the same information for Amodel A-1145 HS. As expected, the more glass reinforcement in the compound, the better the creep resistance.

Tensile Creep Rupture

Creep rupture is defined as a failure or rupture that occurs as a result of a sustained load. Because the stress level at which rupture occurs due to sustained load is lower than the short-term strength, creep rupture can be the limiting design property.

The objective of tensile creep rupture testing is to determine the time required for a sustained load to produce a rupture. A plot of stress versus the time to rupture is commonly known as a "creep rupture envelope". Because the strength of a material varies with temperature, a "creep rupture envelope" can be generated for each temperature of concern.

Creep rupture envelopes were developed in accordance with ASTM D2990. Tensile specimens were 3.2 mm (0.125 inch) thick injection molded ASTM D638 Type I tensile bars. The environments were the same as in the tensile creep testing above. The samples were loaded in tension using pneumatically actuated bellows to maintain indicated stress levels.

The tensile creep rupture envelopes for Amodel AS-1133 HS resin are shown in Figure 46 at 65, 100, and 150°C.

Figure 44: Isochronous Stress-Strain of A-1133 HS PPA

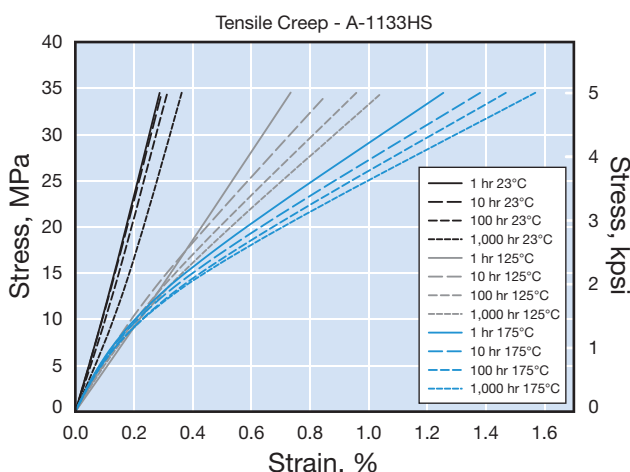


Figure 45: Isochronous Stress-Strain of A-1145 HS PPA

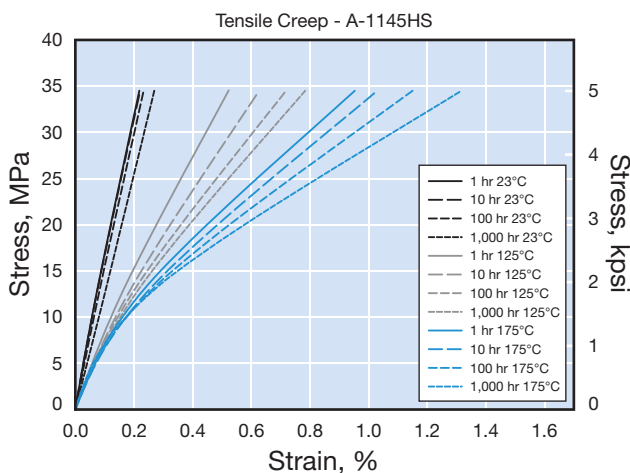


Figure 46: Tensile Creep Rupture of AS-1133 HS

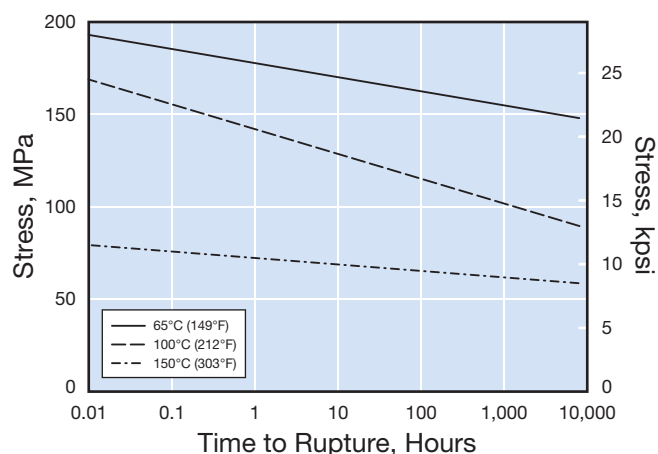


Figure 47: Apparent Flex Modulus at 69 MPa (10 kpsi) at 23°C (73°F)

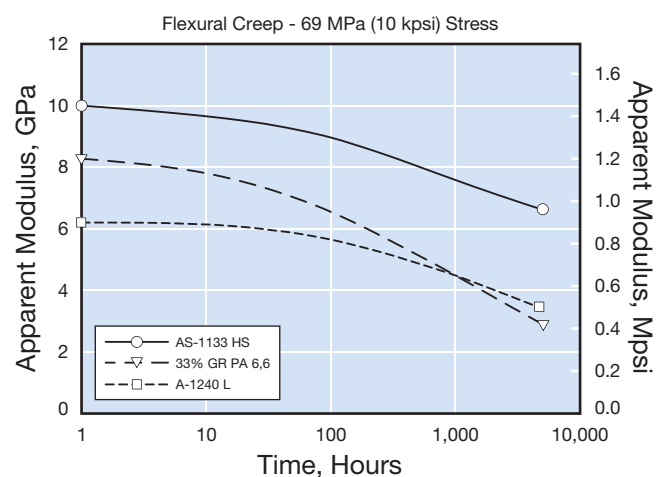
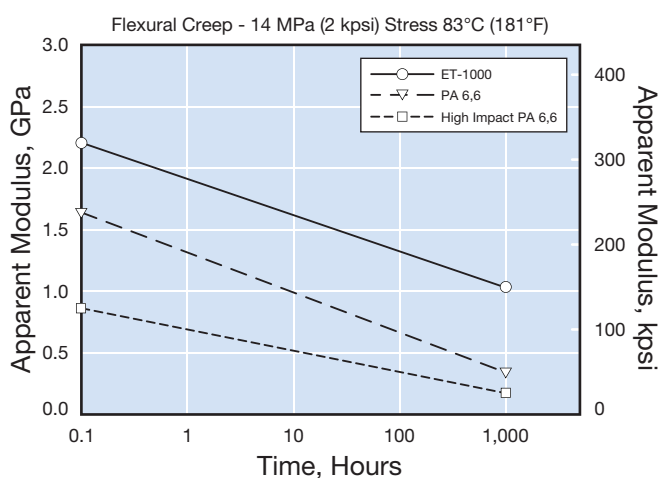


Figure 48: Apparent Flex Modulus at 14 MPa (2 kpsi) at 83°C (181°F)



Flexural Creep

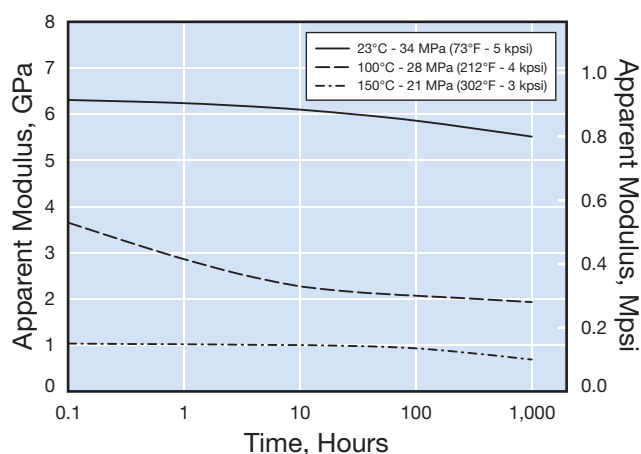
Flexural creep was determined according to ASTM D2990 using the three-point bending mode with a 50.8 mm (2 inch) span. Test specimens were 127 mm x 12.7 mm x 3.2 mm (5.0 inch x 0.5 inch x 0.125 inch) injection molded bars placed on test "dry, as molded". The environment was maintained at 50% relative humidity and 23°C (73°F). Stress levels were predetermined from flexural strength versus temperature curves and chosen to be 25% - 35% of the ultimate strength of the material at the test temperature.

Creep resistance can be predicted to a large extent by the relationship of the service temperature to the material's glass transition temperature. Typically, creep resistance is good at service temperatures much lower than T_g , and becomes poorer as service temperature approaches T_g . Therefore, it is not surprising that Amodel resins have creep resistance superior to many traditional semi-crystalline thermoplastics. For example, Amodel A-1000 resin has a glass transition temperature of 123°C (253°F) as determined by Differential Scanning Calorimetry (ASTM D3418). The corresponding T_g for PA 6,6 is 65°C (149°F). At all temperatures up to its T_g , Amodel resins do have superior creep resistance.

Figure 47 compares the apparent flexural modulus of Amodel AS-1133 HS and A-1240 L resins to a 33% glass reinforced PA 6,6. While the AS-1133 HS resin is clearly superior to the glass reinforced PA, even the mineral filled grade – Amodel A-1240 resin – has an effectively higher creep modulus after 1000 hours under load.

Figure 48 compares the apparent flexural modulus of Amodel ET-1000 resin with that of unreinforced and impact modified grades of PA 6,6 at 83°C (181°F) and 14 MPa (2 kpsi).

Figure 49: Apparent Compressive Modulus of AS-1133 HS



Compressive Creep

Compressive creep was determined according to ASTM D2990. Test specimens were 12.7mm x 12.7mm x 25.4 mm (0.5 inch x 0.5 inch x 1.0 inch) injection molded bars. The ends of the bars were machined until they were parallel to each other within 0.025 mm (0.001 inch) and perpendicular to the axis. Displacement was monitored with bonded strain gauges. As in the flexural creep experiments, the stress levels were chosen to be less than 35% of the compressive strength at the temperature of the test.

Figure 49 shows the compressive creep moduli of Amodel AS-1133 HS resin at 23°C, 100°C, and 150°C (73°F, 212°F, and 302°F). These moduli are lower than the flexural creep moduli given in Figure 47. This is due to less fiber orientation in the direction of the induced strain.

In most applications where Amodel resin will be loaded in a compressive manner, the load will be applied in the direction transverse to flow direction and consequently the fiber orientation. Therefore, the apparent moduli presented here are representative of the material's performance in typical applications.

Fatigue Resistance

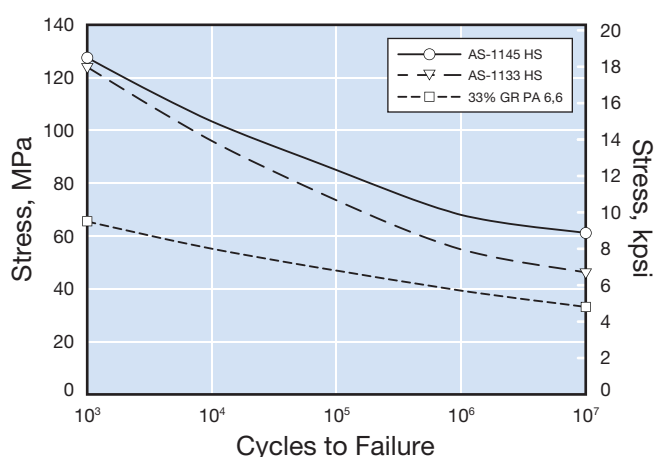
When a material is stressed cyclically, failure or rupture will occur at stress levels much lower than its short-term ultimate strength. Examples of cyclic stress would include components subjected to severe vibration, components of reciprocating or rotating devices where loading is cyclic, and mechanical devices such as gears where the cyclic load is a function of position.

This phenomenon is well known in metals. Metallurgists have defined the term "Fatigue Endurance Limit" to represent the maximum cyclical stress that a material can be subjected to without failure. Normally, this stress level corresponds to the highest stress level that does not cause failure in 10 million (10⁷) cycles.

While the term "Fatigue Endurance Limit" is sometimes used in design discussions involving plastic materials, the response of plastics to cyclic stress is more complex than the response of metals, and the term is not strictly applicable. Fatigue data is typically presented by plotting stress versus number of cycles at rupture. A smooth curve is calculated that represents the best fit to the data. For component design purposes, this S-N (stress-number of cycles) curve provides strength values appropriate for the components required life.

When designing a component that will be subjected to cyclic loading, the establishment of fatigue strength requirements is desirable. However, analysis of the fatigue strength requirements is complicated by a large number of factors that may influence them. Some of these factors are: the shape of the component; stress concentration factors; the rate of load application; any temperature change caused by load application; type of stress induced by load, that is, tensile, compressive, or shear, etc.; environmental factors, such as, chemicals, radiation, ambient temperature; residual stresses; the duty cycle; and the desired component life.

Figure 50: Flex Fatigue of GR Resins at 23°C (73°F) and 32 Hz



Fatigue Strength of Amodel Resin

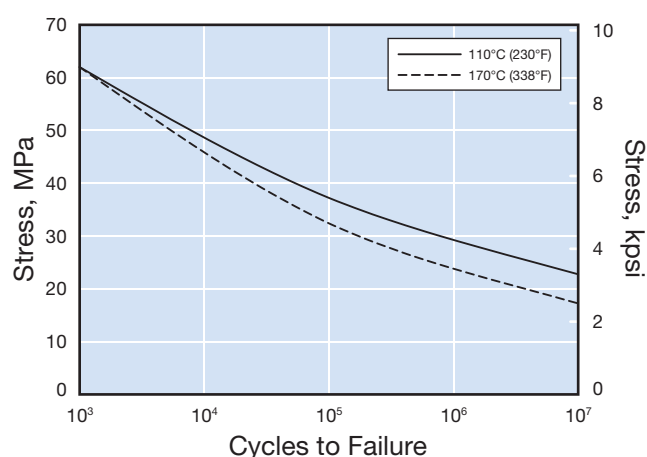
When measuring and/or comparing the fatigue strength of plastic materials, it is critical to specify the mode (tensile, compressive, or flexural), the frequency, and the stress profile.

The fatigue strength of Amodel resins was determined in accordance with ASTM test method D671. This method uses a cantilever beam configuration with a constant deflection. The results shown in Figure 50 were generated at a frequency of 32 Hz. Failure was defined when the stress level decayed to 90% of its initial value. The Amodel resins resist higher cyclic loads longer than PA 6,6.

Figure 51 gives the fatigue behavior of Amodel AS-1145 HS resin at 110° and 170°C (230° and 338°F). As expected, raising the temperature reduces the amount of cyclic stress that can be endured.

A good example of an application involving cyclical stress is a gear. As the driving gear causes the driven gear to rotate, each tooth is subject to stress. This is then followed by a period of time at low or zero stress. In designing a gear tooth, the appropriate strength criteria is the fatigue endurance limit of the material at the operating conditions of the gear.

Figure 51: Flex Fatigue of AS-1145 Resin at Elevated Temperature



After all of the calculations have been made, the part design can be modified to best utilize the properties of the selected material. Conversely, the material grade can be modified to best suit the application requirements. An extremely useful tool to verify a design is to perform Finite Element Analysis (FEA). In FEA, the part is electronically modeled and a computer program is used to simulate the anticipated loads and stresses. The resulting strain levels can be evaluated and, if necessary, part design or material changes can be made. It is much easier to make changes to the FEA model than to a fabricated part or tooling.

Even after calculations and FEA's have been performed, the best way of evaluating a material for a component subject to dynamic stresses is actual prototype testing. Prototype parts can be machined from available stock shapes and subject to performance testing under the requirements of the application. Stock shapes are usually available as extruded slabs or rods and generally exhibit slightly lower mechanical properties than the injection molded part. Additionally, the machining operations usually induce stresses that would not normally be present in an injection molded part. As a result of this, a successful prototype test imparts an extremely high confidence level in the reliability of the design.

Moisture Effects

As with most thermoplastic resins, parts made from Amodel resins can absorb moisture from the atmosphere. This absorption is a physical, not a chemical change and is therefore reversible, in that parts can be "dried out" under proper conditions. Amodel polyphthalamide resins have significant amounts of aromatic character in the polymeric "backbone" and this causes them to absorb much less moisture than aliphatic polyamides such as PA 6,6 and PA 6. As a result, the dimensions, strength, and stiffness of Amodel parts will be significantly less affected by the absorption of moisture than traditional aliphatic PA parts. Since moisture is ubiquitous, knowledge of the effects of moisture on the properties of a material is critical to the design engineer trying to meet end use requirements.

Significance of Moisture Absorption

When a polymer absorbs atmospheric moisture, a number of changes may occur. Obviously, the part weight will increase and this weight increase is typically used to measure the amount of moisture absorbed. Additionally, there may be some dimensional changes, generally an increase; parts will become larger. The presence of reinforcing fillers such as fiberglass may result in anisotropic dimensional change due to the fact that the fibers align themselves in the direction of polymer flow as the resin fills the tool. Similar to mold shrinkage values, dimensional changes due to moisture absorption are often reported in flow and transverse directions.

Mechanical properties may also be affected by moisture absorption. Generally, a slight decrease in physical properties such as tensile and flexural strength are seen. The respective moduli also decrease slightly. Impact strength values tend to increase slightly since the presence of moisture can tend to plasticize the polymer. Since water is a conductor, absorbed moisture can have a negative effect on the dielectric properties of a molded part.

Manufacturers of polymers that absorb moisture usually publish two sets of data, one listing test results on test specimens that have no absorbed moisture, commonly referred to as "Dry-As Molded" (DAM), and a second set of data that is generated on test specimens that have been allowed to come to an equilibrium weight in a 50% Relative Humidity environment, known as "50% RH". Polymers like PA 6 and PA 6,6 absorb moisture relatively quickly and reach equilibrium in a 50% Relative Humidity environment quickly. Providing 50% RH data for these materials is fairly easy and extremely relevant to design, as will be understood in the subsequent discussion.

On the other hand, polymers like Amodel PPA absorb moisture very slowly and can take years to reach an equilibrium at 50% RH. In order to provide 50% RH data, a method was developed to accelerate the conditioning of test specimens. This involves boiling the test specimens in an aqueous solution of potassium acetate until constant specimen weight is obtained, typically for several days. As would be expected, this accelerated procedure has some side effects which influence the test values. In the accelerated procedure, the test specimens are annealed and stress relieved, which may actually cause an improvement in the property test results. Conversely, exposure to boiling water can cause some hydrolysis of the polymer, yielding a loss in properties. Additionally, exposure to the boiling salt solution has been shown to degrade the bond between the polymer and a reinforcing media, such as fiberglass, resulting in a loss of mechanical properties such as tensile, flexural and impact. Nonetheless, the effect of absorbed moisture on Amodel resins is minimal.

Moisture Absorption and Glass Transition Temperature (T_g)

Perhaps much more significant than the effect of moisture absorption on room temperature properties is the effect of moisture absorption on the Glass Transition Temperature (T_g) of a polymer. By definition, the T_g of a polymer is the temperature above which, the crystalline region of the polymer matrix is no longer dominant over the amorphous region. Above the T_g , the amorphous region is dominant and there is a noticeable loss in mechanical properties as seen in the discussion on mechanical properties vs. temperature. In unreinforced grades, this is very significant in that the properties drop to levels which are essentially useless from a mechanical design perspective. In the reinforced grades, while the properties above T_g are still useful from a design perspective, the loss of mechanical properties is significant enough to make major design considerations.

The effect of absorbed moisture on semi-crystalline polymers is to lower the glass transition temperature. The severity of reduction is dependent on the specific polymer and the amount of moisture absorbed.

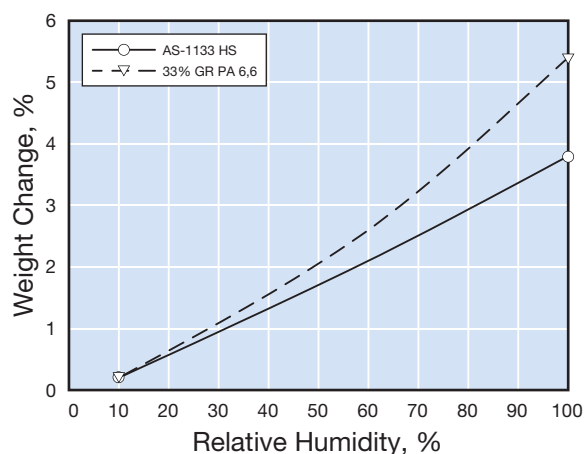
This phenomenon becomes of significant concern when designing with a polymer that has a T_g near or below 100°C (212°F). For example, a polymer with a T_g of 80°C (Dry as molded) might exhibit a T_g of only 60°C after absorbing moisture. The designer must consider the significant loss in properties above 60°C due to the reduction in T_g when making decisions. Polymers with even lower dry T_g 's can have a T_g reduction to at or near room temperature with moisture absorption. This can create a significant design consideration.

Alternatively, consider the Amodel A-1000 series polymers, which have a dry T_g of 123°C. Absorption of moisture at room temperature can reduce this T_g to 84°C and have a slight reduction in "room temperature" properties. However, since moisture absorption is a reversible phenomenon (moisture absorption is a physical, not a chemical reaction), at temperatures above 100°C, the polymer actually dries out, returning the T_g to the original 123°C value. Therefore, the T_g reduction due to moisture absorption is essentially insignificant for Amodel resins. The following data are presented for consideration in applications in which moisture absorption is expected at ambient temperatures and a slight loss of properties may be anticipated. Since the polymer "desorbs" moisture and regains dry properties on exposure to temperatures above 100°C, moisturized test data above 100°C is irrelevant for Amodel resins, but quite important for polymers that have a T_g near or below 100°C.

Absorption Amount

As has been mentioned, water absorption is a reversible process. At each specified relative humidity and temperature, a resin will absorb moisture until an equilibrium is established. At equilibrium, a polymer absorbs moisture at the same rate it releases moisture, achieving a constant weight. Since the polymer, not the filler or reinforcement additives absorb the moisture, the amount of water absorbed is proportional to the amount of polymer present in each grade, the more highly filled grades will have lower absorption than the unfilled grades. Figure 52 compares the increase in weight due to moisture absorption of Amodel AS-1133 HS to that of 33% glass reinforced PA 6,6 at room temperature and specified relative humidities. The 33% glass reinforced PA 6,6 absorbs significantly more moisture than Amodel AS-1133 HS resin. The amount of time required for Amodel resins to reach equilibrium is also significantly longer than PA 6,6.

Figure 52: Moisture Absorption of GR Resins



Effect of Moisture on Strength and Stiffness

Figure 53 compares the tensile strength of Amodel AS-1133 HS resin to that of 33% glass reinforced PA 6,6 at 73°F (23°C) and specified moisture content. The tensile strength of the Amodel resin is superior to that of the PA "dry, as molded" and the difference increases with higher moisture levels.

Figure 53: Effect of Moisture on Tensile Strength of GR Resins

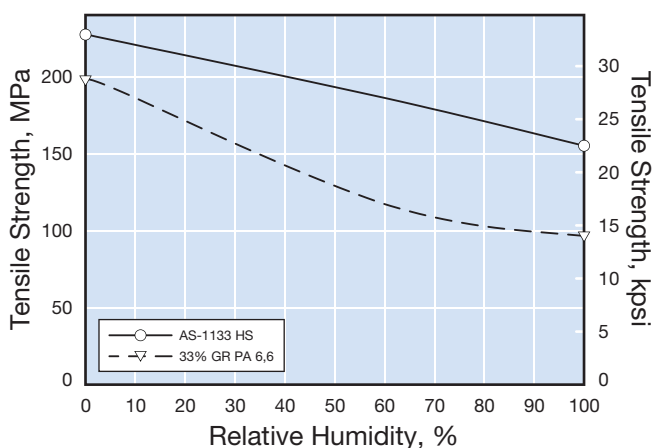


Figure 54: Effect of Moisture on Flex Modulus of GR Resins

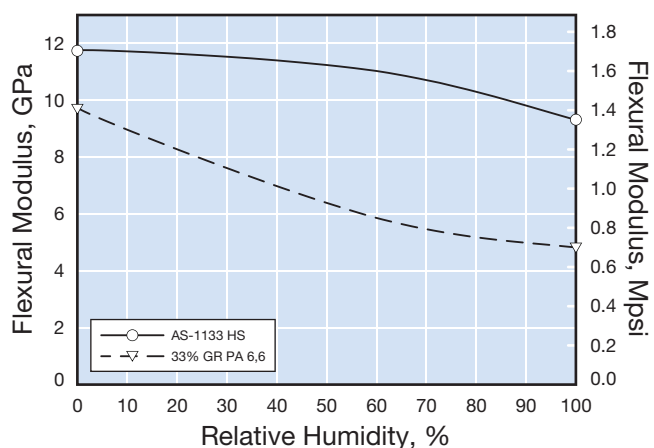
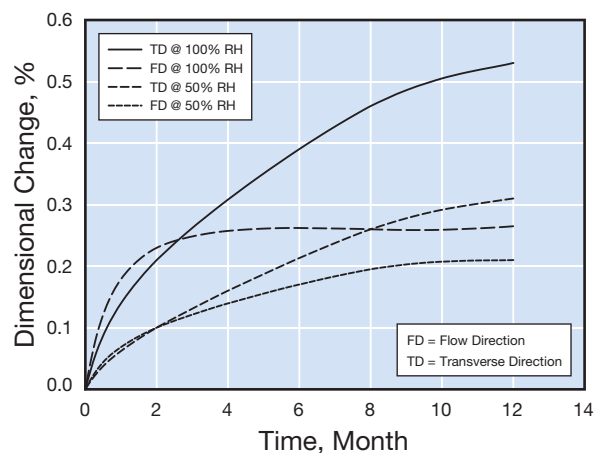


Figure 54 compares the flexural modulus of Amodel AS-1133 HS resin to that of a 33% glass reinforced PA 6,6 at 73°F (23°C) and various moisture contents. The modulus of the Amodel resin is higher as molded and remains relatively constant. The modulus of the PA resin drops rapidly with increasing moisture level and temperature due to the fact that the T_g of PA 6,6 is below 100°C and decreases further with moisture absorption.

Figure 55: Dimensional Change of 33% GR PPA



Dimensional Change due to Moisture

To evaluate the effect of moisture absorption on part dimensions, plaques 102 mm x 102 mm x 3.6 mm (4 inch x 4 inch x 0.125 inch) were molded, measured, and then placed into environments at room temperature, 23°C (73°F), and either 50% or 100% relative humidity. Periodically the plaques were removed and measured. The direction of flow during the molding process was noted and data for both the flow direction and transverse to flow was reported. The dimensional change was calculated by subtracting the initial length from the final length, dividing the result by the original length, and multiplying the result by 100 to express the change in percent.

Figure 55 shows the results of this testing for Amodel AS-1133 resin. Even at 100% relative humidity, the dimensions continue to change for a considerable length of time. These graphs show that after one year, the rate of change has greatly diminished but the dimensions are still changing. Dimensions in the flow direction change less than the transverse direction, most likely due to alignment of the reinforcement fiber in the flow direction. The magnitude of the dimensional change is relatively small (less than 0.6%), but could be important in applications requiring extremely tight dimensional tolerances and stability.

Figure 56: Dimensional Change of 40% Mineral Filled PPA

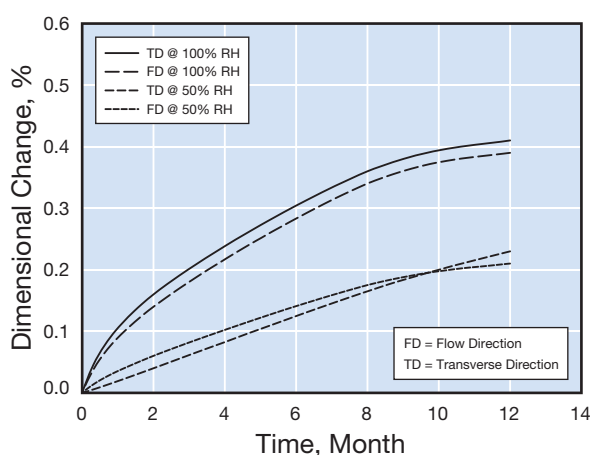
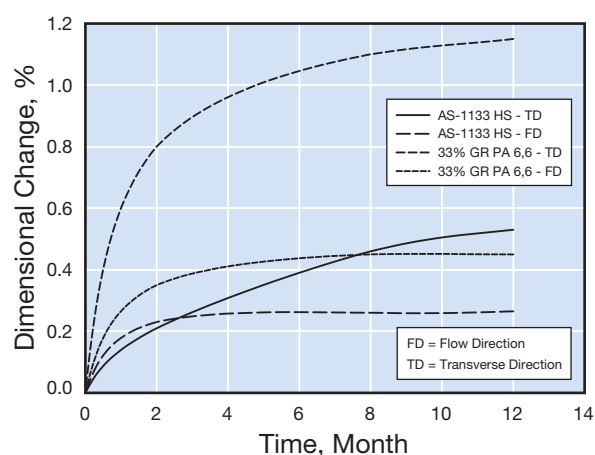


Figure 56 shows the same results for Amodel A-1340 PPA, a 40% mineral filled grade. Not only is the magnitude of the dimensional change smaller, but the difference between flow and transverse direction is almost negligible.

Dimensional Change Compared to PA 6,6

Figure 57 compares the dimensional change due to moisture absorption of Amodel AS-1133 HS resin with that of 33% glass reinforced PA 6,6 at 100% RH. To ensure a valid comparison, both resins were molded under conditions that promote maximum crystallinity. In the case of the Amodel resin, a mold temperature of 135°C (275°F) was used. For the PA 6,6, the mold temperature was 93°C (200°F). Plaques with a thickness of 3.2 mm (0.125 inch) were exposed to 100% RH at room temperature.

Figure 57: Dimensional Comparison of GR PA 6,6 to GR PPA at 100% RH



Amodel resin absorbs moisture much more slowly than PA 6,6, because the diffusion coefficient at room temperature of water in PA 6,6 is approximately five times larger than that of Amodel resins. Therefore, for these plaques, PA 6,6 reaches equilibrium in approximately four months while Amodel AS-1133 HS resin requires over two years.

Thermal Properties

In general, the thermal properties characterize the way a material responds to changing temperatures, both in the short and long term. Thermal properties include the effects of temperature on:

- Strength and stiffness
- Dimensions
- Chemical changes in the polymer itself due to thermal or oxidative degradation
- Softening, melting, or distortion
- Morphology

The properties of the material in the molten state are discussed in the Amodel PPA Processing literature. The behavior of the material while burning is discussed in the section on combustion properties.

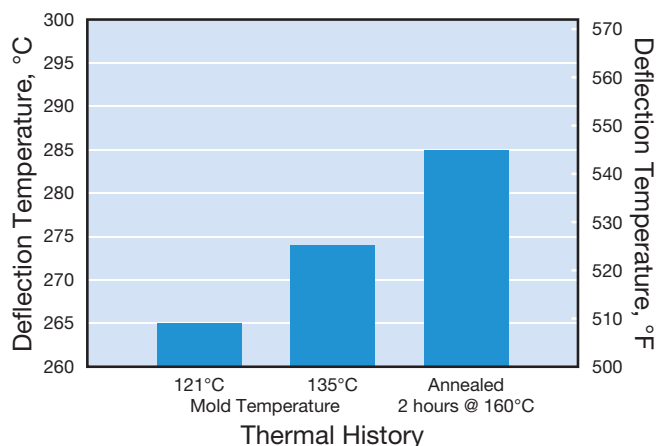
Heat Deflection Temperature – HDT

The tests most commonly used by the plastics industry to measure short-term thermal capability are ASTM D648, *Standard Test Method for Deflection Temperature of Plastics Under Flexural Load* and ISO 75, *Plastics - Determination of Temperature of Deflection Under Load*. These tests are commonly referred to as Heat Distortion Temperature (HDT) or Deflection Temperature under Load (DTUL). Both tests are similar in that the test specimen is supported at two points while a load is applied to the center. The temperature is increased at a constant rate until the specimen deflects a specified amount as indicated by a dial micrometer.

Although details such as specimen geometry, deflection endpoint, specimen orientation, and distance between the supports are different for these methods, the desired stress levels for both methods includes a loading of 1.8 MPa (264 psi) and 0.45 MPa (66 psi). When comparing data from multiple sources, it is important to verify that the same test method was used for all the data being compared. In the product property tables starting on page 6, data collected using both methods is listed. Examination of the data will reveal a considerable amount of difference between the values for some grades.

Certain test parameters can have a significant influence upon the results obtained in this test. The designer should be certain that data from multiple sources are comparable. The most common and critical error is to compare the results from testing performed at 1.8 MPa (264 psi) with results obtained from testing at 0.45 MPa (66 psi). All Amodel resins are tested at 1.8 MPa, unless otherwise specified. The other test parameters that should be considered are specimen thickness and thermal history. The test may be performed as molded or after heat treating or "annealing" for several hours at

Figure 58: Mold Temperature and Annealing Effects on HDT of Amodel AS-1133 HS

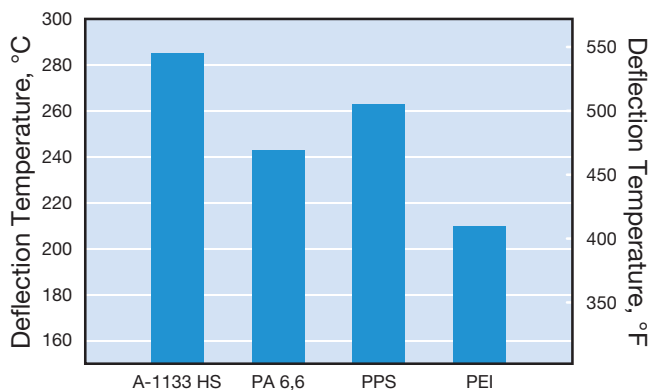


a temperature slightly above the glass transition temperature, or about 160°C (320°F) for Amodel PPA.

In general, annealing reduces the variability in deflection temperature measurements, in addition to raising the value slightly. Figure 58 shows the effects of mold temperature and annealing on deflection temperature at 1.8 MPa (264 psi) for Amodel AS-1133 HS resin. As can be seen, mold temperature and/or annealing effects can cause the deflection temperature to vary by as much as 17°C (30°F). The deflection temperature data in this manual were generated on specimens annealed at 160°C (320°F) for 2 hours.

Deflection Temperature is a modulus at temperature measurement. Classical stress/strain analysis indicates that the ASTM D648 test actually measures the temperature at which the flexural modulus is 240 MPa (35,000 psi) when the applied stress is 0.45 MPa (66 psi), or 965 MPa (140,000 psi) when the applied stress is 1.8 MPa (264 psi). Because the test method directs that the indicator be re-zeroed after five minutes, any creep strain that occurs in the first five minutes is effectively subtracted from the endpoint strain lowering the actual modulus at the end point of the test. The initial modulus can be related to the creep strain.

Figure 59: HDT of 30% - 33% GR Resins



In summary, deflection temperature does not measure thermal capability, it simply provides one point on the modulus versus temperature curve.

In general, HDT can only be used as a general indicator of short-term thermal capability. It is useful for comparing similar materials but can be misleading if, for example, an amorphous material is compared to a semi-crystalline material. It doesn't provide any information about long-term thermal stability. The actual loads and performance requirements will dictate the suitability of the material. Many semi-crystalline resins can be used in applications that experience temperatures higher than their deflection temperature value.

Deflection Temperature Values for Amodel Resins

Deflection temperature values by both ASTM D648 and ISO 75Af for 19 representative grades of Amodel PPA are shown in the Tables starting on page 7.

Figure 59 compares the deflection temperature at 1.8 MPa (264 psi) of Amodel AS-1133 HS resin with a 33% glass fiber reinforced PA 6,6, a 30% glass fiber reinforced polyphenylene sulfide, and a 30% glass fiber reinforced polyetherimide. Amodel resin offers a 75°C HDT advantage relative to PEI, a 42°C advantage relative to PA 6,6, and a 22°C advantage relative to PPS.

Coefficient of Linear Thermal Expansion

The dimensions of most materials increase with increasing temperature. The coefficient of linear thermal expansion (α) is the ratio of the change in length to the change in temperature.

If the coefficient α is known, the change in length of a uniform straight bar raised to a temperature T_f can be calculated from:

$$\Delta L = \alpha L (T_f - T_o)$$

where

ΔL = change in length

L = original length

α = coefficient of linear thermal expansion

T_f = final temperature

T_o = original temperature

The coefficient of linear thermal expansion (α), as measured by ASTM E831, of several Amodel grades and some common metals is given in Table 19. This method provides an average value for the expansion coefficient over a temperature range.

The thermal expansion behavior of metals is uniform over the temperature range of concern. As shown in Table 19, the thermal expansion coefficients of the polymer materials are a function of the temperature range used for the measurement. In general, the polymer materials expand slightly more above their glass transition temperature than they do below it and the behavior in the vicinity of the T_g is also somewhat non-linear. However, over large temperature ranges, the variations are usually insignificant and excellent prediction of dimensional properties can be obtained using the values provided in the table. Also, the addition of glass fiber and other reinforcing additives results in the thermal expansion becoming directional. Since fibers tend to become oriented in the flow direction, and since glass has a lower thermal expansion coefficient than the polymers, the coefficient of expansion are generally lower in the flow direction than the transverse direction.

The values shown in Table 19 should allow the design engineer to estimate the magnitude of the thermal stresses in parts molded from Amodel resins due to thermal expansion.

Table 19: Coefficients of Linear Thermal Expansion

 Values are 10⁻⁶ L/L per degree where L is Length

Temperature	0-50 °C (32-122°F)				50-100 °C (122-212°F)				100-150 °C (212-302°F)				150-200 °C (302-392°F)			
	FD ⁽¹⁾		TD ⁽²⁾		FD		TD		FD		TD		FD*		TD	
Direction																
Units	/°C	/°F	/°C	/°F	/°C	/°F	/°C	/°F	/°C	/°F	/°C	/°F	/°C	/°F	/°C	/°F
Glass-Reinforced Grades																
A-1133 HS	24	13	50	28	24	13	60	33	27	15	99	55	27	15	130	72
A-1145 HS	22	12	49	27	21	12	58	32	27	15	88	49	15	8	122	68
A-6135 HN	23	13	59	33	21	12	63	35	16	9	96	53	15	8	109	61
AS-4133 HS	20	11	64	36	20	11	87	48	20	11	114	63	9	5	126	70
Toughened Grades																
AT-1002 HS	70	39	84	47	85	47	101	56	145	81	126	70	112	62	153	85
ET-1000 HS	68	38	80	44	85	47	81	45	147	82	97	54	142	79	113	63
ET-1001 L	71	39	69	38	94	52	80	44	167	93	88	49	170	94	118	66
AT-5001	93	52	106	59	136	76	144	80	184	102	184	102	153	85	142	79
Toughened Glass-Reinforced Grades																
AT-1116 HS	20	11	72	40	23	13	77	43	16	9	116	64	16	9	133	74
AT-6115 HS	23	13	83	46	21	12	97	54	34	19	116	64	26	14	121	67
Flame Retardant Grades																
AFA-1633 VO Z	18	10	56	31	16	9	72	40	11	6	93	52	3	2	120	67
Mineral and Mineral/Glass Filled Grades																
A-1240 L	26	14	68	38	19	11	91	51	18	10	117	65	15	8	121	67
A-1340 HS	34	19	50	28	42	23	60	33	51	28	103	57	19	11	103	57
A-1565 HS	20	11	34	19	20	11	39	22	20	11	72	40	14	8	89	49
AS-1566 HS	17	9	36	20	17	9	44	24	17	9	59	33	16	9	85	47
AP-9240 NL	54	30	48	27	87	48	61	34	110	61	81	45	87	48	110	61
Common Metals																
Zinc Alloy	27	15	27	15	27	15	27	15	27	15	27	15	27	15	27	15
Aluminum Alloy A-360	21	12	21	12	21	12	21	12	21	12	21	12	23	13	23	13
Stainless Steel	17	9	17	9	17	9	17	9	17	9	17	9	18	10	18	10
Carbon Steel	11	6	11	6	11	6	11	6	11	6	11	6	12	7	12	7

⁽¹⁾ FD = Flow Direction

⁽²⁾ TD = Transverse Direction or Perpendicular to Flow Direction

Table 20: Thermal Conductivity of Amodel PPA Resins

Grades	Additive	Amount, %	Average Temperature					
			40°C (104°F)		100°C (212°F)		150°C (302°F)	
			W/ mK	Btu in/ hr ft ² °F	W/ mK	Btu in/ hr ft ² °F	W/ mK	Btu in/ hr ft ² °F
A-1115 HS	glass	15	0.289	2.00	0.307	2.13	0.324	2.25
AS-1133 HS	glass	33	0.341	2.37	0.360	2.50	0.376	2.61
AS-1145 HS	glass	45	0.372	2.58	0.393	2.73	0.409	2.84
A-1240 L	mineral	40	0.377	2.62	0.388	2.69	0.399	2.77
A-1340 HS	mineral/glass	25/15	0.422	2.93	0.430	2.98	0.436	3.02

Thermal Conductivity

Thermal conductivity is the rate at which heat energy will flow through a material. This property is important in applications where the polymeric material is used as a thermal insulator, or where heat dissipation is of concern.

The measurement of thermal conductivity was performed in accordance with ASTM F433. The test is conducted by placing a sample between plates controlled at different temperatures and monitoring the heat flow through the sample. The thermal conductivity was determined at three average temperatures, 40°C (104°F), 100°C (212°F), and 150°C (302°F), by setting the hot plate about 7°C (12°F) above the average and setting the cold plate about 7°C (12°F) below the average temperature.

The thermal conductivity of various grades of Amodel resin was measured at each of the stated temperatures and the results are presented in Table 20. Higher thermal conductivity values indicate greater heat flow, while lower values indicate better thermal insulating characteristics.

Figure 60 shows that the thermal conductivity increases with glass content and temperature.

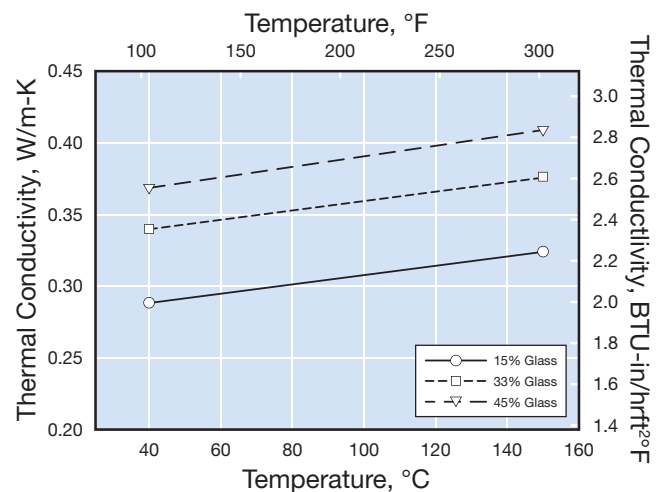
Figure 60: Thermal Conductivity of Glass Reinforced Amodel PPA

Figure 61: Amodel A-1000 PPA, Specific Heat vs. Temperature

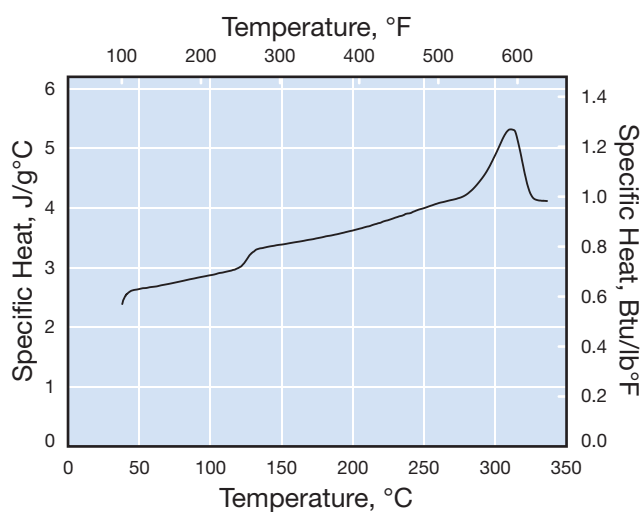


Figure 63: Amodel A-5000, Specific Heat vs. Temperature

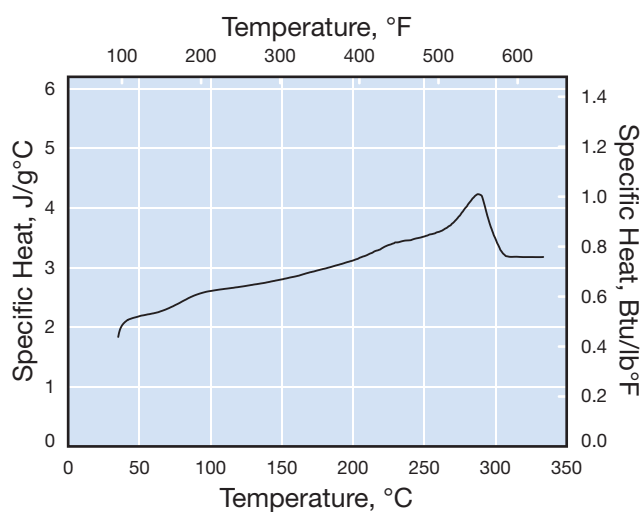


Figure 62: Amodel A-4000, Specific Heat vs. Temperature

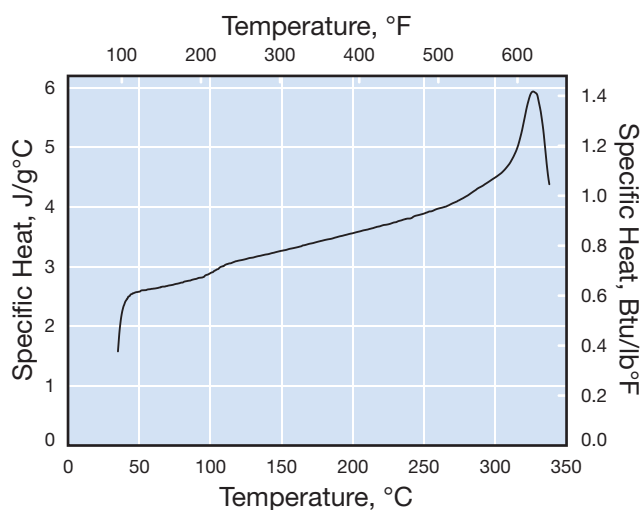
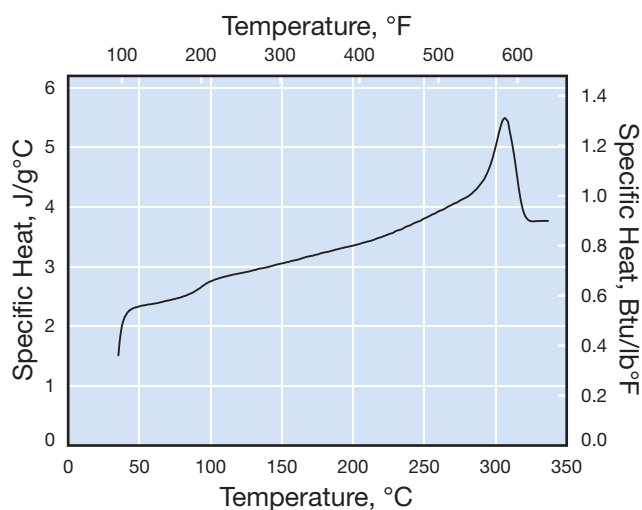


Figure 64: Amodel A-6000, Specific Heat vs. Temperature



Specific Heat

Specific heat is defined as the amount of heat required to change the temperature of a unit mass one degree. Figures 61 through 64 show the specific heat as a function of temperature for the Amodel base resins. Notice that the specific heat changes significantly at the melting point. This behavior is typical of semi-crystalline thermoplastics.

This information can be used by process engineers to calculate the heat input needed to process Amodel resins on equipment such as extruders or injection molding machines.

Thermal Stability

The general term, thermal stability, is used to describe the ability of a material to resist loss of properties due to heat. Various methods are used to evaluate this tendency. In the next section, we will discuss several of these methods, including thermogravimetric analysis, and long-term heat aging.

Thermogravimetric Analysis (TGA)

Thermogravimetric analysis is performed by increasing the temperature of a small sample of the test material at a constant rate while monitoring its weight. The atmosphere is controlled and the test can be performed using air or an inert atmosphere, such as nitrogen. Figure 65 shows the weight loss of Amodel A-1000 resin as a function of temperature in air at a heating rate of 10°C/min (18°F/min). The graph shows that Amodel PPA resins are thermally stable beyond the recommended upper processing temperature limit of 350°C (662°F).

Thermal Aging

Nearly all polymeric materials exhibit some loss of performance properties after long-term exposure to elevated temperatures. While some polymers are more stable than others, the property loss is typically a function of both exposure time and temperature. Because the property losses result from both oxidative attack and thermal degradation, the term "thermal oxidative stability" is frequently used.

Thermal oxidative stability limits the acceptable long-term use temperature of some polymers. To evaluate these long-term effects on the properties of Amodel polyphthalamide, molded test specimens of Amodel resins were placed in circulating air ovens at several elevated temperatures. Specimens were removed from the oven at regular intervals, then tested at room temperature for tensile strength and impact resistance.

Typically, these aging tests are run until the property being monitored has been reduced to one-half its starting value. The aging tests are conducted at several aging temperatures and an "Arrhenius Plot" is prepared. An "Arrhenius plot" plots the heat aging time required to reduce a property to one-half of its starting value, sometimes referred to as its half-life, against the reciprocal of the aging temperature in degrees Kelvin. The advantage of analyzing the data in this manner is that the plot is theoretically a straight line and, therefore, easily extrapolated.

Figure 65: Thermogravimetric Analysis of A-1000 in Air

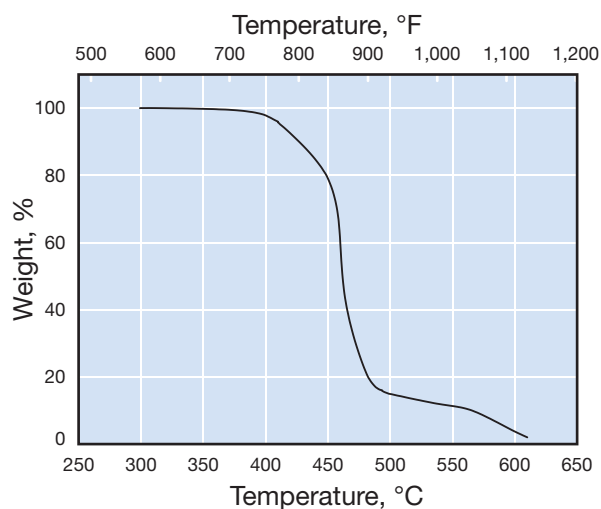


Figure 66: Thermal Aging Comparison - Tensile Strength

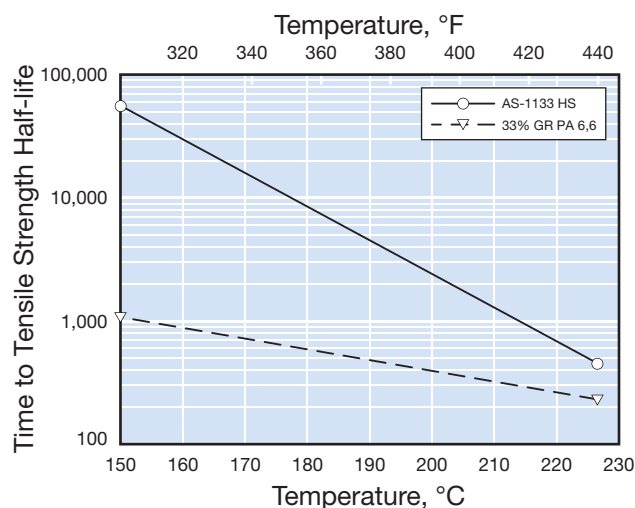


Figure 66 shows the plot of tensile strength half lives of Amodel AS-1133 HS resin and GR PA 6,6 versus the aging temperature. Amodel PPA maintains its tensile strength longer than PA 6,6 does.

Figure 67: Thermal Aging Comparison - Izod Impact

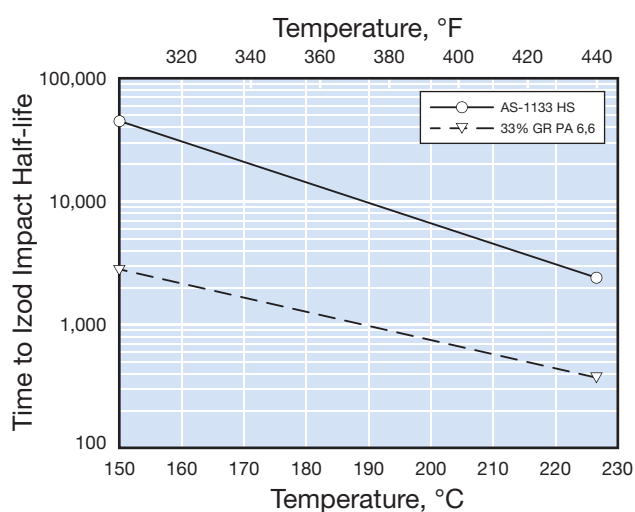


Figure 67 shows the thermal aging curves for notched Izod half lives of Amodel AS-1133 HS resin and GR PA 6,6 versus aging temperature. Amodel PPA also requires longer aging times before loss of impact resistance occurs than the PA 6,6 resin.

Thermal aging tests like this are used to compare plastic materials and to estimate their service life. The service life of a material at a particular end use temperature will be largely dependent upon the requirements of the application and should be judged on the basis of its heat aging data and actual or simulated end use testing.

Relative Thermal Index (UL)

A primary function of Underwriters Laboratories Inc is to assist in the assessment of the risk of fire associated with electrical devices. Because insulating materials may deteriorate over time some method of evaluating this tendency and providing guidance to designers and users of electrical devices was required. Underwriters Laboratories (UL) has developed a method and rating system for this purpose. This method is UL Standard 746B, Polymeric Materials, Long-Term Property Evaluation. A similar method is ASTM D3045, Standard Practice for Heat Aging of Plastics Without Load.

Based on the results of aging tests as described in the previous section, Underwriters Laboratories assigns a rating called the "Relative Thermal Index" to insulating materials. Because all material properties do not decay at the same rate, a material may have different Relative Thermal Indices for electrical properties, mechanical properties without impact, and mechanical properties with impact.

The Relative Thermal Index or RTI is determined by a statistical analysis of thermal aging data for the properties being evaluated. The RTI predicts the aging temperature that a material can endure for 100,000 hours and still retain at least fifty percent of the initial property or properties being measured.

Because the rate of decay is greater for thinner specimens, UL gives RTI ratings for each thickness tested.

To obtain a UL RTI rating, a long-term heat aging program is performed. Sets of test specimens molded from the material to be tested are put into ovens at preset temperatures. Periodically specimens are removed and tested. The results for each aging temperature are plotted on a time versus property graph, until the property being measured has declined to 50% or less of its initial value. This combination of time and aging temperature can be referred to as the "half-life" for that property, material, and thickness.

The half-lives (time to 50% or less) for a particular property, which were experimentally determined at four aging temperatures, are plotted against the reciprocal of the absolute aging temperature. The points should establish a straight line which can be extrapolated to predict the half-life of the material for the particular property at other temperatures. This is called an "Arrhenius plot".

To estimate the RTI for the material, the best fit straight line is drawn through the four half-life points for tensile strength and extended to 100,000 hours. The temperature at which this line crosses the 100,000 hours line is an estimate of the RTI for the material. If only three half-life points are available, such as when the data for the fourth temperature is still under test, then a provisional RTI can be granted. The RTI assigned by UL may be somewhat lower as statistical methods are used to compensate for experimental variability.

Testing of Amodel resins for the establishment of UL Relative Thermal Indices is a continuing long-term activity. The UL ratings of some Amodel resins when this manual was printed is shown in Table 21. Because this testing is ongoing, the Underwriters Laboratories website (<http://data.ul.com>) should be consulted for the latest RTI's.

Table 21: Relative Thermal Indices of Amodel PPA Grades

Grade	Color	Thickness, mm	Relative Thermal Index (RTI), °C		
			Electical	Mechanical	
				With Impact	Without Impact
AFA-4133 V0 Z	ALL	0.75	130	130	130
		1.5	130	130	130
		3.0	130	130	130
AFA-6133 V0 Z	ALL	0.75	130	130	130
		1.5	130	130	130
		3.0	130	130	130
AFA-6145 V0 Z	ALL	0.75	140	—	130
		1.5	140	—	130
		3.0	140	140	140

Combustion Properties

This section describes the resistance of Amodel resins to burning and ignition, and the smoke density characteristics of the material once it has been ignited. Described below are glow wire test results, classifications according to UL 94 and ASTM smoke density test results.

Glow Wire Testing

The ability to support and sustain ignition in plastic materials may be characterized by the standardized glow wire test. This test simulates conditions present when an exposed, current carrying conductor contacts an insulating material during faulty or overloaded operation. The test method followed is referenced in IEC 695-2-1/3.

The glow wire test apparatus consists of a loop of heavy gauge nickel-chromium resistance wire, a thermocouple, and a sample mounting bracket.

During the test, an electrical current is passed through a nickel-chromium loop in order to obtain a predetermined temperature. The sample is then brought in contact with the wire for 30 seconds. The test is passed if after withdrawal, the sample displays no flame or glowing, or if so, it is self-extinguishing after 30 seconds.

The test can be applied at one or more recommended temperatures and at any wall thickness needed. Recommended temperatures are 550°C (1022°F), 650°C (1202°F), 750°C (1382°F), 850°C (1562°F), and 960°C (1760°F). Thickness is usually mandated by the design or the requirements of the device. It is most difficult to resist ignition at the high glow wire temperature and thinner wall sections.

The UL definitions for the parameters usually reported are shown in Table 22.

Amodel resins have passed glow wire testing as shown in Table 23.

Table 22: UL Definitions of GWIT and GWFI

IEC Glow-Wire Ignitability Temperature (GWIT)

In accordance with IEC 695-2-1/3, is expressed as the temperature (in °C), which is 25°C hotter than the maximum temperature of the tip of the glow wire which does not cause ignition of the material during three subsequent tests

IEC Glow-Wire Flammability Temperature (GWFI)

In accordance with IEC 695-2-1/2, is expressed as the highest temperature (in °C) at which, during three subsequent tests, flaming or glowing of the test specimen extinguish within 30 seconds after removal of the glow wire without ignition of the indicator by burning drips or particles.

Table 23: Glow Wire Results

Grade ⁽¹⁾	GWIT		GWFI	
	°C	°F	°C	°F
A(AS)-1133 HS	725	1,337	725	1,337
AT-6115 HS	750	1,382	800	1,472
AT-6130	725	1,337	750	1,382
AS-1566 HS	775	1,427	800	1,472
AS-4133 HS	750	1,382	750	1,382
AFA-6133 V0 Z	960	1,760	960	1,760

⁽¹⁾All samples tested at 0.8 mm (0.031 inch) thickness

Table 24: Smoke Density

Grade	D _s @ 4 min	D _m	D _m Corr.
Flaming Mode			
AS-1133 HS	565	510	469
Non-Flaming Mode			
AS-1133 HS	3	162	162

Smoke Density Test (NBS)

When a material burns, smoke is generated. The quantity and density of the generated smoke is important in many applications. ASTM E662, Standard Test Method for Specific Optical Density of Smoke Generated by Solid Materials, provides a standard technique for evaluating relative smoke density. This test was originally developed by the National Bureau of Standards (NBS), and is often referred to as the NBS Smoke Density test. The data in Table 24 was generated in both flaming and non-flaming modes. A six tube burner is used to apply a row of flamelets across the lower edge of the specimen. A photometric system aimed vertically is used to measure light transmittance as the smoke accumulates. The specific optical density (D_s) is calculated from the light transmittance. The maximum optical density is called D_m.

Vertical Flammability per UL 94

The UL 94 flammability standard established by Underwriters' Laboratories is a system by which plastic materials can be classified with respect to their ability to withstand combustion. The flammability rating given to a plastic material is dependent upon the response of the material to heat and flame under controlled laboratory conditions and serves as a preliminary indicator of its acceptability with respect to flammability for a particular application. The actual response to heat and flame of a thermoplastic depends on other factors such as the size, form, and end-use of the product using the material. Additionally, characteristics in end-use application such as ease of ignition, burning rate, flame spread, fuel contribution, intensity of burning, and products of combustion will affect the combustion response of the material.

Three primary test methods comprise the UL 94 standard. They are the Horizontal Burning Test, the 20 MM Vertical Burning Test, and the 500 MW Vertical Burning Test.

Horizontal Burning Test

For a 94HB classification rating, injection molded test specimens are limited to a 125 mm (5.0 inch) length, 13 mm (0.5 inch) width and the minimum thickness for which the rating is desired. The samples are clamped in a horizontal position with a 20 mm blue flame applied to the unclamped edge of the specimen at a 45 degree angle for 30 seconds or so as soon as the combustion front reaches a premarked line 25 mm from the edge of the bar. After the flame is removed, the rate of burn for the combustion front to travel from the 25 mm line to a premarked 100 mm line is calculated. At least three specimens are tested in this manner. A plastic obtains an HB rating by not exceeding a burn rate of 40 mm/min for specimens having a thickness greater than 3 mm or 75 mm/min for bars less than 3 mm thick. The rating is also extended to products that do not support combustion to the 100 mm reference mark.

Amodel AS-1133 HS resin has obtained a 94HB rating in the Horizontal Burning Test, at thicknesses down to 0.8 mm in a black color.

20 MM Vertical Burn Test

Materials can be classified V-0, V-1, or V-2 on the basis of results obtained from the combustion of samples clamped in a vertical position. The 20 MM Vertical Burn Test is more aggressive than the HB test and is done on samples that measure 125 mm long, 13 mm wide, and the minimum thickness at which the rating is desired (typically 0.8 mm or 1.57 mm). The samples are clamped in a vertical position with a 20 mm high blue flame applied to the lower edge of the clamped specimen. The flame is applied for 10 seconds and removed. When the specimen stops burning, the flame is reapplied for an additional 10 seconds and then removed. A total of five bars are tested in this manner. Table 25 lists the criteria by which a material is classified in this test.

Table 25: UL Criteria for Classifying Materials V-0, V-1, or V-2

Criteria Conditions	V-0	V-1	V-2
Afterflame time for each individual specimen, (t_1 or t_2)	$\leq 10s$	$\leq 30s$	$\leq 30s$
Total afterflame time for any condition set ($t_1 + t_2$ for the 5 specimens)	$\leq 50s$	$\leq 250s$	$\leq 250s$
Afterflame plus afterglow time for each individual specimen after the second flame application ($t_2 + t_3$)	$\leq 30s$	$\leq 60s$	$\leq 60s$
Afterflame or afterglow of any specimen up to the holding clamp	No	No	No
Cotton indicator ignited by flaming particles or drops	No	No	Yes

500 W Vertical Burning Test

A material which passes the flammability requirements established by the 500 W Vertical Burning Test earns either a 5VA or 5VB rating. This particular test is the most severe of the three described. The dimensions of the molded bars used in this test are identical to those used for the 20 MM Vertical Burning Test. Additionally, plaques are required that measure 150 mm (5.9 inch) by 150 mm (5.9 inch) by the minimum and maximum thicknesses required for the application. The bars are clamped in a vertical position with a 125 mm high flame applied five times for five seconds each time with a five second interval between each application. The plaques are clamped in a horizontal, flat position with a 125 mm high flame applied to the bottom surface at a 20° angle using the same burn times described for the bars. Table 26 lists the criteria that must be met to obtain a 5VA or 5VB rating.

Table 27 lists the current UL 94 ratings of some Amodel resins. Because ratings may change and additional products rated please consult the Underwriters Laboratories website for the latest information.

Table 26: UL Criteria for Classifying Materials 5VA or 5VB

Criteria Conditions	5VA	5VB
Afterflame time plus afterglow time after fifth flame application for each individual bar specimen	$\leq 60s$	$\leq 60s$
Cotton indicator ignited by flaming particles or drops from any bar specimen	No	No
Burn-through (hole) of any plaque specimen	No	Yes

Table 27: UL 94 Ratings of Amodel PPA Grades

Grade	Color	Thickness, mm	UL 94 Rating
AFA-4133 V0 Z	ALL	0.75	V-0
		1.5	V-0
		3.0	V-0
AFA-6133 V0 Z	ALL	0.75	V-0
		1.5	V-0
		3.0	V-0
AFA-6145 V0 Z	ALL	0.75	V-0
		1.5	V-0
		3.0	V-0

Electrical Properties

Many applications for thermoplastic resins depend upon their ability to function as electrical insulators. A wide variety of tests have been developed to measure specific aspects of material performance in electrical applications. A brief description of some of the more common tests follows:

Dielectric Breakdown Voltage and Strength - ASTM D149

Dielectric strength is a measure of the ability of a material to resist high voltage without dielectric breakdown. It is measured by placing a specimen between two electrodes and increasing the applied voltage until dielectric breakdown occurs. The dielectric strength is reported at the highest voltage prior to failure. Of the various methods included in ASTM D149, UL 746A specifies the short-time test using a uniform rate of voltage increase of 500 volts per second.

Although the results are reported in units of kV/mm (volts/mil), the dielectric strength is a function of thickness, moisture content, and temperature. Therefore, data on different materials are comparable only for equivalent sample thickness, moisture content, and test temperature.

Table 28 shows the dielectric strengths of several Amodel grades. The dielectric strength of samples conditioned to 50% RH are the same as the dry as molded samples.

Volume Resistivity - ASTM D257

The volume resistivity of a material is defined as the electrical resistance of a unit cube of material. The material is subjected to 500 volts DC for 1 minute, and the current through the material is measured. Materials with higher volume resistivity are more effective at electrically isolating components.

UL 746A specifies that the test be run on two sets of specimens: one set conditioned for 48 hours at 23°C (73°F) and 50% relative humidity; and the other conditioned for 96 hours at 35°C (95°F) and 90% relative humidity.

Volume resistivity is particularly sensitive to temperature changes as well as changes in humidity. Data on different materials are comparable only for equivalent moisture content and temperatures. Materials with resistivities above 108 ohm-cm are considered insulators, while those with values of 103 to 108 ohm-cm are partial conductors.

Table 28: Dielectric Strength of Selected Amodel Grades

Grade	Cond. ⁽¹⁾	Thickness			
		3.2 mm (1/8")		1.6 mm (1/16")	
		kV/mm	V/mil	kV/mm	V/mil
A-1133 HS	dry	21	533	32	813
A-1133 HS	50% RH	21	533		
A-1145 HS	dry	23	584		
A-1145 HS	50% RH	23	584		
AS-4133 HS	dry	21	533	32	813
AS-4133 HS	50% RH	21	533		
AT-1002 HS	dry	17	432		
AT-1002 HS	50% RH	17	432		
AT-5001	dry	17	432		
AT-5001	50% RH	17	432		
AT-6115 HS	dry			28	711
AFA-6133 V0 Z	dry	24	610	27	686
A-1340 HS	dry			32	813
AS-1566 HS	dry			29	737

⁽¹⁾ Condition: dry is dry as molded, 50% RH is moisture conditioned as described on page 6

Surface Resistivity - ASTM D257

The surface resistivity of a material is the electrical resistance between two electrodes on the surface of the specimen. The material is subjected to 500 volts DC for 1 minute, and the current along the surface of the material is measured. Although some finite thickness of material is actually carrying the current, this thickness is not measurable, therefore, this property is an approximate measure. Surface resistivity is affected by surface contamination and is not considered a basic material property. UL specifies the same specimen conditioning used for volume resistivity. Data from this test are best used to compare materials for use in applications where surface leakage is a concern.

Table 29: Volume and Surface Resistivity of Amodel Resins

Grade	Cond. ⁽¹⁾	Volume Resistivity, ohm-cm	Surface Resistivity, ohm
A-1133 HS	dry	1 x 10 ¹⁶	1 x 10 ¹⁵
A-1133 HS	50% RH	2 x 10 ¹⁵	
A-1145 HS	dry	1 x 10 ¹⁶	
A-1145 HS	50% RH	2 x 10 ¹⁵	
AS-4133 HS	dry	1 x 10 ¹⁶	1 x 10 ¹⁵
AS-4133 HS	50% RH	5 x 10 ¹⁴	
AT-1002 HS	dry	1 x 10 ¹⁶	8 x 10 ¹³
AT-1002 HS	50% RH	7 x 10 ¹⁴	2 x 10 ¹³
AT-5001	dry	4 x 10 ¹⁵	4 x 10 ¹⁵
AT-5001	50% RH	2 x 10 ¹⁵	2 x 10 ¹⁵
AT-6115 HS	dry	1 x 10 ¹⁶	1 x 10 ¹⁵
AFA-6133 V0 Z	dry	1 x 10 ¹⁶	1 x 10 ¹⁵
A-1240 L	dry	9 x 10 ¹⁵	
A-1240 L	50% RH	2 x 10 ¹⁵	
A-1340 HS	dry	1 x 10 ¹⁶	
A-1340 HS	50% RH	1 x 10 ¹⁶	1 x 10 ¹⁵
A-1565 HS	dry	4 x 10 ¹⁴	
AS-1566 HS	dry	1 x 10 ¹⁶	1 x 10 ¹⁵

⁽¹⁾ Condition: dry is dry as molded, 50% RH is moisture conditioned as described on page 6

Dielectric Constant - ASTM D150

The dielectric constant is defined as the ratio of the capacitance of a condenser using the test material as the dielectric to the capacitance of the same condenser with a vacuum replacing the dielectric. Insulating materials are used in two very distinct ways. First, to support and insulate components from each other and the ground, and second, to function as a capacitor dielectric. In the first case, it is desirable to have a low dielectric constant. In the second case, a high dielectric constant allows the capacitor to be physically smaller. Dielectric constants have been found to change rapidly with increasing temperature or moisture contents, hence data on different materials are comparable only at equivalent moisture content and temperature.

Table 30: Dielectric Constant of Amodel Resins

Grade	Cond. ⁽¹⁾	Frequency			
		60 Hz	100 Hz	10 ⁶ Hz	10 ⁹ Hz
A-1133 HS	dry	4.4	5.1	4.2	3.7
A-1133 HS	50% RH	4.7		4.3	
A-1145 HS	dry	4.6		4.4	
A-1145 HS	50% RH	4.9		4.5	
AS-4133 HS	dry	3.8	4.6	3.6	3.6
AS-4133 HS	50% RH	4.3		3.4	
AT-1002 HS	dry	3.3		3.3	
AT-1002 HS	50% RH	3.8		3.8	
AT-5001	dry	3.2		3.2	
AT-5001	50% RH	3.6		3.6	
AT-6115 HS	dry		4.0	3.3	3.1
AFA-6133 V0 Z	dry		4.8	4.1	3.7
A-1240L	dry		4.2	4.0	
A-1240L	50% RH		4.4	4.0	
A-1340 HS	dry		4.5	4.3	
A-1340 HS	50% RH		4.5	4.3	3.8
AS-1566 HS	dry		5.7	4.7	4.5

⁽¹⁾ Condition: dry is dry as molded, 50% RH is moisture conditioned as described on page 6

Dissipation Factor - ASTM D150

Dissipation Factor (also referred to as loss tangent or tan delta) is a measure of the dielectric loss, or energy dissipated, when alternating current loses energy to an insulator. In general, low dissipation factors are desirable because they correspond to a better dielectric material. Contamination, testing frequency, temperature, and humidity can affect the dissipation factor.

UL 746A Short-Term Properties

Certain electrical properties are included in the Underwriters' Laboratories (UL) Standard 746A entitled Standard for Polymeric Materials Short-term Property Evaluations and these properties are reported by "Performance Level Category" (PLC). For each property, UL has specified test result ranges and corresponding Performance Level Categories. Desired or best performance is assigned to a PLC of 0, therefore, the lower the PLC, the better the performance in that test.

Table 31: Dissipation Factor of Amodel Resins

Grade	Cond. ⁽¹⁾	Frequency			
		60 Hz	100 Hz	10 ⁶ Hz	10 ⁹ Hz
A-1133 HS	dry	0.005		0.017	0.016
A-1133 HS	50% RH	0.009		0.022	
A-1145 HS	dry	0.005		0.016	
A-1145 HS	50% RH	0.009		0.021	
AS-4133 HS	dry	0.004		0.012	0.013
AS-4133 HS	50% RH	0.020		0.019	
AT-1002 HS	dry	0.004		0.016	
AT-1002 HS	50% RH	0.018		0.035	
AT-5001	dry	0.004		0.016	
AT-5001	50% RH	0.012		0.027	
AT-6115 HS	dry			0.013	0.011
AFA-6133 V0 Z	dry			0.011	
A-1240L	dry		0.006	0.017	
A-1240L	50% RH		0.007	0.019	
A-1340 HS	dry		0.005	0.017	
A-1340 HS	50% RH		0.008	0.017	0.014
AS-1566 HS	dry			0.011	0.011

⁽¹⁾ Condition: dry is dry as molded, 50% RH is moisture conditioned as described on page 6

Table 32: High-Voltage, Low-Current, Dry Arc Resistance Performance Level Categories (PLC)

Value Range, Sec.		Assigned PLC
≥	<	
420		0
360	420	1
300	360	2
240	300	3
180	240	4
120	180	5
60	120	6
0	60	7

Table 33: Comparative Tracking Index Performance Level Categories

Value Range, Volts		Assigned PLC
≥	<	
600		0
400	600	1
250	400	2
175	250	3
100	175	4
0	100	5

High-Voltage, Low-Current, Dry Arc Resistance – ASTM D495

This test measures the time, in seconds, that a 12,500 volt arc can travel between two tungsten rod electrodes on the surface of a material, following a specified test sequence of increasing severity, until a conductive path or track is formed. This test is intended to approximate service conditions in alternating-current circuits operating at high voltage with currents generally limited to less than 0.1 ampere. Table 32 shows the relationship between the arc resistance and the UL assigned Performance Level Categories.

Comparative Tracking Index (CTI) – ASTM D3638

The Comparative Tracking Index is defined as the voltage that causes the formation of a permanent electrically conductive carbon path when 50 drops of electrolyte are applied at a rate of 1 drop every 30 seconds. This test measures the susceptibility of an insulating material to tracking. Table 33 shows the relationship between the voltage obtained and the PLC.

High-Voltage Arc-Tracking-Rate (HVTR)

This test measures the susceptibility of an insulating material to form a visible carbonized conducting path (track) over its surface when subjected to repeated high-voltage, low-current arcing. The high-voltage arc-tracking-rate value is the rate, in mm/minute, at which a conducting path is produced on the surface of a material under standardized test conditions. This test simulates a malfunctioning high-voltage power supply with lower values indicating better performance. Table 34 shows the HVTR values and the corresponding PLC.

Hot Wire Ignition (HWI) - ASTM D3874

This test measures the relative resistance of plastic materials to ignition by an electrically heated wire. A portion of a test specimen is wrapped with a heater wire under specified conditions and a current is passed through the wire at a linear power density of 6.5 0.26 W/mm (W/inch). The current flow is maintained until ignition occurs, and the time to ignition is recorded.

Under certain operational or malfunction conditions, components become abnormally hot. If these overheated components are in intimate contact with the insulating materials, the insulating material may ignite. The intention of this test is to determine relative resistance of insulating materials to ignition under these conditions. Table 35 shows the hot wire ignition times and the assigned PLC.

High-Current Arc Ignition (HAI)

This test measures the relative resistance of insulating materials to ignition from arcing electrical sources. Under certain conditions, insulating materials may be in proximity to arcing. If the intensity and duration of the arcing are severe, the insulating material can ignite. This test measures the number of 240-volt 32.5 ampere arcs on the surface of a material required to cause ignition or a hole. The distance between the electrodes is increased at a rate of 254 mm (10 inch) per second. The maximum number of arcs to be used is 200.

This test measures the performance of an insulating material in close proximity to arcing.

Table 36 shows the relationship between the High-Current Arc Ignition value and the UL assigned Performance Level Categories.

High-Voltage Arc Resistance to Ignition

This test measures the susceptibility of a material to resist ignition or form a visible carbonized conducting path when subjected to high-voltage, low-current arcing. The application of the high-voltage arc is continued until ignition, a hole is burned through the specimen, or 5 minutes. If ignition occurs, the time to ignition is reported. If ignition does not occur the value >300 is reported.

The relationship between the mean time to ignition and the Performance Level Categories is given in Table 37.

Table 34: High-Voltage Arc-Tracking-Rate Performance Level Categories

Value Range, mm/min		Assigned PLC
>	≤	
0	10	0
10	25.4	1
25.4	80	2
80	150	3
150		4

Table 35: Hot Wire Ignition Performance Level Categories

Value Range, Sec.		Assigned PLC
<	≥	
	120	0
120	60	1
60	30	2
30	15	3
15	7	4
7	0	5

Table 36: High-Current Arc Ignition Performance Level Categories

Value Range, Sec.		Assigned PLC
<	≥	
	120	0
120	60	1
60	30	2
30	15	3
15	7	4
7	0	5

Table 37: High Voltage Arc Resistance to Ignition Performance Level Categories

HVAR - Mean Time to Ignition, Sec.		Assigned PLC
<	≥	
	300	0
300	120	1
120	30	2
30	0	3

UL 746A Properties of Amodel Resins

Selected UL 746A properties for selected Amodel grades are shown in Table 38. The grades selected are the ones most often used for electrically insulating applications.

UL Relative Thermal Indices

The UL Relative Thermal Indices are the result of thermal aging tests and, therefore, appear in the Thermal Stability section on page 49.

Table 38: UL 746A Property PLC for Amodel PPA Grades

Grade	mm ⁽¹⁾	HWI	HAI	HVTR	CTI
A(AS)-1133 HS	0.80	0	0	4	0
AT-6115 HS	0.80	0 ⁽²⁾	0	1	0
AT-6130	0.80	4	0	1	0
AS-1566 HS	0.80	—	0	0	0
A-1340 HS	0.80	0 ⁽²⁾	0	1	1
AS-4133 HS	0.80	0 ⁽²⁾	0	1	0
AFA-4133 V0 Z	0.75	0	0	1	1
AFA-6133 V0 Z	0.75	0	0	1	1
AFA-6145 V0 Z	0.75	0	1	—	1

⁽¹⁾ Minimum thickness, mm

⁽²⁾ This value measured at 1.5 mm thickness

Environmental Resistance

As previously mentioned, the performance of polymeric materials may be reduced by environmental factors. This section discusses the effects of environmental factors, such as chemical exposure, conditions likely to promote hydrolysis, exposure to gamma and/or ultraviolet radiation, on the performance of Amodel resins. When appropriate, the effects of these environmental factors on the performance of competitive resins is included for comparison.

Chemical Resistance

Amodel resins are semi-crystalline polyphthalamides, and like other members of the semi-crystalline polyamide family, they exhibit excellent chemical resistance to common organic solvents. However, the chemical structure of Amodel resins is highly aromatic — imparting an even greater degree of chemical resistance to an even broader range of chemicals.

It is difficult to predict the exact effect of chemical exposure on a polymeric component because the reagent, the concentration of the reagent, the exposure time, the temperature of the reagent, the temperature of the polymeric component, and the stress on the component all affect the extent of attack and any change in performance. While the only reliable method for evaluating the effect of chemical attack on the performance of a polymeric component is prototype testing, screening tests are often performed to provide general guidance and compare materials.

Screening chemical resistance testing was performed by immersing ASTM D638 Type I tensile bars in various chemicals for 30 days at the indicated test temperatures. The Amodel resin used was the 33% fiber glass reinforced grade — Amodel AS-1133 HS. Data on 33% glass reinforced PA 6,6 and 30% glass reinforced polyethylene terephthalate (PET) is provided for comparison.

Table 39: Key to Chemical Resistance Ratings

Symbol	Rating	% Reduction in Tensile Strength
E	Excellent	≤ 10
A	Acceptable	≤ 50 but ≥ 10
U	Unacceptable	> 50

The material performance was rated as shown in Table 39. In addition to the performance rating, data on the percent change in tensile strength, length, and weight are reported.

The chemicals used for the screening tests were classified into three groups:

- Organic solvents (Table 40)
- Aqueous solutions (Table 41)
- Automotive fluids (Table 42)

The screening evaluation using aqueous solutions at elevated temperatures showed a loss in tensile strength for all three of the resins tested. This phenomenon is common to all glass reinforced thermoplastics. The loss of tensile strength for Amodel AS-1133 HS resin in deionized water at 93°C (200°F) is initially rapid due to loss of interfacial adhesion between the glass fibers and the resin matrix, and then slows to a gradual rate reflecting hydrolytic attack. Aqueous solutions of antifreeze or zinc chloride produce a similar effect. PA 6,6 is severely attacked by the zinc chloride solution. PET is severely attacked by the antifreeze solution and even badly hydrolyzed by distilled water at elevated temperatures.

Table 40: Screening Chemical Resistance Tests – Organic Chemicals
30 Day Immersion at 23°C (73°F)

Reagent	Resin	Rating	Tensile Strength% Retained	Change in Length%	Change in Weight%
Acetone	Amodel AS-1133 HS	E	97	0.1	0.2
	33% Glass PA 6,6	E	99	0.2	0.2
	30% Glass PET	A	72	0.3	3.2
Isopropanol	Amodel AS-1133 HS	E	99	0.0	0.2
	33% Glass PA 6,6	E	112	0.0	0.3
	30% Glass PET	E	109	0.0	0.3
Methanol	Amodel AS-1133 HS	A	83	0.1	2.9
	33% Glass PA 6,6	A	68	0.5	5.6
	30% Glass PET	E	96	0.1	0.5
Methylene Chloride	Amodel AS-1133 HS	E	94	0.0	1.1
	33% Glass PA 6,6	E	90	0.1	2.4
	30% Glass PET	A	71	2.0	9.5
Methyl Ethyl Ketone	Amodel AS-1133 HS	E	103	0.0	0.1
	33% Glass PA 6,6	A	113	0.0	0.1
	30% Glass PET	A	72	0.1	3.0
Toluene	Amodel AS-1133 HS	E	101	0.0	0.1
	33% Glass PA 6,6	E	109	0.1	0.2
	30% Glass PET	E	91	0.1	1.6
1,1,1 Trichloroethane	Amodel AS-1133 HS	E	99	0.0	0.2
	33% Glass PA 6,6	E	110	0.0	0.2
	30% Glass PET	E	100	0.0	2.3
Trichloroethylene	Amodel AS-1133 HS	E	102	0.0	0.3
	33% Glass PA 6,6	E	97	0.0	0.4
Freon® 113	Amodel AS-1133 HS	E	96	0.0	0.1
	33% Glass PA 6,6	E	99	0.0	0.2
n-Heptane	Amodel AS-1133 HS	E	104	0.0	0.1
	33% Glass PA 6,6	E	96	0.0	0.2

Freon is a registered trademark of E. I. duPont de Nemours and Company.

Table 41: Screening Chemical Resistance Tests – Aqueous Chemical Solutions
30 Day Immersion at Indicated Temperature

Reagent	Conc.	Temperature		Resin	Rating	Tensile Strength, % Retained	Change in Length, %	Change in Weight, %
		°C	°F					
Ammonium Hydroxide	10%	23	73	Amodel AS-1133 HS	E	96	0.1	0.8
				33% Glass PA 6,6	A	61	0.2	4.5
				30% Glass PET	E	95	0.2	0.4
Deionized Water	100%	93	200	Amodel AS-1133 HS	A	69	0.2	3.4
				33% Glass PA 6,6	A	62	0.2	5.0
				30% Glass PET	U	19	0.0	2.4
Sodium Chloride	10%	23	73	Amodel AS-1133 HS	E	97	0.1	2.1
				33% Glass PA 6,6	A	67	0.2	3.3
				30% Glass PET	E	98	0.0	0.3
Zinc Chloride	50%	93	200	Amodel AS-1133 HS	A	66	0.1	4.8
				33% Glass PA 6,6	U	0	*	*
				30% Glass PET	A	54	-0.1	0.6
Sulfuric Acid	36%	23	73	Amodel AS-1133 HS	E	92	0.0	1.8
				33% Glass PA 6,6	U	0	*	*
				30% Glass PET	E	94	0.0	0.3
Sodium Hydroxide	10%	23	73	Amodel AS-1133 HS	E	93	0.0	1.6
				33% Glass PA 6,6	A	62	0.0	3.1
				30% Glass PET	A	70	0.0	-4.2
Sodium Hypochlorite	5%	23	73	Amodel A-1133 HS	E	94	0.0	1.4
				33% Glass PA 6,6	A	57	0.0	-1.5
				30% Glass PET	E	94	0.0	0.4

* = Attacked

Table 42: Screening Chemical Resistance Tests – Transportation Fluids
30 Day Immersion at Indicated Temperature

Fluid	Temperature		Resin	Rating	Tensile Strength, % Retained	Change in Length, %	Change in Weight, %
	°C	°F					
50% Antifreeze Solution	104	220	Amodel AS-1133 HS	A	77	0.2	5.6
			33% Glass PA 6,6	A	54	0.3	8.3
			30% Glass PET	U	0	*	*
Brake Fluid	49	120	Amodel AS-1133 HS	E	99	0.0	0.4
			33% Glass PA 6,6	E	105	-0.1	0.2
			30% Glass PET	E	97	0.0	1.0
Diesel Fuel	23	73	Amodel AS-1133 HS	E	98	0.0	0.1
			33% Glass PA 6,6	E	100	0.0	0.3
			30% Glass PET	E	100	-0.1	0.0
Gasohol (10% Ethanol)	23	73	Amodel AS-1133 HS	A	86	0.0	1.4
			33% Glass PA 6,6	A	65	0.1	3.5
			30% Glass PET	E	93	-0.1	0.7
Hydraulic Fluid	49	120	Amodel AS-1133 HS	E	92	0.0	0.3
			33% Glass PA 6,6	E	103	0.0	0.3
			30% Glass PET	E	105	-0.1	0.1
JP-4 Jet Fuel	23	73	Amodel AS-1133 HS	E	95	0.0	0.4
			33% Glass PA 6,6	E	100	0.0	0.3
			30% Glass PET	E	100	0.0	0.1
Motor Oil	121	250	Amodel AS-1133 HS	E	100	0.0	0.1
			33% Glass PA 6,6	E	106	0.0	-0.2
			30% Glass PET	E	91	-0.1	-0.6
Power Steering Fluid	49	120	Amodel AS-1133 HS	E	97	0.0	0.1
			33% Glass PA 6,6	E	106	0.0	0.2
			30% Glass PET	E	108	0.0	0.0
Transmission Fluid	121	250	Amodel AS-1133 HS	E	97	0.0	0.1
			33% Glass PA 6,6	E	105	-0.1	-0.2
			30% Glass PET	A	64	0.1	-0.5
Unleaded Gasoline	23	73	Amodel AS-1133 HS	E	96	0.1	0.0
			33% Glass PA 6,6	E	99	0.1	0.1
			30% Glass filled PET	E	99	0.0	0.1

* = Attacked

Table 43: General Chemical Compatibility Guidelines for Amodel PPA Resins

Reagent	Rating
Aliphatic Hydrocarbons	E
Aromatic Hydrocarbons	E
Oils	E
Greases	E
Chlorinated Hydrocarbons	E
Methylene Chloride	A
Chloro-Fluoro Carbons	E
Ketones	E
Esters	E
Higher Alcohols	E
Methanol	A
Phenols	U
Strong Acids	A
Alkalis	E

Table 44: Effect of Gamma Radiation on Amodel AS-1133 HS

% Retention of	5 mrad Exposure
Tensile Strength, psi	90
Tensile Elongation, %	100

Chemical Compatibility

Table 43 can be used as a general guide to the chemical resistance of Amodel resins. However, this data should be used for screening only. As mentioned earlier, the performance of Amodel resins under actual chemical exposure conditions will vary with differences in mechanical stress, concentration, time and/or temperature. It is recommended that tests be conducted under conditions close to those anticipated in the actual application to get reliable performance information.

Gamma Radiation

Amodel AS-1133 HS resin has excellent resistance to gamma radiation. Tests on injection molded tensile bars exposed to 5.0 megarads of gamma radiation indicate essentially no significant affect on the mechanical properties of Amodel AS-1133 HS resin. Results are given in Table 44.

In this section, basic design principles and general recommendations are presented to assist the design engineer in designing plastic components that meet the cost/performance requirements of their applications. Guidelines are given on the effects of stresses caused by assembly, temperature changes, environmental factors, and time as it relates to creep.

Of the various materials available to a design engineer, thermoplastics offer the greatest variety, versatility and freedom of design. Plastics can be translucent or opaque, rigid or flexible, hard or soft. Plastic materials are available that provide a wide range of chemical resistance, from chemically inert to selective solubility in certain environments. Broad versatility is also available for other properties like strength, stiffness and impact resistance, lubricity and thermal capability. Blends and alloys are possible that further increase the material choices for a particular application.

At times, designing with plastics may appear more complicated than with metals. But the diversity of products, conversion processes, and secondary operations (welding, inserts, printing, painting, metallizing) available with plastics gives the designer unprecedented freedom as shown in Table 45.

A designer may be tempted to make a plastic part that merely duplicates the dimensions of a metal part without taking advantage of the versatility of the plastic material or the design freedom offered. This approach can lead to inefficient designs or parts that are difficult to produce, or whose performance is less than optimal.

The following sections discuss those areas of mechanical design and stress analysis that relate to designing with plastics, comparing metal to plastics and discussing factors that are specific to plastics alone.

Table 45: Design Benefits of Amodel Resin over Metals

Amodel Resin Characteristics	Benefit in Design
Amodel resins are fabricated by the injection molding process, which allows substantial design freedom	Ribs, bosses, or cored sections can be readily incorporated.
	Snap fits can be molded in, simplifying assembly.
	Eliminate many secondary operations such as drilling, tapping, boring, deburring, and grinding.
	Metal inserts can be easily used where necessary to optimize part strength.
Amodel resins are thermoplastic	Features from several metal parts of an assembly may be combined into a single part, simplifying assembly and reducing cost.
	Parts may be joined with ultrasonic or vibration welding rather than fasteners.
Amodel resins resist chemicals	Color may be molded-in rather than added afterward as paint.
	Parts will not rust, and resist corrosion.

Mechanical Design

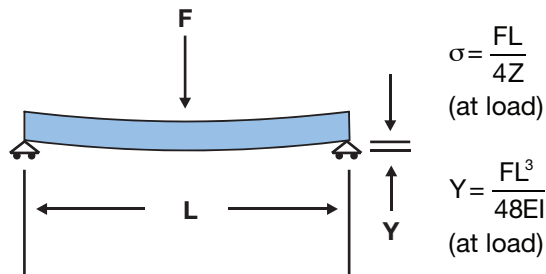
The use of classical stress and deflection equations provide starting points for part design. Mechanical design calculations for Amodel resins will be similar to those used with any engineering material. As with all plastics, however, the analysis used must reflect the viscoelastic nature of the material. In addition, the material properties can vary with strain rate, temperature, and chemical environment or with fiber orientation for fiber reinforced plastics. Therefore, the analysis must be appropriate for all anticipated service conditions. For example, if the service condition involves enduring load for a long period of time, then the apparent or creep modulus should be used instead of the short-term elastic modulus. Or if the loading is cyclical and long term, the fatigue strength at the design life will be the limiting factor.

The initial step in any part design analysis is the determination of the loads the part will be subjected to, and calculation of the resultant stress and deformation or strain. The loads may be externally applied or result from stresses due to temperature changes or assembly.

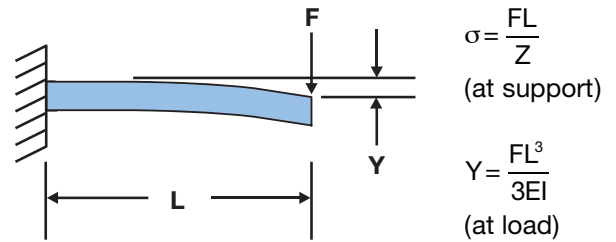
An example of an externally applied load is the weight of medical instruments on a sterilizer tray. Examples of assembly loads are the loads on a housing flange when it is bolted to an engine or the load on the hub of a pulley when a bearing is pressed into it. Thermally induced stresses can arise when the temperature of the assembly increases and the dimensions of the plastic part change more or less than the metal part to which it is attached.

Table 46: Maximum Stress and Deflection Equations

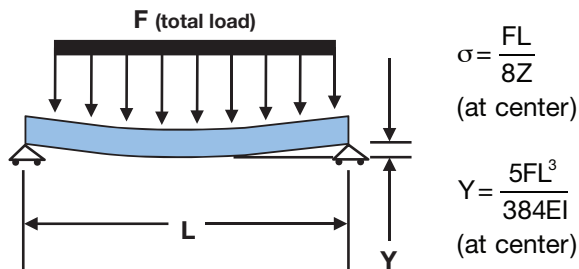
**Simply Supported Beam
Concentrated Load at Center**



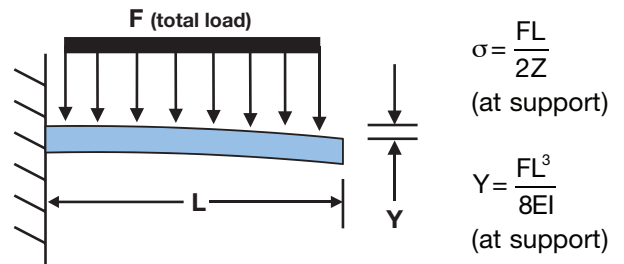
**Cantilevered Beam (One End Fixed)
Concentrated Load at Free End**



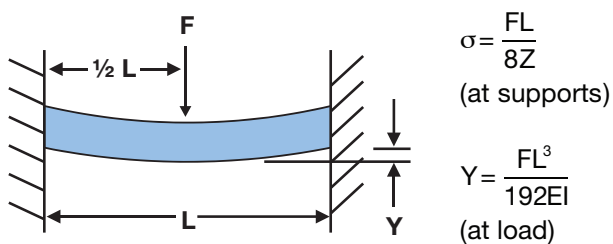
**Simply Supported Beam
Uniformly Distributed Load**



**Cantilevered Beam (One End Fixed)
Uniformly Distributed Load**



**Both Ends Fixed
Concentrated Load at Center**



**Both Ends Fixed
Uniformly Distributed Load**

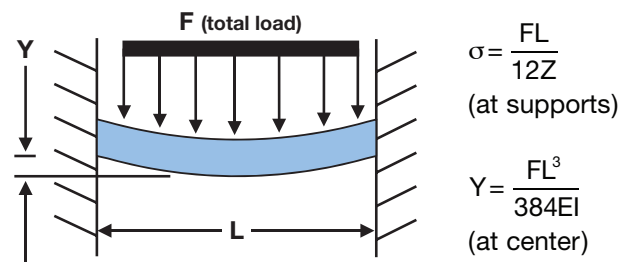
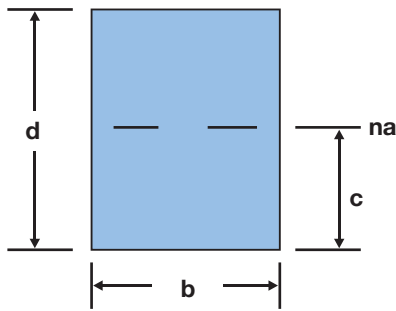


Table 47: Area and Moment Equations for Selected Cross Sections

Rectangular



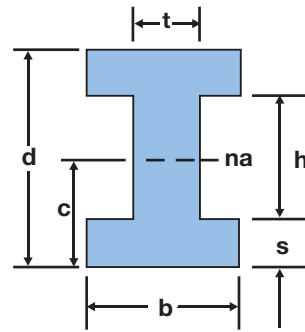
$$A = bd$$

$$c = \frac{d}{2}$$

$$I = \frac{bd^3}{12}$$

$$Z = \frac{bd^2}{6}$$

I-Beam



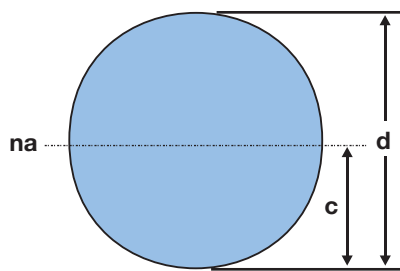
$$A = bd - h(b - t)$$

$$c = \frac{d}{2}$$

$$I = \frac{bd^3 - h^3(b - t)}{12}$$

$$Z = \frac{bd^3 - h^3(b - t)}{6d}$$

Circular



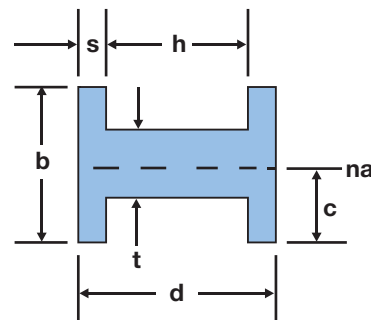
$$A = \frac{\pi d^2}{4}$$

$$c = \frac{d}{2}$$

$$I = \frac{\pi d^4}{64}$$

$$Z = \frac{\pi d^3}{32}$$

H-Beam



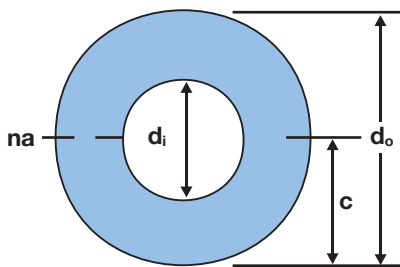
$$A = bd - h(b - t)$$

$$c = \frac{b}{2}$$

$$I = \frac{2sb^3 + ht^3}{12}$$

$$Z = \frac{2sb^3 + ht^3}{6b}$$

Tube



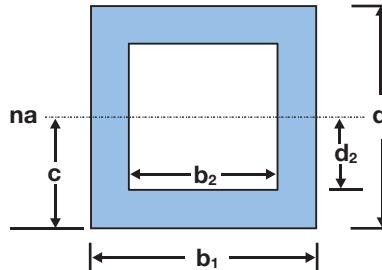
$$A = \frac{\pi(d_o^2 - d_i^2)}{4}$$

$$c = \frac{d_o}{2}$$

$$I = \frac{\pi(d_o^4 - d_i^4)}{64}$$

$$Z = \frac{\pi(d_o^4 - d_i^4)}{32d_o}$$

Hollow Rectangular



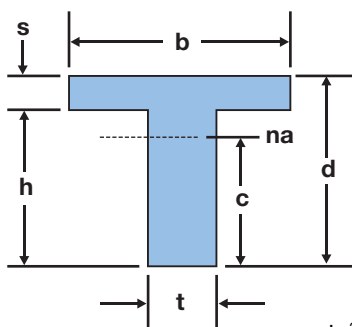
$$A = b_1d_1 - b_2d_2$$

$$c = \frac{d_1}{2}$$

$$I = \frac{b_1d_1^3 - b_2d_2^3}{12}$$

$$Z = \frac{b_1d_1^3 - b_2d_2^3}{6d_1}$$

T-Beam or Rib



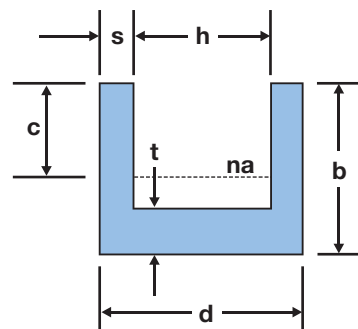
$$A = bs + ht$$

$$c = d - \frac{d^2t + s^2(b - t)}{2(bs + ht)}$$

$$Z = \frac{I}{c}$$

$$I = \frac{tc^3 + b(d - c)^3 - (b - t)(d - c - s)^3}{3}$$

U-Beam



$$A = bd - h(b - t)$$

$$c = b - \frac{2b^2s + ht^2}{2A}$$

$$I = \frac{2b^3s + ht^3}{3} - A(b - c)^2$$

$$Z = \frac{I}{c}$$

Using Classical Stress/Strain Equations

To use the classical equations, the following simplifying assumptions are necessary:

- The part can be analyzed as one or more simple structures
- The material can be considered linearly elastic and isotropic
- The load is a single concentrated or distributed static load gradually applied for a short time
- The part has low residual or molded-in stresses

While all of these assumptions may not be strictly valid for a particular situation, the classical equations can provide a starting point for analysis. The design engineer can then modify the analysis to take into consideration the effects of the simplifying assumptions.

A variety of parts can be analyzed using a beam bending model. Table 46 lists the equations for maximum stress and deflection for some selected beams.

The maximum stress (σ) occurs at the surface of the beam furthest from the neutral surface, and is given by:

$$\sigma = \frac{Mc}{I} = \frac{M}{Z}$$

where

M = bending moment, N · m (inlb)

c = distance from neutral axis, m (in)

I = moment of inertia, m⁴ (in⁴)

$Z = \frac{I}{c}$ = section modulus, m³ (in³)

Table 47 gives the cross sectional area (A), the moment of inertia (I), the distance from the neutral axis (c), and the section modulus (Z) for some common cross sections.

For other crosssections and/or geometries, the design engineer can consult stress analysis handbooks or employ finite element analysis.

Limitations of Design Calculations

The designs given by the application of the classical mechanical design equations are useful as starting points, but some critical factors are simply not adequately considered by these analyses. The viscoelastic behavior of polymeric materials limits application of some of the design equations to, for example, low deflection cases. Often the calculation

of maximum stress contains a number of simplifying assumptions which can diminish the credibility of the results, or the expected failure mode is buckling or shear, where the appropriate property data is lacking.

Also, the impact resistance of a design is directly related to its ability to absorb impact energy without fracture. It is difficult to predict the ability of a design to absorb energy. In addition, even armed with the energy absorption requirements, practical toughness constants for engineering resins don't exist. The results of laboratory testing vary with the type and speed of the impact test, even for fixed geometries. Therefore, the ability of the design to withstand impact must be checked by impact testing of prototype parts.

Similarly, fatigue test results will vary depending on the cyclic rate chosen for the test, the dynamics of the test, and the test specimen used. Therefore, they should only be used as a rough indication of a material's ability to perform in a fatigue application.

Deflection Calculations

To determine the deflection of a proposed part design using classical equations, a modulus of elasticity value is required. It is important that the appropriate value be used. The value must represent the modulus of the material at or near the temperature and humidity expected in the application. Room and elevated temperature values can be found in the property tables on pages 7 to 20. If the load is sustained, then the apparent or creep modulus should be used. Values are given in the isochronous stress/strain curves, Figures 44 and 45 on page 34.

Stress Calculations

After the designer has calculated the maximum stress, those values are then compared to the appropriate material property, i.e., tensile, compressive, or shear strength. The comparison should be appropriate in terms of temperature and humidity to the requirements of the application.

Reinforcing Fiber Orientation Considerations

When designing with plastics, especially filled plastics, the designer must be cognizant of the effects of the fillers and reinforcing fibers on the mechanical properties of the plastic. The processing of filled plastics tends to cause orientation of fibers or high-aspect-ratio fillers parallel to the direction of flow. Throughout this manual, properties have been given both with and across flow direction whenever practical.

Since the design of the part and the processing are interrelated, the designer should consider what portions of the part are likely to be oriented and how the properties will be affected. Shrinkage, strength,

stiffness, and coefficient of thermal expansion will differ depending on the aspect ratio of the fiber (the ratio of its length to its diameter) and the degree of fiber orientation. Perpendicular to the fiber orientation, the fibers act more as fillers than as reinforcing agents.

When molding polymers, there are instances where melt fronts meet (commonly known as weld lines) such as when the plastic melt flows around a core pin. However, the reinforcement in the plastic, if present, does not cross the weld line. Thus the weld line does not have the strength of the reinforced polymer and at times can even be less than the matrix polymer itself. These factors must be taken into account when designing parts with reinforced plastics.

Designing for Equivalent Part Stiffness

Sometimes, a design engineer wants to replace a metal part with one made of plastic, but still wants to retain the rigidity of the metal part. There are two fairly simple ways to maintain the stiffness of a part when substituting one material with another material — even though the materials have different moduli of elasticity.

In the first method, the cross sectional thickness is increased to provide the stiffness. In the second, ribs are added to achieve greater stiffness. An example of each approach follows.

Changing Section Thickness

In reviewing the deflection equations in Table 46, the deflection is always proportional to the load and length and inversely proportional to the modulus of elasticity and moment of inertia.

Selecting one case, for example, both ends fixed with a uniformly distributed load, the deflection is determined by:

$$Y = \frac{FL^3}{384EI}$$

Therefore, to equate the stiffness using two different materials, the deflections are equated as follows:

$$\left\{ \frac{FL^3}{384EI} \right\}_{\text{metal}} = Y = \left\{ \frac{FL^3}{384EI} \right\}_{\text{plastic}}$$

Since the load and length are to remain the same, the FL^3 becomes a constant on both sides of the equation and what remains is:

Equation 1

$$\{EI\}_{\text{metal}} = \{EI\}_{\text{plastic}}$$

This, then, is the governing equation for equating part stiffness.

If the metal part were magnesium having a modulus of elasticity E of 44.8 GPa (6.5 Mpsi) and the thermoplastic chosen to replace it was Amodel AS-1145 HS resin having a modulus of elasticity of 13.8 GPa (2.0 Mpsi), we need to increase the moment of inertia I of the plastic version by increasing the part thickness or adding ribs.

Substituting the E values in equation 1:

$$(44.8 \times 10^9)I_{\text{metal}} = (13.8 \times 10^9)I_{\text{Amodel}}$$

$$3.25 I_{\text{metal}} = I_{\text{Amodel}}$$

From Table 47, the moment of inertia for rectangular sections is:

$$I = \frac{bd^3}{12}$$

where b is the width and d is the thickness of the section, substituting into our equation to determine the required thickness yields:

$$3.25 d_{\text{metal}}^3 = d_{\text{Amodel}}^3$$

If d for the metal part is 2.54 mm (0.10 inch) then the thickness is Amodel resin is:

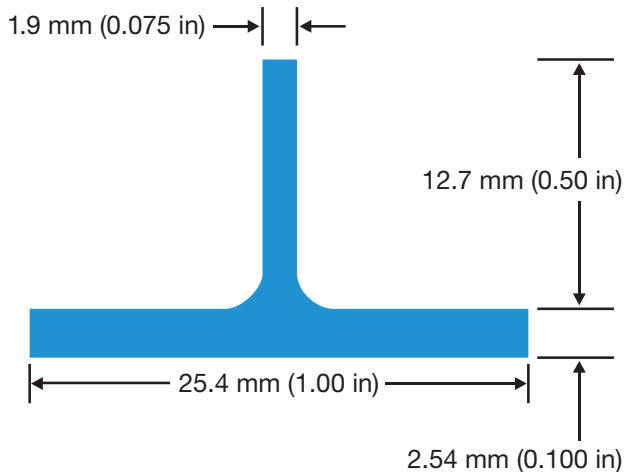
$$d_{\text{Amodel}} = \sqrt[3]{3.25(2.54)^3} = 3.76 \text{ mm (0.148 in.)}$$

or 48% thicker than the magnesium part. However, ribs can be used to effectively increase the moment of inertia as discussed in the next section.

Adding Ribs to Maintain Stiffness

In the last section, it was determined that if a metal part were to be replaced with a part molded of Amodel AS-1145 HS resin, a part thickness of 3.7 mm (0.148 inch) would be required to equal the stiffness of a 2.5 mm (0.100 inch) thick magnesium part.

By incorporating ribs into the Amodel design, the wall thickness and weight can be reduced very efficiently and yet be as stiff as the magnesium part.

Figure 68: Adding Ribs to Increase Stiffness

To demonstrate this, the moment of inertia (I) of the new rib design can be equated with that of the 3.7 mm (0.148 inch) thick plate design. Selecting the same material, Amodel AS-1145 HS, the modulus of elasticity remains 13.8 GPa (2.0 Mpsi) in both cases; therefore, if the moment of inertia of the ribbed design is equal to the plate design, the parts will have equivalent deflection and/or stiffness.

From Table 47, the I for a ribbed section is selected. By assuming that the section width "b" is the same for both, the I_{rib} has to be equal or greater than the I_{plate} . Assigning a section width "b" = 25.4 mm (1.0 inch), the moment of inertia of a ribbed construction that will satisfy that condition can be calculated.

The moment of inertia for the plate design is:

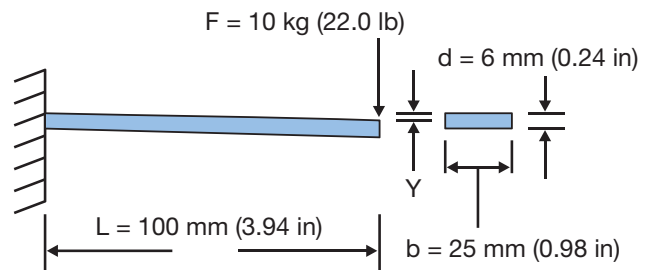
$$I_{plate} = \frac{bh^3}{12} = \frac{2.54 \times (3.76)^3}{12} = 112.5 \text{ mm}^4 (2.70 \times 10^{-4} \text{ in}^4)$$

By choosing the arbitrary rib design shown in Figure 68, and working through the calculations, the moment of inertia is found to be:

$$I_{rib} = 1379 \text{ mm}^4 (33.19 \times 10^{-4} \text{ in}^4)$$

Therefore, the ribbed design will be 9.5 times stiffer than the Amodel plate design or the original magnesium part that was 2.5 mm (0.100 inch) thick.

The same rib having half the height would still produce a part twice as stiff as the magnesium part. The ribbed design shown requires placing a rib every 25 mm (1 inch) of section width.

Figure 69: Cantilever Beam, Bending Load Example

Designing for Sustained Load

Up to this point, the stress strain calculations and examples have dealt with immediate stress/strain response and therefore short-term properties. If the part in question must sustain loads for long periods of time or at elevated temperatures, apparent (creep) modulus values must be used to account for the additional strain and part deflection that may occur. An example showing how the calculations are modified for sustained load follows.

Calculating Deflection

If a cantilever beam with a rectangular cross-section, as shown in Figure 69, is loaded with a 10 kg (22.0 lb) force at the free end, what is the deflection after 1,000 hours?

From Table 46 on page 65, the deflection of a cantilever beam is given by:

$$Y = \frac{FL^3}{3EI}$$

where I , the moment of inertia, as shown in Table 47 is:

$$I = \frac{bd^3}{12}$$

and E is the flexural modulus of the material.

Calculating the moment of inertia for this example gives:

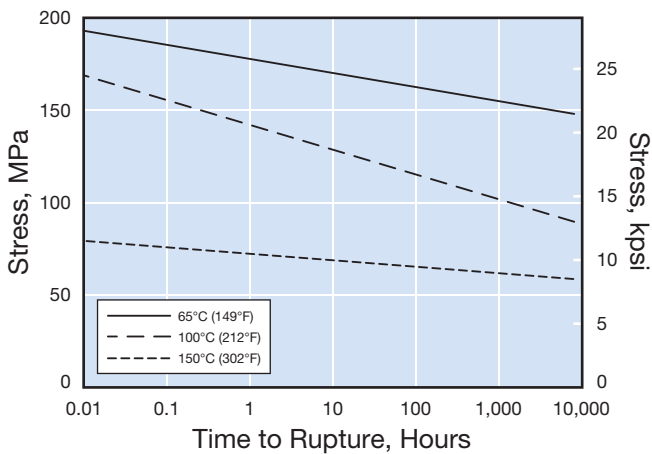
$$I = \frac{(25)(6)^3}{12} = 450 \text{ mm}^4 (1.081 \times 10^3 \text{ in}^4)$$

The data sheet for Amodel A-1133 HS resin gives 11.6 GPa (1.68 Mpsi) for the flexural modulus. Using this value and the equation previously cited, the short-term room temperature deflection can be calculated by:

$$Y = \frac{(10 \text{ kg} \times 9.8066)(.1\text{m})^3}{3(11.6 \times 10^9 \text{ Pa})(4.5 \times 10^{-10} \text{ m}^4)}$$

$$Y = 6.3 \text{ mm (0.25 in)}$$

Figure 70: Tensile Creep Rupture, Amodel A-1133 HS Resin



If the application requires that the load be sustained for a long time, we would expect the deflection to be greater than this because of creep. To calculate the deflection considering the creep, we would use the apparent modulus instead of the short-term flexural modulus. The value of apparent modulus shown for Amodel A-1133 HS resin at 1000 hours in Figure 70 is 7.58 GPa (1.10 Mpsi). Therefore the calculated deflection is:

$$Y = \frac{(10 \text{ kg} \times 9.8066)(.1\text{m})^3}{3(7.58 \times 10^9 \text{ Pa})(4.5 \times 10^{-10} \text{ m}^4)}$$

$$Y = 9.6 \text{ mm (0.38 in)}$$

The deflection is about 50% greater when a sustained load is considered.

Calculating Allowable Stress - Creep Rupture

If a load is sustained for a long time and if the load and/or temperature are high enough, rupture of the part will eventually occur due to creep.

To estimate the combinations of time, temperature, and load that will cause this type of failure, creep rupture tests are conducted at various temperatures as shown in Figure 70. This figure illustrates the actual time to failure for different levels of stress so that a creep rupture envelope can be obtained. From this envelope, the safety factor in time or stress can be determined for that particular temperature.

For instance, if the application life is 1,000 hours at 65°C (149°F) for a part molded from Amodel A-1133 HS resin, the curve indicates that rupture will occur within that time frame if the part is exposed to a stress level of approximately 158 MPa (23 kpsi).

If the part can be redesigned to reduce the stress to 124 MPa (18 kpsi), the predicted time to rupture is now well beyond 10,000 hours. This automatically builds a safety factor into the design. Actual part testing is still recommended to confirm these results.

For operating temperatures that are different from the tested temperatures, information is usually extrapolated from known creep rupture envelopes to approximate the envelope for the temperature of interest.

Considering Stress Concentrations

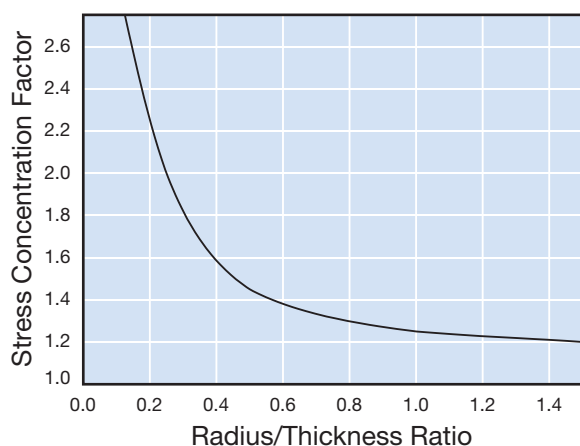
Classical mechanical design may result in a component design which fails prematurely or at a much lower stress than predicted. This could arise due to stress concentration. Stress concentrations may occur at sharp corners, around holes, or other part features. Impact and fatigue situations are especially sensitive to stress concentrations.

Minimizing sharp corners reduces stress concentrations and results in parts with greater structural strength. To avoid stress concentration problems, inside corner radii should be equal to at least half of the nominal wall thickness. A fillet radius of 0.4 mm (0.015 inch) should be considered minimum.

Figure 71 shows the effect of inside corner radius on the stress concentration factor. For example, if the nominal wall thickness is 2 mm (0.080 inch) and an inside corner radius is 0.5 mm (0.020 inch), then the radius to thickness ratio is 0.25 and the stress concentration factor will be over two. A stress of x will have the effect of over $2x$ on the part.

Outside corners should have a radius equal to the sum of the radius of the inside corner and the wall thickness to maintain a uniform wall thickness.

Figure 71: Stress Concentration Factor at Inside Corners



Considering Thermal Stresses

When a plastic part attached to metal undergoes temperature changes, stresses may be induced that should be considered by the designer in the development of the part design.

Figure 72 illustrates a typical plastic flange fastened by a steel bolt to a steel frame. Because the thermal expansion of the plastic is significantly greater than that of the steel, an increase in temperature will produce an increase in compressive stresses in the plastic and tension in the bolt. It is the increase in compressive stress under the washer that must be considered if creep and loss of torque load on the bolt is of concern.

For example, the change in length of a material when exposed to a change in temperature is given by:

$$\Delta L = L (T_F - T_O)\alpha$$

where

ΔL = change in length

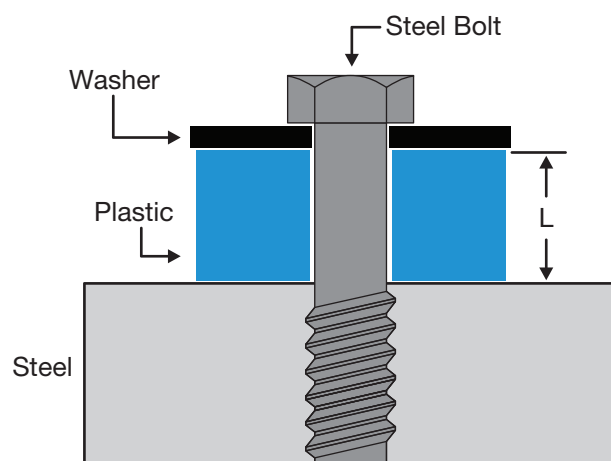
L = original length

α = coefficient of thermal expansion

T_F = final temperature

T_O = original temperature

Figure 72: Thermal Stress Example



Since the plastic is constrained, the unit elongation, combining both thermal expansion and strain, of both the steel bolt and the plastic, will be as follows:

$$\alpha_s(T_F - T_O) + \frac{F}{A_s E_s} = \alpha_p(T_F - T_O) - \frac{F}{A_p E_p}$$

where

A_s = cross sectional area of the bolt

A_p = cross sectional area of the washer

E_s = modulus of steel

E_p = modulus of plastic

α_s = coefficient of thermal expansion of steel

α_p = coefficient of thermal expansion of plastic

F = increase in the tensile force of the bolt

Solving for F

$$F = \frac{(\alpha_p - \alpha_s)(T_F - T_O) A_s E_s}{1 + \frac{A_s E_s}{A_p E_p}}$$

and the increase in compressive stress on the plastic will be:

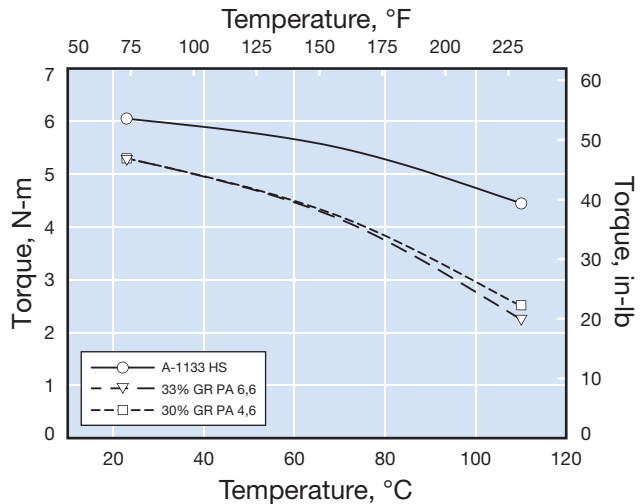
$$\sigma = \frac{F}{A_p}$$

Loss of Bolt Tightness Due to Creep

When threaded metal fasteners are used to retain or secure plastic parts to an assembly, and the assembly is subjected to changes in temperature, the difference between the thermal expansion coefficients of the metal and the plastic can cause problems. When a threaded fastener is tightened, the fastener is elongated slightly and a compressive stress is generated on the substrate. This compressive stress maintains the tightness of the bolt.

When the assembly is heated, both the plastic part and the metal fastener will expand. The plastic part, however, is constrained by the metal fastener, and cannot expand. This results in increased compressive stresses in the plastic, and a corresponding increased tendency for compressive creep or stress relaxation to occur. The relaxation of the compressive stress will result in reduced torque retention in the bolts.

Figure 73: Bolt Torque Retention



To evaluate this tendency, 6.4 mm (0.250 inch) thick plaques of Amodel A-1133 HS resin, 33% glass reinforced PA 6,6 and 30% glass reinforced PA 4,6 were bolted to a metal surface with steel machine bolts tightened to 6.8 N-m (60 in-lb) of torque with a torque wrench compressing the plastic plaque under the bolt face. The temperature of the bolted assemblies was then raised to the indicated temperatures shown in Figure 73, held for one hour, and then cooled to room temperature. The torque required to loosen the bolts was then measured.

Figure 73 compares the amount of torque retained versus temperature. The coefficient of linear thermal expansion of Amodel resin is lower than those of the other materials tested, and therefore closer to that of the steel.

The smaller difference in thermal expansion results in lower induced stress due to the compressive strain caused by the thermal excursion in the constrained part. This translates to lower creep and therefore better torque retention for such bolted assemblies.

Designing for Assembly

Interference or Press Fits

One of the most economical methods that can be used to assemble two parts is a press fit. The joint is achieved by pressing or forcing the shaft into a hole whose diameter is smaller than the diameter of the shaft. The difference in diameter between the hole and shaft is referred to as the diametrical interference. The force maintaining the joint is primarily a compressive stress on the shaft resulting from the hoop stress in the hub created by the insertion of the shaft. Depending upon the relative moduli of the shaft and hub materials, the compressive stress in the shaft can also contribute to maintaining the joint. The stress holding an interference fit will exhibit relaxation over time in a manner that is analogous to creep, because the apparent modulus of the polymeric material decreases over time.

Calculating the Allowable Interference

The allowable interference between a shaft and a hub can be determined by using the general equation:

$$I = \frac{S_d D_s}{F} \left\{ \frac{F + \nu_h}{E_h} + \frac{1 - \nu_s}{E_s} \right\}$$

and the geometry factor is given by:

$$F = \frac{1 + \left(\frac{D_s}{D_h} \right)^2}{1 - \left(\frac{D_s}{D_h} \right)^2}$$

where

I = Diametrical interference

S_d = Working stress

D_h = Outside diameter of the hub

D_s = Diameter of the shaft

E_h = Modulus of the hub material

E_s = Modulus of the shaft material

ν_h = Poisson's Ratio of the hub material

ν_s = Poisson's Ratio of the shaft material

F = Geometry factor

If the shaft and hub are made from the same grade of Amodel resin, then:

$$E_h = E_s = E$$

and the interference is:

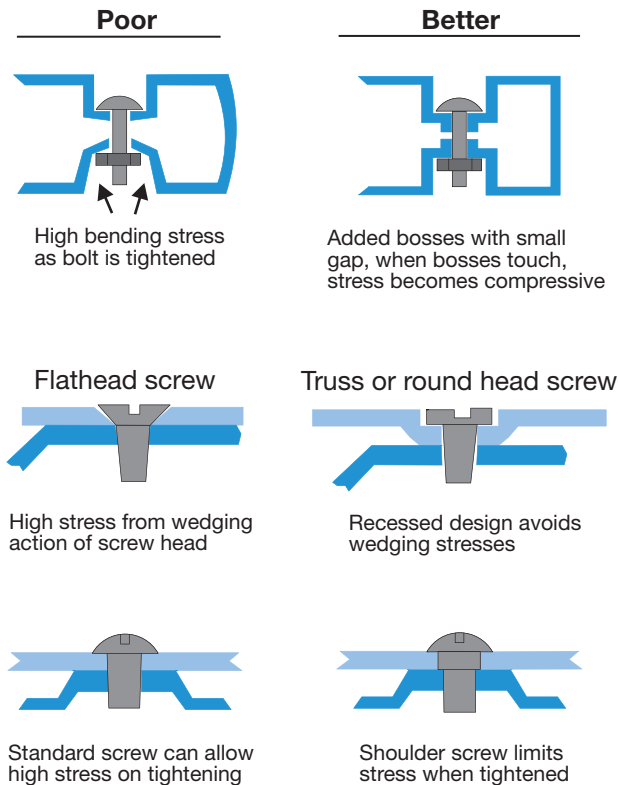
$$I = \frac{S_d}{E} D_s \left(\frac{F+1}{F} \right)$$

If the hub is made from Amodel resin and the shaft is made from metal, then the interference is:

$$I = \frac{S_d D_s}{F} \frac{F + \nu_h}{E_h}$$

When a press fit is used with dissimilar materials, the differences in thermal expansion can increase or decrease the interference between two mating parts. This could increase or reduce the stress affecting joint strength.

A press fit can creep or stress relax over time. This could cause a decrease in the retention force of the assembly. Therefore, testing the assembly under its expected operating conditions is highly recommended.

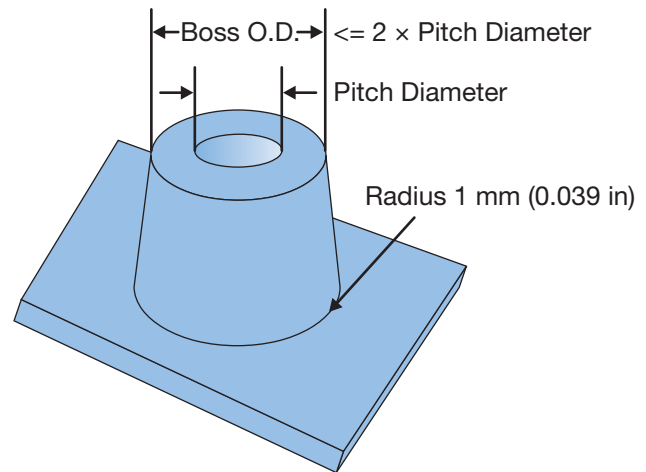
Figure 74: Designing for Mechanical Fasteners

Mechanical Fasteners

Mechanical fasteners provide an economical method of joining dissimilar materials together. Fasteners frequently used with injection molded plastic parts include screws, bolts, nuts, lock washers and lock nuts. When using metal mechanical fasteners, good design practice should be used to prevent the plastic parts being assembled from becoming overstressed.

The most obvious procedure for preventing a highly stressed assembly is to control the tightening of the mechanical fasteners with torque limiting drivers. When torque cannot be controlled, as might be the case with field assembly, shoulder screws will limit compression on the plastic part. Other alternatives may be to use flange-head screws, large washers or shoulder washers. Figure 74 presents some preferred designs when using mechanical fasteners.

Repeated assembling and disassembling should be avoided when using self-tapping screws. If repeated assembly is required, thread-forming screws are recommended.

Figure 75: Boss Design for Self-Tapping Screws

Self-Tapping Screws

A common type of mechanical fastener used with plastics is a self-tapping screw. A self-tapping screw cuts or forms threads as it is inserted into the plastic and eliminates the need for molding internal threads or the secondary operation of tapping the thread form by machining. The major types are thread-forming and thread-cutting.

The modulus of elasticity of the plastic material plays an important role in deciding what type of self-tapping screw is most suitable for the application. For plastic materials with a modulus less than 3.0 GPa (440 kpsi), such as most unreinforced resins, thread-forming screws are best since the plastic is ductile enough to be deformed without cracking or shearing. For glass and mineral filled grades, thread-cutting screws are preferred.

For optimum strip-out torque, the hole diameter of the boss should be equal to the pitch diameter of the screw. The outer diameter of the boss should be equal to two or three times the hole diameter and the boss height should be more than twice the thickness of the boss.

Figure 75 illustrates the basic boss design for use with self-tapping screws.

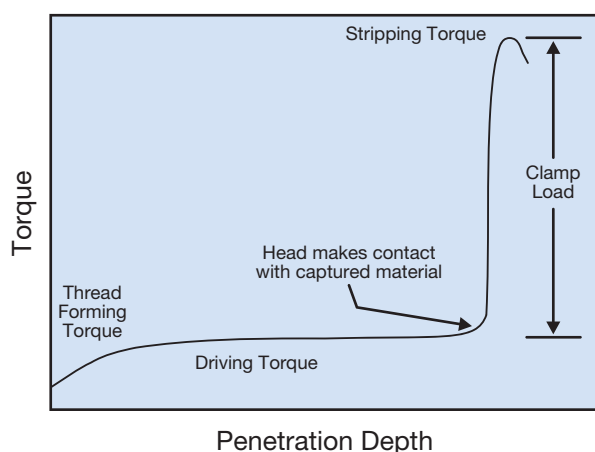
To avoid stripping or high stress assemblies, torque controlled drivers should be used on assembly lines.

Improving Torque Retention

To minimize the loss of torque due to creep, reduce the compressive stress under the screw head by:

- Increasing the screw head diameter
- Using a large-diameter flat washer
- Reducing the clamping torque
- Using a spring or spiral washer
- Using shoulder bolt to reduce stresses on plastic part
- Using a metal bushing

Figure 76: Torque Developed During Screw Installation



Tightening Torque

Figure 76 shows how torque changes as a function of screw penetration. Tightening torque must be high enough to fully engage the screw threads and develop clamp load but lower than the torque that would cause failure of the threads, known as the stripping torque.

The tightening torque is the recommended installation torque for a given application. It should be sufficiently high so as to fully drive the screw and generate clamp load, yet low enough to avoid stripping.

The optimum tightening torque value can be calculated from the average driving torque and the average stripping torque using the following equation.

$$T_T = \frac{1}{2} \left(\frac{3}{2} T_D + \frac{1}{2} T_S \right)$$

where

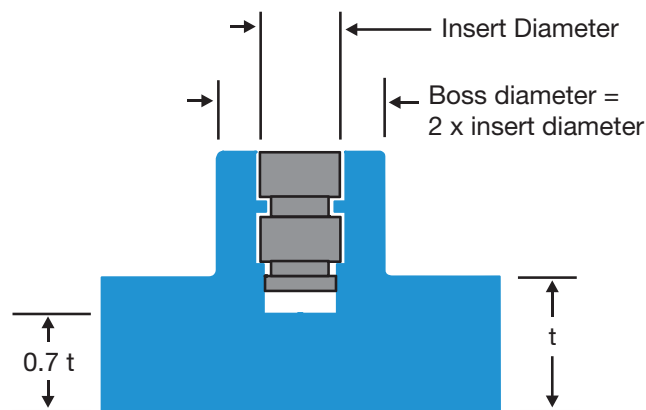
T_T = Tightening torque

T_D = Average driving torque

T_S = Average stripping torque

Some self-tapping screws have been designed specifically for use with plastics and these have the advantage of having a greater difference between driving and stripping torque than the typical screws designed for metal. These special fasteners can provide an additional safety factor for automated assembly.

Figure 77: Boss Design for Ultrasonic Inserts



Pull Out Force Calculation

The strength of a joint can be characterized by the amount of force required to pull-out a screw. The pull out force can be estimated by using the following equation:

$$F = \pi S D L$$

where

F = Pull out force

S = Shear strength

D = Pitch diameter

L = Thread engagement length

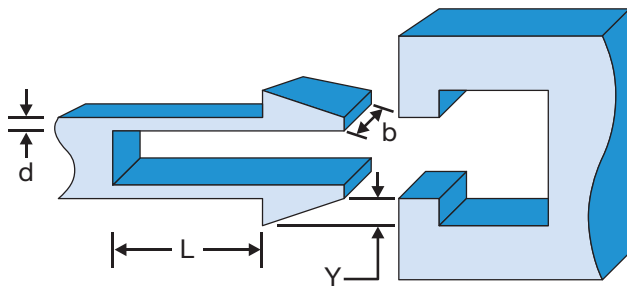
When repeated assembly and disassembly are required or expected, threaded metal inserts should be used instead of self-tapping screws.

Threaded Inserts

Threaded metal inserts can be used to provide permanent metal threads in a plastic part; a wide variety of sizes and types are available. Inserts are usually installed in molded bosses whose internal diameter is designed for the insert. The most commonly used metal inserts are either molded-in or ultrasonically placed in the part as a secondary operation. In the case of the molded-in insert, the insert is placed in the mold and the plastic is injected around it. Stress will develop when the plastic cools around the insert. To reduce this stress, heat the inserts to the temperature of the mold.

The ultrasonic insert is pressed into the plastic by melting the plastic with high frequency vibrations, generated by an ultrasonic welding machine. The ultrasonic welding melts material around the metal insert as it is being installed, forming a bond between the insert and the plastic that is usually strong and relatively free of stress.

Figure 77 depicts the recommended insert and boss designs for use with Amodel PPA resin.

Figure 78: Cantilever Type Snap Fit

Molded-In Threads

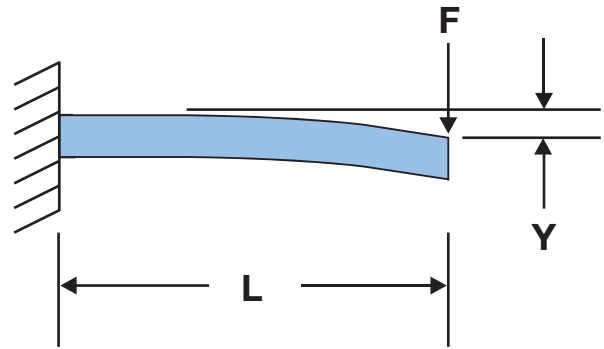
One of the benefits of using plastic materials instead of metals is the ability to mold thread forms directly into the part. This eliminates the secondary machining operations needed with metal parts to form the threads. molded-in threads can be either external or internal. In the case of internal threads, some type of unscrewing or collapsible core is required. External threads can be formed more easily if the parting line of the mold is perpendicular to the thread.

Designing with Snap Fits

The use of snap fits in plastics is very prevalent. All snap fit designs require the plastic to flex like a cantilever spring as it moves past an interference that is designed on the mating part. Once the flexible arm moves past the interference, it returns to its normal unflexed, unstressed position. Usually a step or protrusion has been designed on the cantilever that engages and locks into the mating part, creating a simple assembly method without additional parts. This is shown in Figure 78.

Each cantilever arm must deflect a distance "Y" in order to be inserted. The key to proper snap design is to not exceed the strain/stress limits of the material being used. A snap fit design that has been used for a ductile, low modulus plastic will probably not be suitable for a highly reinforced, very rigid plastic.

For rigid materials, the length of the cantilever may be increased or the interference deflection "Y" reduced. Adding a "stop" can prevent over deflection of the cantilever during assembly.

Figure 79: Boss Design for Self-Tapping Screws

Straight Cantilever Beam Equation

The relationship between maximum deflection and strain for a straight cantilevered beam was calculated as follows: From Table 46, the cantilever beam was chosen and the drawing is repeated as Figure 79. The maximum stress, is given by the following:

$$\sigma = \frac{FL}{Z}$$

Since this beam has a rectangular cross section,

$$Z = \frac{bd^2}{6} \text{ and}$$

$$I = \frac{bd^3}{12}$$

Therefore:

$$\sigma = \frac{FLd}{2I}$$

The deflection of the beam, Y, is given by:

$$Y = \frac{FL^3}{3EI}$$

Table 48: Strain Recommendations for Cantilever Snap-Fits

Grade	Maximum Strain, %
ET-1000 HS	1.0
A-1230 L	0.5
AS-1133 HS	1.0

Solving the deflection equation for F, the force needed to deflect the beam can be calculated as follows:

Equation 1

$$F = \frac{3YEI}{L^3}$$

The modulus of elasticity, E, is defined as:

$$E = \frac{\sigma}{\epsilon} \quad \text{and therefore} \quad \epsilon = \frac{\sigma}{E}$$

substituting that in the cantilever stress equation:

Equation 2

$$\epsilon = \frac{FLd}{2EI}$$

Using the relationship of equation 1 and substituting for F in equation 2 the relationship between strain and deflection is derived:

Equation 3

$$\epsilon = \frac{3Yd}{2L^2}$$

This equation allows the designer to calculate the strain required from the maximum deflection of a design. Table 48 summarizes maximum strain recommendations for several grades of Amodel resins.

Once a suitable grade of Amodel resin has been selected, the basic equations can be used to find the load, F, needed to deflect the cantilever the required amount.

In a cantilever snap fit, the stress and strain are maximum at the base of the cantilever and become proportionately lower toward the tip where the load is applied. In fact the stress and strain at any point can be calculated by substituting a different L, the distance from the load toward the fixed end. Therefore, if the cantilever thickness was gradually reduced from fixed end to tip, the beam will be able to deflect more than in the fixed thickness cantilever without incurring higher maximum stresses. In this way, the capability of the material can be maximized.

Figure 80: Snap Fit Design Using Tapered Beam

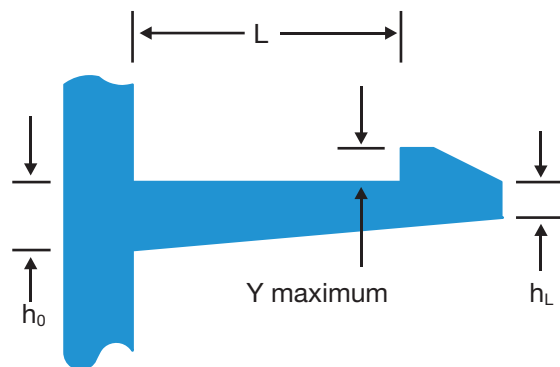
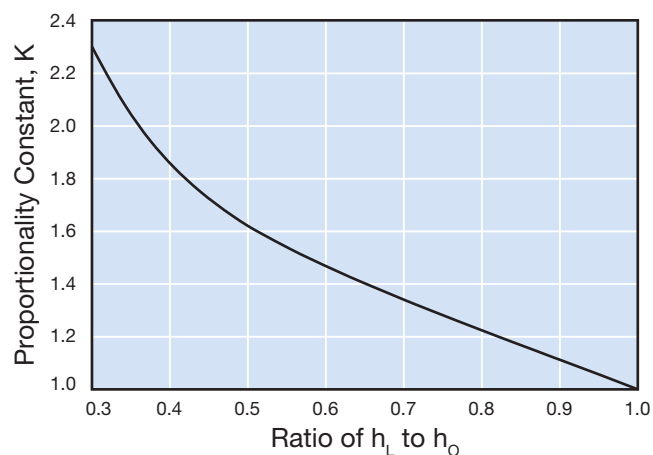


Figure 81: Proportionality Constant (K) for Tapered Beam



Tapered Cantilever Beam Equation

For the tapered design shown in Figure 80, h_L is the thickness at the free end. The value of the proportionality constant, K, for a tapered beam design can be found in Figure 81. The maximum strain can be calculated from:

Equation 4

$$\epsilon = \frac{3Yh_0}{2L^2K}$$

For example, if the beam thickness has been gradually reduced to half its fixed end thickness; the ratio of h_L to h_0 would be 0.5 and K (from Figure 81) would be 1.6. Therefore, the maximum strain and the corresponding stress would be multiplied the reciprocal of K, 0.625. The strain will be reduced by about 40% of the strain of a constant thickness cantilever beam design with equal deflection.

Designing for Injection Molding

Many of the applications for Amodel PPA resins will be manufactured using the injection molding process. An engineer who has designed a part to meet the performance requirements of the application must also take into account the fact that there are elements in the part design that can influence moldability. These factors include wall thickness and wall thickness transitions, draft, ribs, bosses, and coring. The effect of these factors on moldability should be considered by the design engineer before a mold is built to make the part.

Wall Thickness

In general, parts should be designed with the thinnest wall that will have sufficient structural strength to support the expected loads, keep deflection within design criteria limits, have adequate flow, and meet flammability and impact requirements. Parts designed in this manner will have the lowest possible weight, and therefore the lowest material cost, and the shortest molding cycle.

Wall Thickness Variation

Part designs that contain uniform wall thicknesses are ideally suited for the injection molding process. They minimize molded-in stress, reduce the potential for sink marks on the surface of the part, and eliminate the potential for voids in a molded part. However, structural, appearance, and draft considerations may require varying wall thicknesses. When changes in wall section thickness are necessary, the designer should consider a gradual transition, such as the tapered or gradual designs shown in Figure 82.

Sharp transitions may create problems in appearance and dimensional stability, because they may result in differential cooling and turbulent flow. A sharp transition may also result in a stress concentration, which may adversely affect part performance under loading or impact.

Draft Angle

To aid in the release of the part from the mold, parts are usually designed with a taper. The taper creates a clearance as soon as the mold begins to move, allowing the part to break free from its mold cavity. The taper is commonly referred to as draft, and the amount of taper as draft angle, as shown in Figure 83.

Figure 82: Wall Thickness Transition

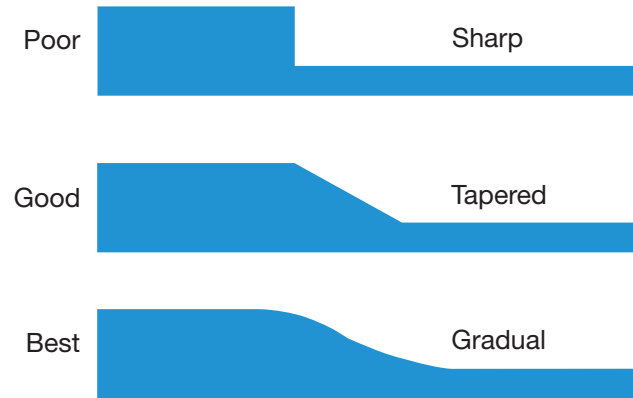
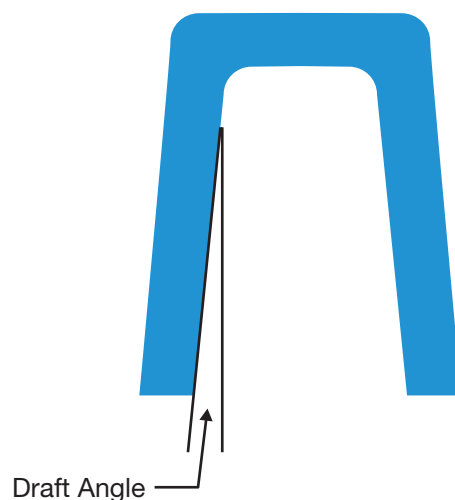


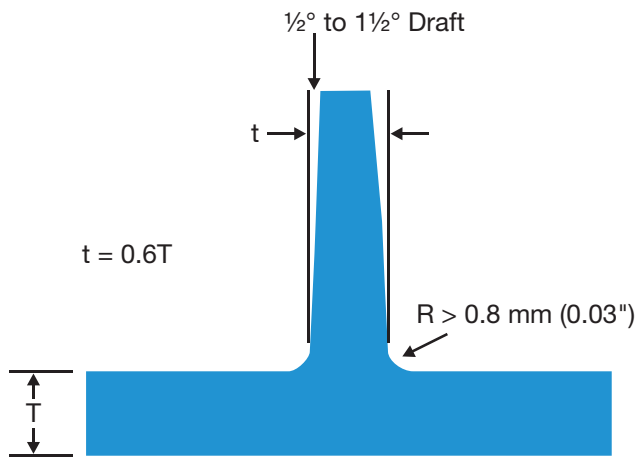
Figure 83: Draft - Designing for Mold Release



Adequate draft angle should be provided to allow easy part removal from the mold. Generally, the designer should allow a draft angle of 0.5° to 1° per side for both inside and outside walls for Amodel resins. However, in some special cases, smaller draft angles, as low as $1/8^\circ$ to $1/4^\circ$, have been used with draw polish on the mold surface.

More draft should be used for deep draws or when cores are used. Textured finishes increase draft requirements by a minimum of 1° per side for each 0.025 mm (0.001 inch) of texture depth.

Figure 84: Draft - Recommended Rib Design



Ribs

The stiffness of a part design can be increased with properly designed and located ribs, without creating thick walls as illustrated in the Design Section entitled "Adding Ribs to Maintain Stiffness" on page 68. Proper rib design will allow for decreased wall thickness. This will save material and weight, and shorten molding cycles. It will also eliminate thick walls, which can cause molding problems like sink marks on the surface of parts or voids on the inside of parts. Ribs that are correctly positioned may also function as internal runners, assisting plastic melt flow during molding.

In general, the following guidelines should be used when designing with ribs. The thickness at the rib base should be no greater than 60% of the adjacent wall thickness. When ribs are opposite appearance areas, the width should be kept as thin as possible. If there are areas in the molded part where structure is more important than appearance, then ribs are often 75%, or even 100%, of the outside wall thickness. Whenever possible, ribs should be smoothly connected to other structural features such as side walls, bosses, and mounting pads. If there are several ribs in a part, they need not be constant in height or width, and are often matched to the stress distribution in the part. All ribs should have a minimum of $\frac{1}{2}^\circ$ of draft per side and should have a minimum radius of 0.8 mm (0.03 inch) at the base to reduce stress concentrations and sink marks.

Figure 84 shows the recommended rib size relationships.

Coring

Proper design practice should include uniform wall thickness throughout a part. Heavy sections in a part can extend cycle time, cause sink marks on the part surface, cause voids within the part and increase molded-in stresses.

Heavy sections should be cored to provide uniform wall thickness. For simplicity and economy in injection molds, cores should be parallel to the line of draw of the mold. Cores placed in any other direction usually create the need for some type of side action or manually loaded and removed loose cores.

Cores which extend into the cavity will be subject to high pressure. For blind cores (cores that are unsupported) that have diameters greater than 1.5 mm (0.060 inch) the core lengths should not exceed three times the diameter, while blind cores with diameters less than 1.5 mm (0.060 inch) should not exceed twice their diameter in length. These recommendations may be doubled for through cores (cores that telescope into or shut off with the opposite side of the mold). Draft should be added to all cores, and all tooling draw polished for best ejection.

Bosses

Bosses are projections from the nominal wall of a part that will eventually be used as mounting or fastening points. The design of bosses is largely dependent upon their role in a given part. Cored bosses can be used for press fits, self-tapping screws, and ultrasonic inserts. Each of these will exert stress on the wall of the boss.

As a general guideline, the outside diameter of a boss should be twice the inside diameter of the hole, and the wall thickness at the base of the boss should not exceed 60% of the part wall thickness unless structural concerns override appearance requirements. Figure 85 illustrates these guidelines.

Additional forces imposed on bosses may tend to be transmitted down the boss and into the nominal wall. For this reason, a minimum radius of 25% of the wall thickness is required at the base of the boss to provide strength and reduce stress concentration. A boss can be further strengthened by using gusset-plate supports around the boss, or attaching it to a nearby wall with a properly designed rib. Bosses should be designed in the same manner as ribs. Heavy sections should be avoided to prevent the occurrence of sink marks on the surface and voids in the interior of the part.

Figure 85: Boss Design - General Guidelines

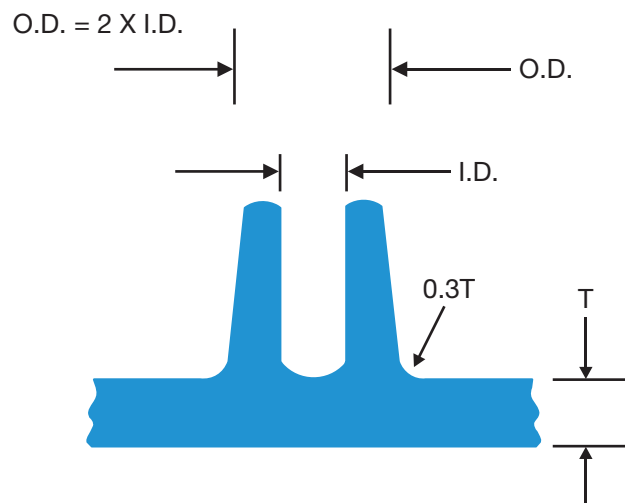


Figure 86: Thermostat Housing Showing Beads



Undercuts

Some design features, depending on orientation, can place portions of the mold in the way of ejecting the part. These features are called undercuts and can require special mold configurations, such as slides or cams, to move prior to ejection. In some cases, the material being molded will have enough flexibility than the part can be pushed off the undercut without damage.

For example, the typical automotive thermostat housing, as shown in Figure 86, has beads to provide for leak-proof hose connections. To provide a smooth surface for the hose connection, the designer has specified that the parting line cannot be in this area. This results in an undercut at each bead.

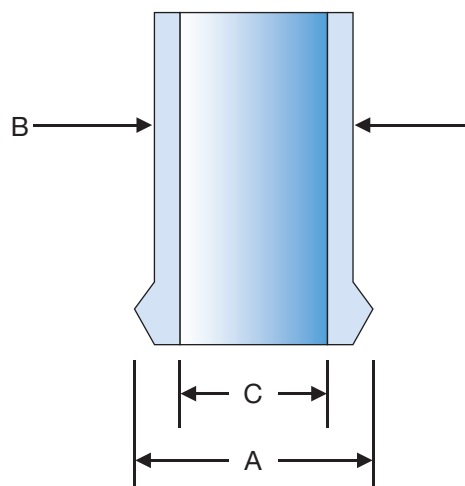
Under some circumstances, it may be possible to eject a part with an undercut if the core can be pulled first and the undercut ratio is 8 or less.

$$\text{Undercut Ratio (R)} = \frac{100 (\text{Bead diameter (A)} - \text{Tube OD (B)})}{\text{Tube ID (C)}}$$

If the part must be molded without side pulls and the undercut ratio calculated is greater than 8, the design should be modified. One possible modification is to taper the tube inside diameter effectively reducing the wall thickness under the bead. For tubes with inside diameters less than 25 mm (1 inch), it may be necessary to modify the bead geometry to get an undercut ratio of 8 or less.

The success of this approach is based upon removing the part from the mold while the part is still hot and therefore more flexible than it will be a room temperature.

Figure 87: Undercut Diagram



Welding

Components produced from Amodel resins can be readily joined using hot-plate, vibration, spin, or ultrasonic welding.

In this section, each welding method is described, and the apparatus and the conditions that produced acceptable welds with Amodel AS-1133 HS resin are discussed. These conditions are the suggested starting points for determining welding conditions for actual applications. Other Amodel grades may require refinement of the noted process conditions. In some instances, additional information will be provided, such as sensitivity to welding conditions, sample geometry, or moisture content.

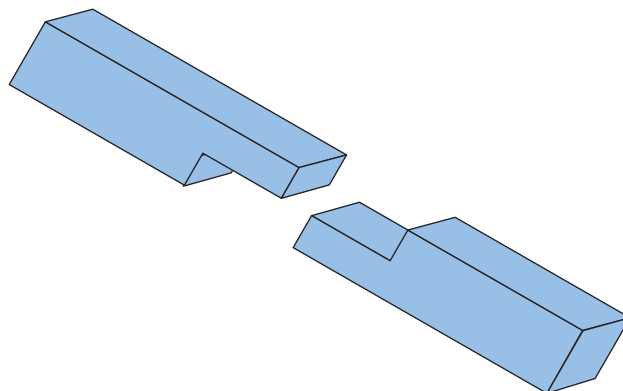
Because Amodel resins absorb moisture, tests were performed on specimens conditioned to three different moisture levels; 0%, 1.8% and 3.8% moisture. These moisture contents were selected to represent the moisture levels for parts molded from Amodel AS-1133 HS resin that had reached equilibrium in air with relative humidity levels of 0%, 50%, and 100% respectively. To simplify the discussion of results, the term dry will be used for the dry, as molded specimens, normal for those containing 1.8% moisture, and saturated for those containing 3.8% moisture.

In summary, acceptable welds can be achieved using all of the welding techniques evaluated and described in this section. Ultrasonic welding does require near-field energy application for strong welds. In general, absorbed moisture does not interfere with welding, but best results are obtained using samples that contain normal amounts of moisture (1.8%) or less.

Hot Plate Welding

In hot plate welding, the thermoplastic samples are pressed against a heated element causing the contact surface to melt. The element is then removed and the samples are forced together under pressure. This welding method typically requires a longer cycle time than other methods, but it allows for the joining of parts that have a much larger surface area. With care, a strong and hermetic bond may be obtained using this method with Amodel resins.

Figure 88: Joint Design for Hot Plate Welding



The hot plate welding machine used was a Bielomatic HV 4806 welding machine manufactured in 1986 by Leuze GMBH. The specimens used were bars 102 mm long x 25 mm wide x 6 mm thick (4 inch x 1 inch x 0.25 inch) thick. The welding machine was set up to provide a nominal lap shear weld of 13mm x 25 mm (0.5 inch x 1 inch). A diagram of the weld joint is shown in Figure 88.

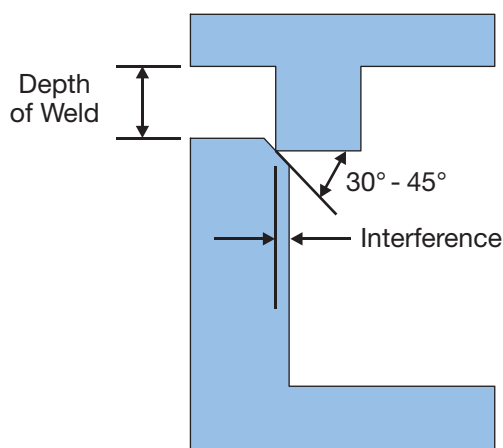
Best results were obtained using a hot plate temperature of 330°C (626°F), a clamping pressure of 207 KPa (30 psi). The optimum heating time for the test samples proved to be 40 seconds, with a holding time of 20 seconds. The strength of the bond produced was comparable to the strength of the material itself, i.e., the majority of the specimens failed at points other than the joint during mechanical testing.

Test plaques occasionally stuck to the hot plate unless a silicone mold release was applied and the hot plate was allowed to reach thermal equilibrium. Tests showed that the use of mold release did not reduce the weld strength. Absorbed moisture did not significantly affect weld strength at dry (0%) and normal (1.8%) levels, but it did reduce weld strength at the saturated (3.8%) condition.

Vibrational Welding

In vibrational welding, friction is used to generate heat at the weld joint. One of the parts to be assembled is held stationary while the mating part vibrates ~0.8 mm to 1.5 mm (0.030 inch to 0.060 inch) in a linear fashion at 100 Hz to 400 Hz. Vibrational welding is limited to flat parts, but has a relatively fast cycle time and a low tooling cost.

Figure 89: Lap Shear Joint Configuration



The machine used for these experiments was a Vinton Hydroweld Vibration welding machine. This machine operates at a nominal frequency of 240 Hz. The specimens used were 102 mm (4 inch) long, by 25 mm (1 inch) wide, by 6 mm (0.25 inch) thick, and they were welded in a 25 by 13 mm (1 by 0.5 inch) lap shear configuration as shown in Figure 89.

This method was very effective and welds as strong as the parent material were easily obtained. This technique proved relatively insensitive to welding conditions, giving good results at weld times as short as 0.60 seconds and pressures as low as 2.20 MPa (320 psig). Best results were obtained using specimens containing a normal (1.8%) amount of moisture.

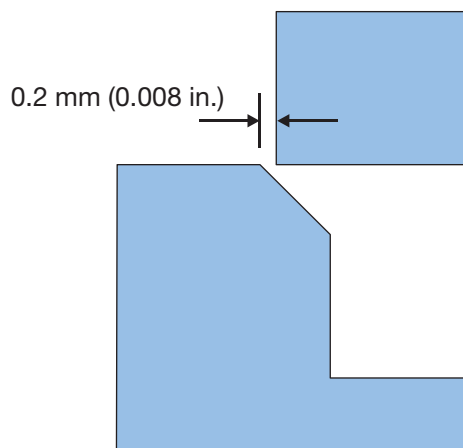
Spin Welding

The spin welding method uses frictional heat to join two cylindrical or spherical mating parts. While one half is held stationary in a nest fixture, the mating part is spun rapidly against it. Friction at the interface raises the temperature of the material until melting occurs. When the spinning action is stopped, the parts are held under pressure until cooled. Obviously, this welding method is limited to parts with circular geometry at the joint. The advantage obtained through spin welding is the increased dispersion of material at the joint compared to other techniques. This allows for the development of hermetic seals and reduces the tolerance requirements on the joint geometry.

Spin welded joints using Amodel PPA should incorporate a design known as a shear joint like that shown in Figure 90. Details known as flash traps may be incorporated to channel the localized flow of the material to one side of the part depending on requirements.

The spin welding machine used for these experiments was a Mechasonic KLN Omega machine, model SPN-063. Typically the important parameters for this welding method are angular speed, in revolutions per minute,

Figure 90: Shear Joint Configuration



normal force, and welding time. Because this specific machine was an inertia- type, the energy available for spinning the sample was limited to that stored in the flywheel. Instead of adjustments per se to speed, the energy stored in the flywheel was controlled. More modern spin welding machines allow for the control of speed, force, time, and in some cases, angular location.

The specimens used for the spin weld testing were injection molded cups with an interference joint design. Excellent weld strength was obtained using this method.

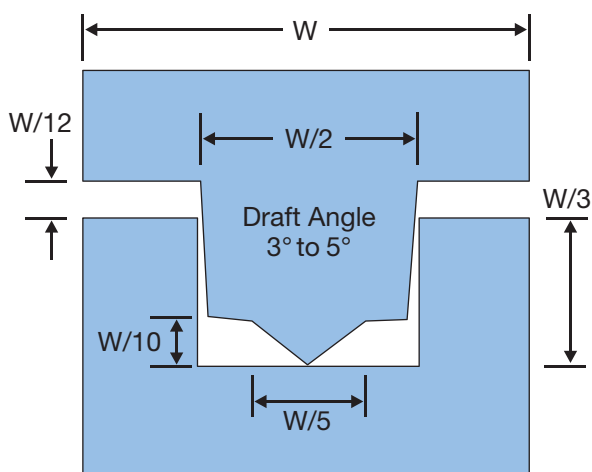
Because the welding condition settings were machine-specific, they are not generally useful in setting a starting point. Rather, it was observed that as forge pressure and angular velocity were increased, weld strength increased up to a maximum and then decreased when an excessive amount of either pressure or velocity were applied. The values for these parameters are strictly dependent on the part geometry and therefore they are not noted here. The explanation of the observed phenomena is that when a weld was made with too high a forge pressure, the spinning motion was stopped too rapidly and not enough polymer melted and flowed to create a sound joint. In the other extreme, a high angular velocity and a low forge pressure, the top part essentially sat on top of the bottom part and freely rotated without being forced into the interference fit. Thus, to assure a good joint, a welding condition must be found so both melting and forging occurs.

Moisture content did not significantly affect weld strength.

Ultrasonic Welding

In the ultrasonic welding of thermoplastic materials, high frequency (10 to 40 KHz) mechanical vibrations are transmitted through one of the mating parts to the joint interface while the other half of the assembly is held stationary. The combination of friction and an applied

Figure 91: Typical Energy-Directing Joint Configuration



force causes the temperature at the joint interface to increase to the melting temperature of the material. Normal force is held after the ultrasonic energy input is removed to achieve a mechanical bond or weld.

Ultrasonic welding has the advantage of being very high speed and is well suited to high volume production. Weld consistency and quality are high using this method; even hermetic seals may be obtained with close tolerance parts.

Aside from the ultrasonic weld equipment, a customized horn must be employed for each assembly to focus the ultrasonic energy for the given part configuration.

An energy-directing joint design is recommended for use with Amodel materials to ensure that there is localized melting at the joint. A typical joint design is shown in Figure 91. The recommended interference using a shear joint design is a minimum of 0.2 mm (0.008 inch).

The ultrasonic welding machine used for this testing was a Branson Model 910 M microprocessor-controlled machine. With this unit it is possible to adjust the amount of ultrasonic energy that is applied to the sample. For testing, the output from the booster was fed to near and far field horns. The samples used were similar to the injection molded cup used for the spin welding evaluation. Aluminum fixtures held the parts in place and a butt weld joint configuration was employed.

Welds produced using a near field horn [defined as 6 mm (0.25 inch) or less measured from the horn to the weld joint] were excellent. Welds made using the far field horn position were weak (one-third of the strength achieved with near field) and are probably not useful. The conditions that gave acceptable weld strength were: weld energy of 750 J and pressure of 4.3 MPa (617 psi).

Adhesive Bonding

Injection molded samples of Amodel A-1133 HS resin were bonded with both an epoxy and a urethane adhesive. Both adhesives were supplied by Lord Corporation. The epoxy was a two part adhesive sold under the trade name Lord® 305-1/-2 and the urethane was a two part system known as Lord® 7500 A®.

To prepare the test specimens for the Lord 305-1/-2, a cure cycle of 30 minutes at 120°C (250°F) followed by conditioning at room temperature for 72 hours was employed. The cure cycle for the Lord 7500 A® adhesive was 10 minutes at 90°C (200°F) followed by a 72-hour room temperature conditioning step.

The bond strength for both materials was tested at low temperature, room temperature, and an elevated temperature. To evaluate the effect of humid aging, specimens were conditioned for 14 days at 38°C (100°F) and 100% relative humidity. Some specimens were tested immediately after conditioning; others were tested 24 hours after conditioning.

Impact performance was determined with a side impact tester according to GM specification #9751P. Lap shear values were measured on an Instron testing machine using a pull rate of 13 mm/min (0.5 inch/min) according to ASTM D1002.

The results are shown in Figures 92 and 93. In general, the epoxy adhesive performed slightly better than the urethane. Acrylic adhesives are not recommended for use with Amodel resins.

Figure 92: Lap Shear Bond Strength

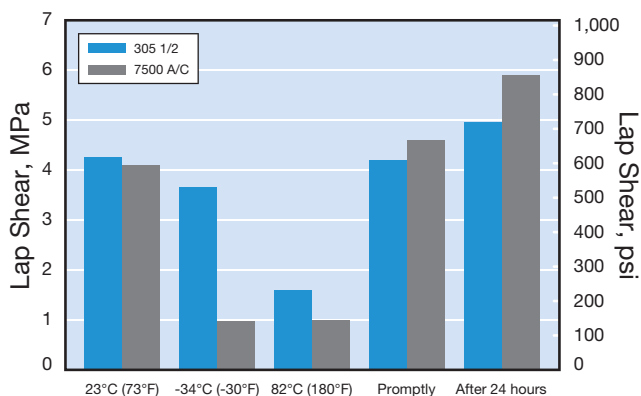


Figure 93: Side Impact Bond Strength

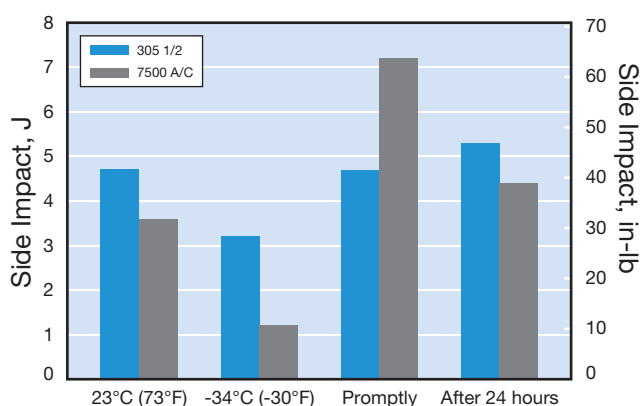


Table 49: Suitable Automotive Primers

Supplier	Primer	Description
BASF	U04KD004	solvent, flexible
	U04AD041	solvent, rigid
	U36AD001	water based
PPG	RPP9870	solvent, high solids
	AHAP9470R	solvent, one coat
Red Spot	AE146	solvent, lacquer
Siebert-Oxidermo	UBP9604	solvent, high solids
	BP2024	solvent
Sherwin-Williams	E75BC2301	solvent
	E75AC6	solvent

Coatings and Surface Finishes

Vacuum Metallizing

Vacuum metallizing involves the evaporation, and subsequent condensation, of a metal onto a substrate in a vacuum chamber. The metal used in most industrial applications is aluminum. When the end use requirement is primarily decorative, the substrate is usually processed with two organic coatings called the basecoat and the topcoat with the metal layer deposited in between. The primary function of the basecoat is to produce a smooth surface on molded plastic parts so that the metal layer will have maximum luster. A secondary function of the basecoat is to maximize adhesion of the metal layer to the substrate. On substrates that tend to outgas in a vacuum, the basecoat also provides a barrier layer. The function of the topcoat is to protect the metal layer from physical, oxidative, or chemical deterioration.

Basecoats that are compatible with Amodel resins include #VB-4315, #VB-4774, and #VB-4836-1 from Pearl Paints, <http://www.pearlpaints.com>. Topcoats that are compatible with Amodel resin include #VT 4316-2, also from Pearl Paints.

Because of the need to vaporize the metal materials during this process, an elevated temperature may be expected in the vacuum chamber. The rate at which parts may be coated is controlled by the thermal characteristics of the substrate material. For this reason, Amodel resin, with its high heat deflection temperature, is an excellent candidate material when metallization is required as comparatively rapid cycle times may be obtained.

Table 50: Suppliers of Laser Marking Equipment

Company	Website
Videojet Systems International, Inc.	www.videojet.com
Panasonic Electric Works Corporation	www.panasoni-electric-works.co.uk
ID Technology	www.idtechnology.com

Table 51: Suppliers of InkJet Printing Equipment

Company	Website
Videojet Systems International, Inc.	www.videojet.com
ID Technology	www.idtechnology.com

Laser Marking

It is possible to obtain a durable, high contrast mark on Amodel resins using commercially available laser marking systems. Depending upon the wavelength and intensity of the laser system used, the appearance of the mark can range from a bleached surface to an engraved mark.

No one set of conditions can be specified for laser marking all Amodel PPA resins. Operating parameters must be adjusted depending upon the particular application and part being marked.

The manufacturers in Table 50 have equipment that should be suitable for marking Amodel PPA resins.

Inkjet Printing

Inkjet printing can be used to provide a highly visible mark on Amodel PPA resin substrates of any color. The durability of marks made using an inkjet system depends upon the environment to which the marked part will be exposed and the type of ink used to make the mark. In many cases the durability of the mark will be satisfactory.

Equipment needs vary depending upon the type of ink used, the speed at which the mark is made, and size of the desired mark. A wide variety of equipment and inks are commercially available. Two sources are shown in Table 51.

Painting

Several grades of Amodel PPA resin were evaluated for their compatibility with various automotive paint systems. Representative glass-reinforced, mineral-reinforced, and mineral/ glass-reinforced compounds were evaluated.

As with all plastic substrates, the primer system is critical. The test specimens were cleaned with isopropyl alcohol then coated with primers and cured as per the manufacturer's instructions. The plaques were tested for tape adhesion (GM9071P, method A) and cross-hatch adhesion (GM9071P, method B) and gravelometer chip resistance (GM9508P and SAEJ400) as coated and after conditioning for 96 hours with water/fog/humidity per GM4465P specification. Table 49 lists primers that meet or exceed all test requirements and represent adequate coating performance for most painted automotive applications.

Overmolding

A process developed by the Bryant Rubber Corporation allows for the overmolding of Amodel materials with soft touch silicone rubber. The silicone rubber materials are ideal for the creation of sealing surfaces, tactile grips, and sound/noise dampening details. While overmolding with silicone rubber is not a new idea, these design details are typically characterized as having poor adhesion to the rigid substrates even if primers, or priming processes, are employed. The adhesion and peel strength achieved through the use of Bryant's Select Primerless Adhesion Polymer System (SPAPS™ Technology) is uniquely better than anything that has previously been achieved. In fact, cohesive failure of the silicone rubber is typical of the SPAPS™ Technology process.

Amodel resins are particularly well suited for use in conjunction with SPAPS™ silicone rubbers due to their excellent properties at high temperatures. This allows for reduced cycle times for the silicone cure process, improving overall economics. The silicone materials match the long-term thermal stability of Amodel resin, more so than other elastomeric materials, ensuring long-term performance in difficult environments.

The SPAPS™ silicone rubbers are offered in the full range of property options available in other common silicon rubbers. The materials are naturally transparent and colorable using liquid colorants during the molding process, with excellent color fastness, even with prolonged ultraviolet light exposure. They are available with durometer ratings of 10 to 85 on the Shore A scale. Their chemical resistance is similar to that of other silicone rubber materials. The unreactive character of the materials will allow for agency approvals, such as NSF, FDA, and U.S.P., of the finished parts.

Further information regarding the overmolding process may be obtained from the Bryant Rubber Corporation at <http://www.bryantrubber.com/>.

A

Absorption Amount	39
Accelerated Moisture Conditioning	6
Adding Ribs to Maintain Stiffness	68
Adhesive Bonding	83
Amodel Polyphthalamide (PPA) Resins	1
Amodel Resin Property Tables	4

B

Bosses	79
------------------	----

C

Calculating Allowable Stress - Creep Rupture.	70
Calculating Deflection	69
Calculating the Allowable Interference.	73
Changing Section Thickness	68
Chemical Compatibility	62
Chemical Resistance	58
Chemistry	1
Coatings and Surface Finishes	84
Coefficient of Linear Thermal Expansion	43
Combustion Properties	50
Comparative Tracking Index (CTI) – ASTM D3638	55
Compressive Strength and Modulus	27
Considering Stress Concentrations	71
Considering Thermal Stresses	71
Coring	79
Creep	31
Crystallinity	2

D

Deflection Calculations	67
Deflection Temperature Values for Amodel Resins.	43
Design Information	63
Designing for Assembly	73
Designing for Equivalent Part Stiffness	68
Designing for Injection Molding	78
Designing for Sustained Load.	69
Designing with Snap Fits	76
Dielectric Breakdown Voltage and Strength - ASTM D149	53
Dielectric Constant - ASTM D150.	54
Dimensional Change Compared to PA 6,6	41
Dimensional Change due to Moisture	40
Dissipation Factor - ASTM D150	54
Draft Angle	78

E

Effect of Moisture on Strength and Stiffness.	39
Electrical Properties.	53
Environmental Resistance.	58

F

Falling Weight Impact Properties	30
Fatigue Resistance	36
Fatigue Strength of Amodel Resin.	37
Flexural Creep	35
Flexural Properties	23
Flexural Properties at Elevated Temperatures	24
Flexural Property Comparison.	24

G

Gamma Radiation.	62
Glow Wire Testing.	50

H

Heat Deflection Temperature – HDT.	42
High-Current Arc Ignition (HAI)	56
High-Voltage Arc Resistance to Ignition	56
High-Voltage Arc-Tracking-Rate (HVTR).	55
High-Voltage, Low-Current, Dry Arc Resistance – ASTM D495	55
Horizontal Burning Test	51
Hot Plate Welding.	81
Hot Wire Ignition (HWI) - ASTM D3874	56

I

Impact Strength.	27
Inkjet Printing	85
Interference or Press Fits	73
Isochronous Stress/Strain Curves.	34
Izod (Cantilevered Beam) Impact	28
Izod Impact Property Comparison	28

L

Laser Marking.	85
Limitations of Design Calculations.	67
Long-term Mechanical Properties.	31
Loss of Bolt Tightness Due to Creep	72

M

Mechanical Design	64
Mechanical Fasteners.	74
Mechanical Properties	19
Moisture Absorption and Glass Transition Temperature (Tg)	38
Moisture Effects.	3, 38
Molded-In Threads	76

N

Nomenclature.	4
-----------------------	---

O

Overmolding	85
-----------------------	----

P

Painting.	85
Poisson's Ratio	30
Product Data	4
Product Selection.	5
Property Data.	6
Pull Out Force Calculation.	75

R

Reinforcing Fiber Orientation Considerations	67
Relative Thermal Index (UL)	48
Ribs.	79

S

Secondary Operations	81
Self-Tapping Screws	74
Shear Properties	26
Short-Term Mechanical Properties	19
Significance of Moisture Absorption.	38
Smoke Density Test (NBS)	51
Specific Heat	46
Spin Welding	82
Straight Cantilever Beam Equation	76
Stress Calculations	67
Surface Resistivity - ASTM D257	53

T

Tapered Cantilever Beam Equation	77
Tensile Creep	32
Tensile Creep Rupture	34
Tensile Properties	19
Tensile Properties for GR PPA vs. Temperature	21
Tensile Properties of A-1000 GR Grades at Elevated Temperatures	22
Tensile Property Comparison	20
Test Methods	19, 23
Thermal Aging	47
Thermal Conductivity	45
Thermal Properties	42
Thermal Stability	47
Thermogravimetric Analysis (TGA)	47
Threaded Inserts	75
Typical Properties	6

U

UL 746A Properties of Amodel Resins	57
UL 746A Short-Term Properties.	54
UL Relative Thermal Indices.	57
Ultrasonic Welding	82
Undercuts.	80
Using Classical Stress/Strain Equations.	66

V

Vacuum Metallizing	84
Vertical Burn Test	51, 52
Vertical Flammability per UL 94	51
Vibrational Welding	81
Volume Resistivity - ASTM D257	53

W

Wall Thickness	78
Wall Thickness Variation.	78
Welding.	81

www.SolvaySpecialtyPolymers.com

Contact Solvay Specialty Polymers

Europe, Middle East and Africa SpecialtyPolymers.EMEA@solvay.com

Americas SpecialtyPolymers.Americas@solvay.com

Asia and Australia SpecialtyPolymers.Asia@solvay.com

Material Safety Data Sheets (MSDS) for products of Solvay Specialty Polymers are available upon request from your sales representative or by emailing us at specialtypolymers@solvay.com. Always consult the appropriate MSDS before using any of our products.

Solvay Specialty Polymers is comprised of the activities of the Solvay Advanced Polymers, Solvay Solexis and Solvay Padanaplast companies along with the Ixan® and Diofan® PVDC products lines. To our actual knowledge, the information contained herein is accurate as of the date of this document. However the companies that comprise Solvay Specialty Polymers and none of their affiliates make any warranty, express or implied, or accepts any liability in connection with this information or its use. Only products designated as part of the Solviva® family of biomaterials may be considered as candidates for implantable medical devices; Solvay Specialty Polymers does not allow or support the use of any other products in any implant applications. This information is for use by technically skilled persons at their own discretion and risk and does not relate to the use of this product in combination with any other substance or any other process. This is not a license under any patent or other proprietary right. The user alone must finally determine suitability of any information or material for any contemplated use in compliance with applicable law, the manner of use and whether any patents are infringed. This information gives typical properties only and is not to be used for specification purposes. All companies comprising Solvay Specialty Polymers reserve the right to make additions, deletions or modifications to the information at any time without prior notification.

All trademarks and registered trademarks are property of the companies that comprise the Solvay Group or their respective owners.
AM-50477 © 2011 Solvay Specialty Polymers USA, LLC. All rights reserved. D 2002 | R 09/2011 | Version 4.0



a Passion for Progress®